U.S. DEPARTMENT OF ENERGY

Prepared for the U.S. Department of Energy
under Contract DE-AC05-76RL01830

PNNL-20184
EMSP-RPT-003

Optical Basicity and Nepheline Crystallization in High Alumina Glasses

CP Rodriguez
JS McCloy
MJ Schweiger
JV Crum
A Winschell

February 2011

Pacific Northwest
NATIONAL LABORATORY

Proudly Operated by Battelle *Since 1965*

DISCLAIMER

PACIFIC NORTHWEST NATIONAL LABORATORY
operated by
BATTELLE
for the
UNITED STATES DEPARTMENT OF ENERGY
under Contract DE-ACO5-76RL01830

Printed in the United States of America

Available to DOE and DOE contractors from the
Office of Scientific and Technical Information,
P.O. Box 62, Oak Ridge, TN 37831-0062;
ph: (865) 576-8401
fax: (865) 576 5728
email: reports@adonis.osti.gov

Available to the public from the National Technical Information Service,
U.S. Department of Commerce, 5285 Port Royal Rd., Springfield, VA 22161
ph: (800) 553-6847
fax: (703) 605-6900
email: orders@nits.fedworld.gov
online ordering: http://www.ntis.gov/ordering.htm

PNNL-20184
EMSP-RPT-003

Optical Basicity and Nepheline Crystallization in High Alumina Glasses

CP Rodriguez
JS McCloy
MJ Schweiger
JV Crum
A Winschell

February 2011

Prepared for the U.S. Department of Energy
under Contract DE-AC05-76RL01830

Pacific Northwest National Laboratory
Richland, Washington 99354

Summary

The purpose of this study was to find compositions that increase waste loading of high-alumina wastes beyond what is currently acceptable while avoiding crystallization of nepheline ($NaAlSiO_4$) on slow cooling. Nepheline crystallization has been shown to have a large impact on the chemical durability of high-level waste glasses. It was hypothesized that there would be some composition regions where high-alumina would not result in nepheline crystal production, compositions not currently allowed by the nepheline discriminator.

Optical basicity (OB) and the nepheline discriminator (ND) are two ways of describing a given complex glass composition. This report presents the theoretical and experimental basis for these models. They are being studied together in a quadrant system as metrics to explore nepheline crystallization and chemical durability as a function of waste glass composition. These metrics were calculated for glasses with existing data and also for theoretical glasses to explore nepheline formation in Quadrant IV (passes OB metric but fails ND metric), where glasses are presumed to have good chemical durability. Several of these compositions were chosen, and glasses were made to fill poorly represented regions in Quadrant IV.

To evaluate nepheline formation and chemical durability of these glasses, quantitative X-ray diffraction (XRD) analysis and the Product Consistency Test were conducted. A large amount of quantitative XRD data is collected here, both from new glasses and from glasses of previous studies that had not previously performed quantitative XRD on the phase assemblage.

Appendix A critically discusses a large dataset to be considered for future quantitative studies on nepheline formation in glass. Appendix B provides a theoretical justification for choice of the oxide coefficients used to compute the OB criterion for nepheline formation.

Abbreviations

ASTM	American Society for Testing and Materials
ARM	Approved reference materials
CCC	canister centerline cooled
DOE	U.S. Department of Energy
DWPF	Defense Waste Processing Facility
EA	environmental assessment
HLW	high-level waste
ICP-MS	Inductively coupled plasma– mass spectrometry
INEEL	Idaho National Engineering and Environmental Laboratory, now Idaho National laboratory
NBO/T	non-bridging oxygen per tetrahedron
ND	nepheline discriminator
NLAS	nepheline-like aluminosilicate
OB	optical basicity
PCT	Product Consistency Test
PDF	powder diffraction file
PNNL	Pacific Northwest National Laboratory
PSD	particle-size distribution
QA	quality assurance
SRNL	Savannah River National Laboratory
3-D	three dimensional
2-D	two dimensional
UV	Ultraviolet
VSL	Vitreous State Laboratory at the Catholic University of America
WL	waste loading
WTP	Hanford Tank Waste Treatment and Immobilization Plant
XRD	X-ray diffraction

Acknowledgements

The authors would like to acknowledge fruitful discussions with Kevin Fox (Savannah River National Laboratory [SRNL]), Dong-Sang Kim (Pacific Northwest National Laboratory [PNNL]), Hong Li (Schott), David Peeler (SRNL), Pavel Hrma (PNNL), Amanda Billings (SRNL), Hao Gan (Vitreous State Laboratory [VSL]), and Jake Amoroso (SRNL). Also, thanks to Kevin Fox and David Peeler for the SRNL NE3, NP2, and SB5NEPH glass samples, and to Ian Pegg (VSL), Wing Kot (VSL), and Hao Gan for the VSL HWI-Al and HLW-E-Al glass samples. Thanks to Michael Lindburg (PNNL) and Fabienne Johnson (SRNL) for analytical chemistry support. Thanks to summer students at PNNL Kevin Swearingen and Rachel Anheier who helped in this study.

PNNL is operated for the U.S. Department of Energy by Battelle under Contract DE-AC05-76RL01830. This work funded in part by the Department of Energy – Office of Environmental Management, Office of Technology Innovation and Development.

Table of Contents

Figures

Tables

1.0 Introduction

The ultimate objective for immobilizing the high-level radioactive tank waste (HLW) is to incorporate and convert the radioactive and hazardous components into a solid waste form that will be chemically durable and meet the conditions for storage in a geologic repository for HLW (NRC 2001). Nepheline crystallization is of concern for HLW glasses because its formation generally reduces the chemical durability of the waste form (Kim, Peeler, & Hrma 1995). The combination of high Al_2O_3 and Na_2O concentrations in the waste, coupled with lower SiO_2 concentrations in the glass as waste loadings (WL) increase, can lead to the crystallization of nepheline ($NaAlSiO_4$) (e.g., Fox et al. 2007). After years of exploration and testing, a nepheline discriminator (ND) was introduced and currently is used as process control constraint at the Defense Waste Processing Facility (DWPF) (Fox et al. 2008, Edwards 2006) and for Hanford (Vienna et al. 2009, Vienna and Kim 2008) models. Proposed by Li et al. (1997), the ND is used as a composition constraint to avoid nepheline precipitation. The ND is defined below and relates the concentrations of SiO_2, Na_2O, and Al_2O_3 (as mass percentages in glass) to a critical value of 0.62 (Fox et al. 2007). Glasses with ND > 0.62 are predicted to be free from nepheline.

$$ND = \frac{mass\%_{SiO_2}}{mass\%_{Al_2O_3} + mass\%_{Na_2O} + mass\%_{SiO_2}} \geq 0.62 \quad (1.1)$$

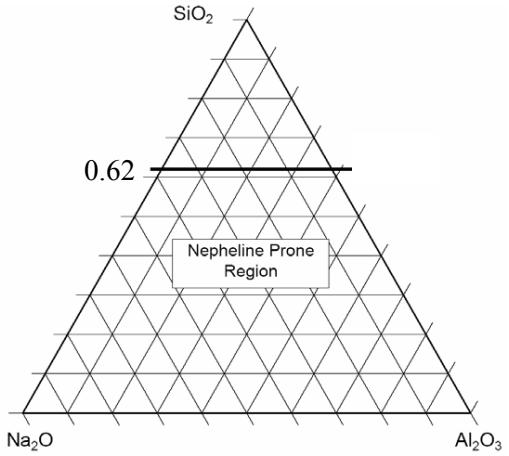

Figure 1.1. Ternary SiO_2-Na_2O-Al_2O_3 Diagram (mass fraction) Showing the Location of the Current ND. Glasses below the 0.62 line are considered prone to nepheline crystallization.

The ND equation uses only the concentrations of the SiO_2, Na_2O, and Al_2O_3 components in the glass in predicting whether nepheline is likely to crystallize. However, several other components have been shown to impact the propensity for nepheline crystallization, including B_2O_3 (Li et al. 2003) and CaO, among others (Fox et al. 2007). This impact is suggested to be explained by the optical basicity (OB) concept, namely, that the more basic cations are more likely to cause nepheline-like aluminosilicates (NLAS) to precipitate as they readily donate their valence electrons and thus become removed from the covalent glass network (McCloy and Vienna 2010). A four-quadrant system (see Table 1.1) was created from the ND and OB threshold criteria ND = 0.62, OB = 0.575 to explore the nepheline crystallization and chemical durability as a function of waste glass composition. The focus was placed on exploring

nepheline formation for glasses in Quadrant IV, which are not hypothesized to be prone to nepheline precipitation, despite being currently unallowable by the ND criterion alone (McCloy and Vienna 2010).

Table 1.1. Quadrant System for the ND and OB

II: ND high enough, OB too high	**I:** ND too low, OB too high
III: ND high enough, OB low enough	**IV:** ND too low, OB low enough

This report presents all the glass compositions that were chosen to fill sparse regions in Quadrant IV that were identified when evaluated according to the previously existing dataset. Data are presented evaluating the presence of nepheline in canister centerline cooled (CCC) glasses by X-ray diffraction (XRD) and its effect on chemical durability as shown by the Product Consistent Test (PCT) (ASTM 2008). Previously undocumented data on quantitative XRD of nepheline formation in previously published glasses as well as a critical review of existing datasets of quantitative nepheline formation is also included in Appendix A. A theoretical justification for the selection of OB coefficients used in this study is provided in Appendix B.

2.0 Experimental Procedure

Glass formulation and fabrication, CCC heat-treatments, crystallinity evaluation by XRD, and chemical durability evaluation by PCT were performed to assess the effects of nepheline formation in simulated HLW glasses. After fabricating the glasses, each of them were heat-treated following a simulated CCC profile. Then a sample of each glass was analyzed by XRD to quantitatively evaluate nepheline or other crystal phase precipitation. A set of glasses was selected for the PCT, and samples were prepared following the American Society for Testing and Materials (ASTM) procedure (ASTM 2008).

The Pacific Northwest National Laboratory (PNNL) quality assurance (QA) program was adhered to during the conduct of this work. This program used Subpart 4.2, Guidance on Graded Application of QA for Nuclear-Related Research and Development (Sp 4.2) of the national standard Nuclear Quality Assurance-1-2000 ASME NQA-1, Quality Assurance Requirements for Nuclear Facility Applications (NQA-1-2000) (along with Sp 2.7, QA Requirements for Computer Software for Nuclear Facility for software). This was done to provide a graded approach to research activities at PNNL and to meet the requirements of 10 CFR 830, Subpart A, and DOE Order 414.1C. All activities related to the work reported here were graded as research activities not impacting the design, construction, or operation of a nuclear facility.

2.1 Glass composition and fabrication

The chemical durability of a glass is affected by nepheline, which is mostly precipitated during cooling. Several sets of glasses were fabricated and/or characterized to fill the sparse regions of the quadrant system (Table 1.1) and to better understand the relationship of nepheline to OB.

Samples of high alumina glasses were provided by Savannah River National Laboratory (SRNL) (NP2-# [Fox and Edwards 2008], NE3-# [Fox and Edwards 2009]) and by Vitreous State Laboratory (VSL) (HLW-E-Al-# [Matlack et al. 2007] and HWI-Al-# [Matlack et al. 2008]) and tested with XRD as well. A set of glasses originally formulated by VSL (HLW-E-ANa-# [Matlack et al. 2007]) were selectively remade and heat-treated by Pacific Northwest National Laboratory (PNNL). Another series of glasses was fabricated using derivative compositions of VSL HLW-E-ANa-# glasses but altering Li, B, Al, Si, Ca, and Mg concentrations to study the effect of this on the glass basicity and nepheline formation. A set of new PNNL glasses (denoted PNNL-Al-24-#) was chosen to fill sparse regions at Quadrant IV. Finally, a set of high Li_2O glasses denoted EM09Li20m-B-# (based on EM09-Li20m-B from McCloy et al. [2010]) was fabricated and tested. All the new glasses were heat-treated following the CCC procedure (Table 2.1). Glasses that were provided to PNNL with previous heat-treatments are summarized in Table A.1 in Appendix A.

To evaluate nepheline formation and explore Quadrant IV in more depth, a series of glass compositions was formulated and fabricated. As previously mentioned, other glasses were obtained from SRNL or VSL and either characterized as received (SRNL) or heat-treated and then characterized (VSL). Another set of 12 VSL compositions (Matlack et al. 2007) were prepared and heat-treated at PNNL: HLWE-ANa-4, 5, 9, 10, 11, 13, 14, 15, 16, 24, 25, 26. A set of 25 more glasses was fabricated at PNNL, based on the VSL HLW-E-ANa-4, 5, 9, 10, 11, 13, 14, 15, 16, 24, 25, 26 compositions by altering Li, B,

Al, Si, Ca, and Mg concentrations. Thirteen new glasses with a composition similar to HLW-E-Al-24 (denoted PNNL-Al-24-#) were also fabricated and heat-treated. Eight new compositions based on EM09-Li20m-B (McCloy et al. 2010) (denoted EM09-Li20m-B-#) and five high Al_2O_3 glasses (denoted A#) (Hrma et al. 2010) were formulated, fabricated, heat-treated. Additional glasses reported to contain nepheline or other NLAS were remade, including some Idaho National Engineering and Environmental Laboratory (INEEL) waste compositions (Riley et al. 2001) (DZr-CV-#) and WTP glass HLW-ALG-27 (Vienna and Kim 2008).

Compositions of the glasses made at PNNL (including VSL compositions) are shown in Table 2.1. Note that all SRNL glasses tested were previously published compositions, and those VSL compositions received from them were also previously published compositions, so the reader is referred to the original works for their compositions (see Table A.1, Appendix A).

Glasses made at PNNL were batched and melted using oxides and carbonates. After batching, each glass was mixed in an agate mill for about 3 minutes and then placed into a platinum crucible (Pt/10%Rh) and melted for ~1 hour at 1150 to 1400°C. The glass then was air quenched by pouring the melt onto a stainless steel pour plate. Most of the glasses showed some undissolved solids (UDS) after cooling. Thus, to facilitate UDS dissolution and increase homogeneity, glass from the first melt was ground to a powder in the tungsten carbide mill (~4 minutes) and melted a second time at the same or slightly lower temperature than the first melt. All the glasses were subsequently air-quenched again on a stainless steel pouring plate. For the most part, glasses had a very uniform appearance after cooling, and no UDS were observed.

Table 2.1. Target Compositions of Remade Glasses from VSL and New Formulations by PNNL. Compositions are listed in mass%.

GLASS ID	Al_2O_3	B_2O_3	BaO	Bi_2O_3	CaO	CdO	Cr_2O_3	F	Fe_2O_3	K_2O	Li_2O	MgO	Na_2O	NiO	P_2O_5	PbO	SiO_2	TiO_2	SO_3	ZnO	ZrO_2
HLW-E-ANa-4	21.34	14.37	0.03	1.16	0.72	0.00	0.71	0.25	2.82	0.66	4.08	0.22	12.71	0.10	2.02	0.09	38.06	0.17	0.22	0.18	0.12
HLW-E-ANa-5	23.61	14.41	0.03	1.28	0.80	0.01	0.79	0.25	3.11	0.73	3.58	0.24	14.06	0.11	2.24	0.10	33.89	0.19	0.24	0.20	0.14
HLW-E-ANa-5(2Al-2Si)	25.61	14.41	0.03	1.28	0.80	0.01	0.79	0.25	3.11	0.73	3.58	0.24	14.06	0.11	2.24	0.10	31.89	0.19	0.24	0.20	0.14
HLW-E-ANa-5(3Al-3Si)	26.61	14.41	0.03	1.28	0.80	0.01	0.79	0.25	3.11	0.73	3.58	0.24	14.06	0.11	2.24	0.10	30.89	0.19	0.24	0.20	0.14
HLW-E-ANa-5(2Al+1B-3Si)	25.61	15.41	0.03	1.28	0.80	0.01	0.79	0.25	3.11	0.73	3.58	0.24	14.06	0.11	2.24	0.10	30.89	0.19	0.24	0.20	0.14
HLW-E-ANa-5(1.5Al+2B-3.5Si)	25.11	16.41	0.03	1.28	0.80	0.01	0.79	0.25	3.11	0.73	3.58	0.24	14.06	0.11	2.24	0.10	30.39	0.19	0.24	0.20	0.14
HLW-E-ANa-5(2Al+1.5B-3.5Si)	25.61	15.91	0.03	1.28	0.80	0.01	0.79	0.25	3.11	0.73	3.58	0.24	14.06	0.11	2.24	0.10	30.39	0.19	0.24	0.20	0.14
HLW-E-ANa-5(2Al+1.5B+1Na-4.5Si)	25.61	15.91	0.03	1.28	0.80	0.01	0.79	0.25	3.11	0.73	3.58	0.24	15.06	0.11	2.24	0.10	29.39	0.19	0.24	0.20	0.14
HLWE-ANa-9	25.88	14.44	0.03	1.40	0.88	0.01	0.86	0.27	3.41	0.80	5.09	0.26	15.41	0.12	2.45	0.11	27.72	0.21	0.26	0.22	0.15
HLWE-ANa-9(0.5B -0.5Li)	25.88	14.94	0.03	1.40	0.88	0.01	0.86	0.27	3.41	0.80	4.59	0.26	15.41	0.12	2.45	0.11	27.72	0.21	0.26	0.22	0.15
HLWE-ANa-9(1.0B, -1.0Li)	25.88	15.44	0.03	1.40	0.88	0.01	0.86	0.27	3.41	0.80	4.09	0.26	15.41	0.12	2.45	0.11	27.72	0.21	0.26	0.22	0.15
HLWE-ANa-10	25.88	15.94	0.03	1.40	0.88	0.01	0.86	0.27	3.41	0.80	3.59	0.26	15.41	0.12	2.45	0.11	27.72	0.21	0.26	0.22	0.15
HLWE-ANa-10(0.5B-0.5Li)	25.88	16.46	0.03	1.40	0.88	0.01	0.86	0.27	3.41	0.80	3.09	0.26	15.41	0.12	2.45	0.11	27.72	0.21	0.26	0.22	0.15
HLWE-ANa-10(1.0B-1.0Li)	25.88	16.96	0.03	1.40	0.88	0.01	0.86	0.27	3.41	0.80	2.59	0.26	15.41	0.12	2.45	0.11	27.72	0.21	0.26	0.22	0.15
HLWE-ANa-10(1.5B-1.5Li)	25.88	17.46	0.03	1.40	0.88	0.01	0.86	0.27	3.41	0.80	2.09	0.26	15.41	0.12	2.45	0.11	27.72	0.21	0.26	0.22	0.15
HLWE-ANa-11	25.88	13.44	0.03	1.40	0.88	0.01	0.86	0.27	3.41	0.80	5.09	0.26	15.41	0.12	2.45	0.11	28.72	0.21	0.26	0.22	0.15
HLWE-ANa-11(0.5B-0.5Li)	25.88	13.94	0.03	1.40	0.88	0.01	0.86	0.27	3.41	0.80	4.59	0.26	15.41	0.12	2.45	0.11	28.72	0.21	0.26	0.22	0.15
HLWE-ANa-11(1.0B-1.0Li)	25.88	14.44	0.03	1.40	0.88	0.01	0.86	0.27	3.41	0.80	4.09	0.26	15.41	0.12	2.45	0.11	28.72	0.21	0.26	0.22	0.15
HLWE-ANa-11(1.5B-1.5Li)	25.88	14.94	0.03	1.40	0.88	0.01	0.86	0.27	3.41	0.80	3.59	0.26	15.41	0.12	2.45	0.11	28.72	0.21	0.26	0.22	0.15
HLWE-ANa-11(2B-2Li)	25.88	15.44	0.03	1.40	0.88	0.01	0.86	0.27	3.41	0.80	3.09	0.26	15.41	0.12	2.45	0.11	28.72	0.21	0.26	0.22	0.15
HLWE-ANa-13	21.34	14.37	0.03	1.16	5.72	0.01	0.71	0.23	2.82	0.66	3.08	0.22	12.71	0.10	2.02	0.09	34.06	0.17	0.22	0.18	0.12
HLWE-ANa-13(1.0Li-1.0Si)	21.34	14.37	0.03	1.16	5.72	0.01	0.71	0.23	2.82	0.66	4.08	0.22	12.71	0.10	2.02	0.09	33.06	0.17	0.22	0.18	0.12
HLWE-ANa-13(3Al - 3 Si)	24.34	14.37	0.03	1.16	5.72	0.01	0.71	0.23	2.82	0.66	3.08	0.22	12.71	0.10	2.02	0.09	31.06	0.17	0.22	0.18	0.12
HLWE-ANa-13(3Al+2B-5Si)	24.34	16.37	0.03	1.16	5.72	0.01	0.71	0.23	2.82	0.66	3.08	0.22	12.71	0.10	2.02	0.09	29.06	0.17	0.22	0.18	0.12
HLWE-ANa-13(1B+1Na+1Al-3Ca)	22.34	15.37	0.03	1.16	3.72	0.01	0.71	0.23	2.82	0.66	3.08	0.22	13.71	0.10	2.02	0.09	34.06	0.17	0.22	0.18	0.12
HLWE-ANa-13(2Na-2Ca)	21.34	14.37	0.03	1.16	3.72	0.01	0.71	0.23	2.82	0.66	3.08	0.22	14.71	0.10	2.02	0.09	34.06	0.17	0.22	0.18	0.12
HLWE-ANa-14	23.61	14.41	0.03	1.28	5.80	0.01	0.79	0.25	3.11	0.73	2.58	0.24	14.06	0.11	2.24	0.10	29.89	0.19	0.24	0.20	0.14
HLWE-ANa-15	23.61	15.41	0.03	1.28	5.80	0.01	0.79	0.25	3.11	0.73	2.58	0.24	14.06	0.11	2.24	0.10	28.89	0.19	0.24	0.20	0.14
HLWE-ANa-15(1Li-1Na)	23.61	15.41	0.03	1.28	5.80	0.01	0.79	0.25	3.11	0.73	3.58	0.24	13.06	0.11	2.24	0.10	28.89	0.19	0.24	0.20	0.14
HLWE-ANa-16	23.61	14.41	0.03	1.28	5.80	0.01	0.79	0.25	3.11	0.73	3.58	0.24	14.06	0.11	2.24	0.10	28.89	0.19	0.24	0.20	0.14
HLWE-ANa-16(1.0B-1.0Ca)	23.61	15.41	0.03	1.28	4.80	0.01	0.79	0.25	3.11	0.73	3.58	0.24	14.06	0.11	2.24	0.10	28.89	0.19	0.24	0.20	0.14
HLWE-ANa-16(2.0B-2.0Ca)	23.61	16.41	0.03	1.28	3.80	0.01	0.79	0.25	3.11	0.73	3.58	0.24	14.06	0.11	2.24	0.10	28.89	0.19	0.24	0.2	0.14
HLWE-ANa-16(1.0Mg-1.0Ca)	23.61	14.41	0.03	1.28	4.80	0.01	0.79	0.25	3.11	0.73	3.58	1.24	14.06	0.11	2.24	0.10	28.89	0.19	0.24	0.2	0.14
HLWE-ANa-16(2.0Mg-2.0Ca)	23.61	14.41	0.03	1.28	3.80	0.01	0.79	0.25	3.11	0.73	3.58	2.24	14.06	0.11	2.24	0.10	28.89	0.19	0.24	0.2	0.14
HLWE-ANa-24	22.70	18.39	0.03	1.23	0.77	0.01	0.76	0.24	3.00	0.71	3.08	0.23	13.52	0.11	2.15	0.10	32.26	0.19	0.23	0.19	0.13
HLWE-ANa-25	22.70	19.39	0.03	1.23	0.77	0.01	0.76	0.24	3.00	0.71	3.08	0.23	13.52	0.11	2.15	0.10	31.26	0.19	0.23	0.19	0.13
HLWE-ANa-26	23.61	19.41	0.03	1.28	0.80	0.01	0.79	0.25	3.11	0.73	3.08	0.24	14.06	0.11	2.24	0.10	29.39	0.19	0.24	0.20	0.14

Table 2.1. Target Compositions of remade glasses from VSL, SRNL and new formulations by PNNL (continuation). Compositions are listed in mass%.

GLASS ID	Al_2O_3	B_2O_3	BaO	Bi_2O_3	CaO	CdO	Cr_2O_3	F	Fe_2O_3	K_2O	Li_2O	MgO	Na_2O	NiO	P_2O_5	PbO	SiO_2	TiO_2	SO_3	ZnO	ZrO_2
PNNL-AL-24-1	17.93	17.69	0.04	0.86	0.81	0.02	0.39	0.50	4.41	0.11	3.39	0.09	11.76	0.41	0.20	1.14	37.32	0.01	0.05	0.07	2.80
PNNL-AL-24-4	16.50	24.25	0.04	0.79	0.74	0.02	0.36	0.46	4.06	0.10	3.12	0.08	10.82	0.38	0.18	1.05	34.35	0.01	0.04	0.06	2.58
PNNL-AL-24-6	17.71	16.77	0.04	0.85	0.80	0.02	0.39	0.49	4.36	0.10	3.35	0.09	11.62	0.41	0.19	1.13	38.78	0.01	0.05	0.07	2.77
PNNL-AL-24-11	17.55	15.67	0.04	0.84	0.79	0.02	0.39	0.49	4.32	0.10	3.32	0.08	11.51	0.41	0.19	1.12	40.30	0.01	0.05	0.07	2.74
PNNL-AL-24-12	17.06	17.99	0.04	0.81	0.77	0.02	0.38	0.48	4.20	0.10	3.23	0.08	11.20	0.40	0.19	1.09	39.19	0.01	0.04	0.07	2.66
PNNL-AL-24-13	16.61	20.18	0.04	0.79	0.75	0.02	0.37	0.46	4.09	0.10	3.15	0.08	10.90	0.38	0.18	1.06	38.14	0.01	0.04	0.06	2.59
PNNL-AL-24-16	17.57	18.29	0.04	0.84	0.79	0.02	0.39	0.49	4.33	0.10	3.33	0.08	12.31	0.41	0.19	1.12	36.83	0.01	0.05	0.07	2.74
PNNL-AL-24-18	16.94	21.26	0.04	0.81	0.76	0.02	0.37	0.47	4.17	0.10	3.21	0.08	11.87	0.39	0.18	1.08	35.49	0.01	0.04	0.07	2.64
PNNL-AL-24-19	16.63	22.67	0.04	0.79	0.75	0.02	0.37	0.46	4.10	0.10	3.15	0.08	11.65	0.39	0.18	1.06	34.86	0.01	0.04	0.06	2.60
PNNL-AL-24-22	15.79	26.60	0.03	0.75	0.71	0.02	0.35	0.44	3.89	0.09	2.99	0.08	11.06	0.37	0.17	1.01	33.08	0.01	0.04	0.06	2.46
PNNL-AL-24-28	17.13	16.68	0.04	0.82	0.77	0.02	0.38	0.48	4.22	0.10	3.24	0.08	12.00	0.40	0.19	1.09	39.57	0.01	0.04	0.07	2.67
PNNL-AL-24-33	16.97	15.62	0.04	0.81	0.76	0.02	0.37	0.47	4.18	0.10	3.21	0.08	11.89	0.39	0.19	1.08	41.03	0.01	0.04	0.07	2.65
PNNL-AL-24-53	17.63	13.38	0.04	0.84	0.79	0.02	0.39	0.49	4.34	0.10	3.34	0.09	11.57	0.41	0.19	1.12	42.38	0.01	0.05	0.07	2.75
PNNL-AL-24-63	17.80	16.37	0.04	0.85	0.80	0.02	0.39	0.50	4.38	0.11	3.37	0.09	11.68	0.41	0.19	1.13	38.97	0.01	0.05	0.07	2.78
PNNL-AL-24-65	14.79	12.02	0.03	0.71	0.67	0.02	0.33	0.41	3.64	0.09	2.80	0.07	16.29	0.34	0.16	0.94	44.28	0.01	0.04	0.06	2.31
A0	24.02	15.19	0.00	1.15	6.08	0.00	0.52	0.67	5.91	0.14	3.57	0.12	9.59	0.40	1.05	0.41	30.51	0.00	0.20	0.08	0.40
A1	24.02	16.69	0.00	1.15	4.58	0.00	0.52	0.67	5.91	0.14	3.57	0.12	9.59	0.40	1.05	0.41	30.51	0.00	0.20	0.08	0.40
A2	24.02	15.19	0.00	1.15	6.08	0.00	0.52	0.67	5.91	0.14	6.77	0.12	6.39	0.40	1.05	0.41	30.51	0.00	0.20	0.08	0.40
A3	24.02	11.19	0.00	1.15	10.08	0.00	0.52	0.67	5.91	0.14	3.57	0.12	9.59	0.40	1.05	0.41	30.51	0.00	0.20	0.08	0.40
A4	24.02	11.99	0.00	1.15	6.08	0.00	0.52	0.67	5.91	0.14	6.77	0.12	9.59	0.40	1.05	0.41	30.51	0.00	0.20	0.08	0.40
A5	24.02	15.19	0.00	1.15	3.58	0.00	0.52	0.67	5.91	0.14	4.83	2.62	8.33	0.40	1.05	0.41	30.51	0.00	0.20	0.08	0.40
EM09-Li20m-B-04	14.10	15.65	0.00	0.18	1.38	0.00	0.25	2.51	2.65	1.04	12.55	0.21	8.07	0.38	0.53	0.13	40.14	0.00	0.00	0.00	0.23
EM09-Li20m-B-09	22.33	14.98	0.00	1.30	1.20	0.00	0.58	0.74	6.56	1.53	5.83	0.13	7.77	0.44	1.17	0.46	34.55	0.00	0.00	0.00	0.44
EM09-Li20m-B-10	21.90	16.59	0.00	1.28	1.18	0.00	0.57	0.73	6.44	1.50	5.71	0.13	7.62	0.43	1.15	0.45	33.89	0.00	0.00	0.00	0.43
EM09-Li20m-B-16	28.18	9.66	0.00	1.37	1.26	0.00	0.62	0.78	6.93	0.16	5.79	0.13	4.21	0.46	1.24	0.48	38.25	0.00	0.00	0.00	0.46
EM09-Li20m-B-26	26.61	9.65	0.00	1.37	1.26	0.00	0.61	0.78	6.93	0.16	7.83	0.13	4.83	0.46	1.24	0.48	37.19	0.00	0.00	0.00	0.46
EM09-Li20m-B-29	24.28	9.96	0.00	1.42	1.30	0.00	0.63	0.80	7.15	0.17	8.08	0.14	4.98	0.48	1.28	0.50	38.37	0.00	0.00	0.00	0.48
EM09-Li20m-B-34	28.21	9.85	0.00	1.40	1.29	0.00	0.63	0.80	7.07	0.17	4.85	0.14	4.93	0.47	1.27	0.49	37.96	0.00	0.00	0.00	0.47
EM09-Li20m-B-38	25.08	10.28	0.00	1.46	1.34	0.00	0.66	0.83	7.38	0.17	5.07	0.14	5.14	0.49	1.32	0.51	39.62	0.00	0.00	0.00	0.46
EM09-Ca20m_B	25.70	8.82	0.00	1.23	15.99	0.00	0.56	0.00	6.32	0.15	0.18	0.13	3.84	0.43	1.13	0.44	33.96	0.00	0.00	0.00	0.42
EM09-Mg20m-B	26.59	9.12	0.00	1.27	1.19	0.00	0.58	0.00	6.54	0.16	0.19	12.01	3.97	0.44	1.17	0.45	35.13	0.00	0.00	0.00	0.44

2.2 Canister Centerline Cooling (CCC)

The Hanford Tank Waste Treatment and Immobilization Plant (WTP) plan for pouring HLW glass into canisters involves pouring glass in distinct batches (or lifts) of roughly 300kg each followed by natural cooling to room temperature. Crystallization is expected to be very high at the center line of the canister where cooling is slow, whereas cooling is expected to be very rapid where glass is in contact with the canister wall. To simulate the glass near the wall of the canister, glasses were melted using (Pt 10%Rh) crucibles and air quenched on a steel plate. To simulate the cooling profile of the slowly cooled glass in the center of a canister, the CCC heat-treatment is performed on previously quenched glasses, Quenched glasses were received from VSL and CCC heat-treated at PNNL. Glasses received from SRNL were previously heat-treated using the DWPF-CCC schedule, which is slightly different than the WTP-CCC schedule performed by PNNL (Figure 2.2).

About 150 g of each glass heat-treated at PNNL was crushed and place to into a 3 × 3 cm^3 box. Boxes with tight lids were formed from Pt foil. Samples were placed in a furnace that was set to run according to the temperature schedule shown in Table 2.2. At heat treatment completion, each sample was removed from the Pt box with care to avoid breaking the sample. Samples were cut from one corner to the opposite corner through the body diagonal, using a diamond saw (Figure 2.1), in order that the resulting sample would include bulk glass, side-wall contact zones, and air contact zones. In this way the various effects of surface nucleated, side-wall nucleated, and bulk nucleated crystallization would be averaged. One of the halves of each sample was used to prepare the powder for the crystalline phase quantification by XRD and the other was used for PCT.

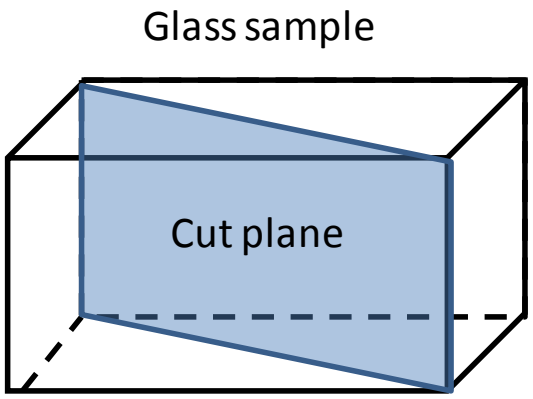

Figure 2.1. CCC Heat-Treated Glass Sample Cutting Method

Table 2.2 shows the temperature schedule of CCC heat-treatment for Hanford HLW glasses used at WTP.[(a)]

(a) Memorandum, "Canister Centerline Cooling Data, Revision 1," CCN: 074851, RPP-WTP (October 29, 2003).

Table 2.2. Temperature Schedule during WTP-CCC Treatment

Segment	Time (min)	Start Temp. (°C)	Rate (°C/min)
1	0-45	1050	-1.556
2	45-107	980	-0.806
3	107-200	930	-0.591
4	200-329	875	-0.388
5	329-527	825	-0.253
6	527-707	775	-0.278
7	707-1776	725	-0.304

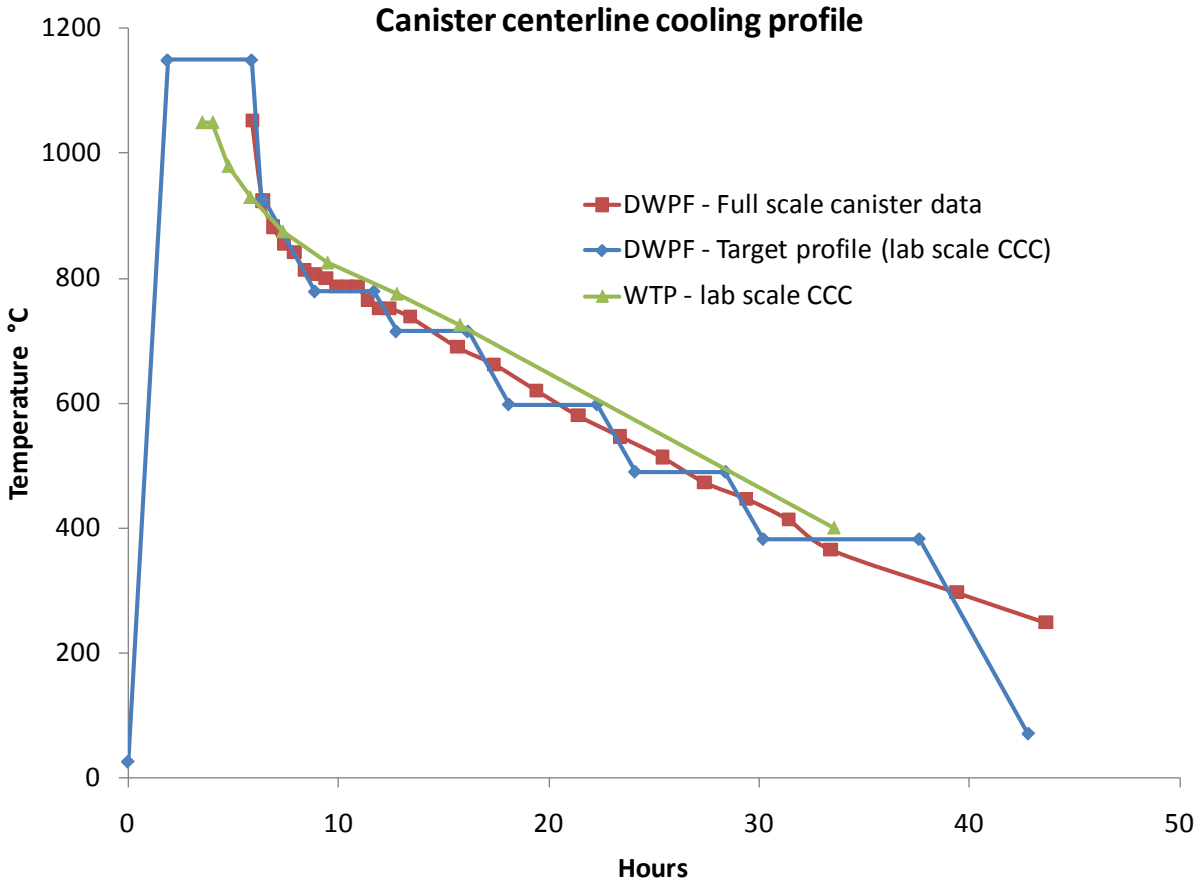

Figure 2.2. Plot of Temperature Schedule During CCC Treatment. Shown for comparison are the DWPF measured and simulated CCC profiles (Marra and Jantzen 1993).

2.3 X-Ray Diffraction Analysis

The amount and type of crystalline phases that formed during slow cooling heat-treatment were analyzed by XRD according to the PNNL procedures APEL-PAD-V and GDL-XRD. Powdered samples were prepared using roughly 5 mass% of CaF_2 as an internal standard phase with a sample of heat-treated glass. Both glass and CaF_2 were milled for 2 minutes in a tungsten carbide mill. Then the samples were loaded in round plastic holders. Once loaded, holders were mounted in an XRD sample holder. XRD was performed using a Bruker (Bruker AXS Inc., Madison, WI, USA) D8 Advance diffractometer with a LynxEye silicon detector. Scan parameters of 0.001486° 2-θ step size from 5 to 70° 2θ scan range, with a 0.300 divergence slit and a 0.0500 anti-scattering slit. Data were analyzed with Jade 6.0 Software (MDI, Materials Data Incorporated, Livermore, CA, USA) for phase identification. Full-pattern Rietveld refinement using RIQAS® 4 (MDI) was performed to quantify the amounts of crystal phases. Sample glasses received from VSL were heat-treated at PNNL, while samples from SRNL were already heat-treated according to the DWPF CCC schedule.

2.4 Product Consistency Test Analysis

A sub-set of glasses not previously tested for PCT were measured using the ASTM (2008); some of the glasses were fabricated at PNNL and some obtained from VSL (HLW-E-Al-#), The purpose of the PCT test is to measure the chemical durability of waste glasses to help qualify them for disposal. Samples were ground, sieved (-100 to +200 mesh), washed, and dried. A dionized water (DIW) blank and standard glasses (Approved Reference Material [ARM] [Mellinger and Daniel 1984] and Environmental Assessment [EA] [Jantzen et al. 1993] glasses) were also included. For every 1.5 g of glass, 15 mL of DIW was added to the glass in stainless steel vessels (304-SS). After placing the sample and water into the vessels, the vessels were sealed and placed into an oven at 90°C for 7 days. At test completion, the pH of the leached solution was measured and then filtered using a 0.45-µm filter. All the solutions were acidified with 1 volume% of concentrated HNO_3 and sent for quantitative analytical chemistry using inductively coupled plasma-optical emission spectrometry (ICP-OES) or inductively coupled plasma-atomic emission spectrometry (ICP-AES) analysis for the following elements: Al, B, Li, Si, and Na. Facilities at PNNL and SRNL were used to perform the PCT analysis. At PNNL, the instrument used for ICP-OES was a Perkin Elmer (Waltham, Massachusetts) OPTIMA 3300 DV. At SRNL the instrument used for ICP-AES was a Varian (Lexington, Massachusetts) Vista-AX. High purity calibration standards were used to generate calibration curves and to verify continuing calibration during the analysis.

3.0 RESULTS

3.1 X-Ray Diffraction

To evaluate the amount and type of crystalline phases that formed during slow cooling heat-treatment (CCC), all the glasses were analyzed by XRD according to the PNNL procedures APEL-PAD-V and GDL-XRD. Results are shown in Table 3.1 through Table 3.5. Note that "structure" in these tables is the phase that best represents the XRD patterns. Table 3.6 summarizes some of the powder diffraction file (PDF) phase identification numbers used for XRD crystalline phase analysis. Some general observations are summarized below.

- Most of the HWLE-ANa-# and HWLE-ANa-#(X) contained between 13 to 50 vol% nepheline and between 1 to 10 vol% of various spinel types, except HWLE-ANa-24 and HWLE-ANa-10(X) (three glasses) that only had spinel. HWLE-ANa-13, 14, 15, 16 and their derivatives HWLE-ANa-13(X), 14(X), 15(X), 16(X) glasses contained a third phase of —fluorapatite —present between 2 and 6 vol%. It is possible that this was another apatite phase, as the fluorine content was low in these glasses, but the XRD software identified as fluorapatite.
- All PNNL-Al-24-# glasses contained between 0.9 to 1.9 vol% of spinel, identified as magnetite. All VSL HLWE-Al-# glasses contained spinel, between 0.6 and 21.5 vol%. Additionally, HLWE-Al-08 contained 2.5 vol% of fluorapatite; HWLE-Al-15 and 17 contained between 1.1 and 2.4 vol% of lithium alumino-silicate (probably eucryptite); only HWLE-Al-23 contained nepheline, at 43.8 vol%.
- HWI-Al-X glasses contained between 4.13 and 8.43 vol% of spinel, mainly magnetite; HWI-Al-2, -3, -13 also contained fluorapatite (1.1 to 2.9 vol%).
- A0 through A5 glasses have spinel between 3.4 and 7.3 vol%; A3 and A4 have large fractions of nepheline (>20 vol%) in addition to a sodalite phase [$Na_8(AlSiO_4)_6(MnO_4)_2$].
- A0 through A5 glasses contained between 3.4 and 7.3 vol% spinel; A3 and A4 contained >20 vol% nepheline in addition to a sodalite phase [identified as $Na_8(AlSiO_4)_6(MnO_4)_2$].
- All EM09-Li20m-B-# glasses except -04 contained spinel (3.7 to 11.2 vol%); most contained a lithium aluminosilicate phase (probably eucryptite) (4.6 to 44.5 vol%). EM09-Li20m-B-04 was amorphous, and EM09-Li20m-B-09 and 10 contained only spinel.
- NE3-# glasses contained various combinations of nepheline (5.6 to 43.5 vol%), spinel (0.4 to 16.5 vol%), and lithium silicate (Li_2SiO_3) (1.9 to 47.8 vol%) phases, with the exception of NE3-09 and 12, which are amorphous.
- NP2-# glasses primarily contained nepheline (7.2 to 39.4 vol%), sometimes spinel or Li_2SiO_3, and rarely other phases; NP2-03, -14, and -22 were amorphous.

Table 3.1. X-Ray Diffraction Data for CCC Heat-Treated Glasses Made at PNNL (HLWE-ANa-# and HLWE-ANa-#(X)

GLASS ID	Nepheline		Spinel		Fluorapatite	
	Vol%	Structure	Vol%	Structure	Vol%	Structure
HLWE-ANa-4	27.8	$Na_{7.11}(Al_{7.2}Si_{8.8}O_{32})$	2.9	Fe_3O_4		
HLWE-ANa-5	50.7	$Na_{7.11}(Al_{7.2}Si_{8.8}O_{32})$	4.2	$NiFe_2O_4$		
HLWE-ANa-5(2Al-2Si)	33.8	$K_{0.25}Na_6A_{l6.24}Si_{9.76}O_{32}$	5.2	Fe_3O_4		
HLWE-ANa-5(3Al-3Si)	36.1	$Na_{5.47}K_{1.40}\ Ca_{.30}Al_{7.47}\ Si_{8.53}$	10.5	$(Zn_{0.3}Al_{0.7})Al_{1.7}\ O_4$		
HLWE-ANa-5(2Al+1B-3Si)	44.4	$Na_{7.11}(Al_{7.2}Si_{8.8}O_{32})$	4.0	$NiFe_2O_4$		
HLWE-ANa-5(1.5Al+2B-3.5Si)	44.0	$Na_{7.11}(Al_{7.2}Si_{8.8}O_{32})$	4.9	$NiFe_2O_4$		
HLWE-ANa-5(2Al+1.5B-3.5Si)	13.9	$Na_{6.65}(A_{l6.24}Si_{9.76}O_{32})$	6.3	$LiFe_3Cr_2O_8$		
HLWE-ANa-5(2Al+1.5B+1Na-4.5Si)	41.7	$Na_{7.11}(Al_{7.2}Si_{8.8}O_{32})$	3.8	$NiFe_2O_4$		
HLWE-ANa-9	43.1	$Na_{6.8}(Al_{6.3}Si_{9.7}O_{32})$				
HLWE-ANa-9(0.5B -0.5Li)	31.2	$Na_{6.65}(A_{l6.24}Si_{9.76}O_{32})$				
HLWE-ANa-9(1.0B, -1.0Li)	42.7	$Na_{6.65}(A_{l6.24}Si_{9.76}O_{32})$				
HLWE-ANa-10	38.1	$Na_6K_{1.2}A_{l7.2}Si_{8.8}O_{32}$	0.8 5.0	$NiFe_2O_4$ Fe_3O_4		
HLWE-ANa-10(0.5B-0.5Li)			4.0	$NiFe_2O_4$		
HLWE-ANa-10(1.0B-1.0Li)			4.6	Fe_3O_4		
HLWE-ANa-10(1.5B-1.5Li)			3.5	Fe_3O_4		
HLWE-ANa-11	48.3	$Na_{7.11}(Al_{7.2}Si_{8.8}O_{32})$	4.4	Fe_3O_4		
HLWE-ANa-11(0.5B-0.5Li)	41.7	$K_{0.25}Na_6Al_{6.24}Si_{9.76}O_{32}$	4.0	Fe_3O_4		
HLWE-ANa-11(1.0B-1.0Li)	38.3	$Na_{6.65}(A_{l6.24}Si_{9.76}O_{32})$	3.9	Fe_3O_4		
HLWE-ANa-11(1.5B-1.5Li)	38.3	$Na_{6.8}(Al_{6.3}Si_{9.7}O_{32})$	4.0	$NiFe_2O_4$		
HLWE-ANa-11(2B-2Li)	34.6	$Na_{6.65}(A_{l6.24}Si_{9.76}O_{32})$	4.1	Fe_3O_4		
HLWE-ANa-13	36.5	$Na_{7.11}(Al_{7.2}Si_{8.8}O_{32})$	1.4	Fe_3O_4	3.3	$Ca_{5.061}(P_{2.87}O_{11.46})F_{0.89}$
HLWE-ANa-13(1.0Li-1.0Si)	36.0	$Na_{7.11}(Al_{7.2}Si_{8.8}O_{32})$	1.5	Fe_3O_4	2.9	$Ca_{5.061}(P_{2.87}O_{11.46})F_{0.89}$
HLWE-ANa-13(3Al - 3 Si)	38.0	$Na_{7.11}(Al_{7.2}Si_{8.8}O_{32})$	2.5	Fe_3O_4	3.4	$Ca_{5.061}(P_{2.87}O_{11.46})F_{0.89}$
HLWE-ANa-13(3Al+2B-5Si)	39.5	$Na_{7.11}(Al_{7.2}Si_{8.8}O_{32})$	2.9	Fe_3O_4	3.7	$Ca_{5.061}(P_{2.87}O_{11.46})F_{0.89}$
HLWE-ANa-13(1B+1Na+1Al-3Ca)	43.4	$Na_{7.11}(Al_{7.2}Si_{8.8}O_{32})$	2.5	Fe_3O_4	3.6	$Ca_{5.061}(P_{2.87}O_{11.46})F_{0.89}$
HLWE-ANa-13(2Na-2Ca)	40.4	$Na_{7.11}(Al_{7.2}Si_{8.8}O_{32})$	0.8	Fe_3O_4	2.7	$Ca_{5.061}(P_{2.87}O_{11.46})F_{0.89}$
HLWE-ANa-14	34.6	$Na_{7.11}(Al_{7.2}Si_{8.8}O_{32})$	3.2	Fe_3O_4	3.7	$Ca_{5.061}(P_{2.87}O_{11.46})F_{0.89}$
HLWE-ANa-15	21.5	$Na_{6.65}(A_{l6.24}Si_{9.76}O_{32})$	2.5	Fe_3O_4	5.0	$Ca_{5.061}(P_{2.87}O_{11.46})F_{0.89}$
HLWE-ANa-15(1Li-1Na)	47.9	$Na_{6.8}(Al_{6.3}Si_{9.7}O_{32})$	3.5	Fe_3O_4	3.9	$Ca_{5.061}(P_{2.87}O_{11.46})F_{0.89}$
HLWE-ANa-16	46.5	$K_{.03}\ Ca_{.05}\ Na_{7.30}\ Al_{7.48}\ Fe_{.03}\ S$	3.8	$MgAl_{.6}Fe_{1.4}O_4$	3.7	$Ca_{5.164}\ (P_{2.892}\ O_{11.523})\ F_{0.959}$
HLWE-ANa-16(2.0B-2.0Ca)	36.3	$Na_{6.3}\ (Al_{6.3}\ Si_{9.7}\ O_{32})$	3.4	Fe_3O_4	3.3	$Ca_5\ (P\ O_4)_3\ F$
HLWE-ANa-16(1.0Mg-1.0Ca)	43.5	$Na_{6.3}\ (Al_{6.3}\ Si_{9.7}\ O_{32})$	3.7	Fe_3O_4	3.1	$Ca_{5.061}(P_{2.87}O_{11.46})F_{0.89}$
HLWE-ANa-16(2.0Mg-2.0Ca)	49.4	$Na_{6.3}\ (Al_{6.3}\ Si_{9.7}\ O_{32})$	4.6	Fe_3O_4	2.9	$Ca_5\ (PO_4)_3\ F$
HLWE-ANa-24			1.7	Fe_3O_4		
HLWE-ANa-25	28.7	$Na_{6.8}(Al_{6.3}Si_{9.7}O_{32})$	2.9	Fe_2O_3		
HLWE-ANa-26	13.7	$Na_{7.11}(Al_{7.2}Si_{8.8}O_{32})$	3.7	Fe_3O_4		

Table 3.2. X-Ray Diffraction Data for CCC Heat-Treated Glasses Made at PNNL (PNNL-AL-24-#) and at VSL (HLWE-AL-#)

GLASS ID	Nepheline		Spinel		Fluorapatite		Silicate		Other	
	Vol%	Structure	Vol%	Structure	Vol%	Structure	Vol%	Structure	Vol%	Structure
PNNL-AL-24-1			1.2	Fe_3O_4						
PNNL-AL-24-4			1.3	Fe_3O_4						
PNNL-AL-24-6			1.6	Fe_3O_4						
PNNL-AL-24-11			1.6	Fe_3O_4						
PNNL-AL-24-12			0.8	Fe_3O_4						
PNNL-AL-24-13			1.4	Fe_3O_4						
PNNL-AL-24-16			1.3	Fe_3O_4						
PNNL-AL-24-18			1.7	Fe_3O_4						
PNNL-AL-24-19			1.7	Fe_3O_4						
PNNL-AL-24-22			1.2	Fe_3O_4						
PNNL-AL-24-28			1.9	Fe_3O_4						
PNNL-AL-24-53			1.9	Fe_3O_4						
PNNL-AL-24-63			1.4	Fe_3O_4						
HLWE-Al-03			6.6	$NiFe_2O_4$						
HLWE-Al-08					2.5	$Ca_5(PO_4)_3F$			21.5	Fe_2O_3
HLWE-Al-09			7.9	$(Fe_{0.793}Al_{0.207})(Al_{1.793}Fe_{0.207})O_4$						
HLWE-Al-10			9.6	$(Fe_{0.793}Al_{0.207})(Al_{1.793}Fe_{0.207})O_4$						
HLWE-Al-14			15.0	Fe_3O_4						
HLWE-Al-15			9.6	$LiFe_3CrO_8$			1.1	$(Li_2Al_2Si_3O_{10})_{.6}$		
HLWE-Al-16			11.0	Fe_3O_4	`					
HLWE-Al-17			12.7 17.3	$(Fe_{0.878}Al_{0.122})(Al_{1.878}Fe_{0.122})O_4$ Al_2MgO_4			2.4	$(LiAlSiO_4)_{.5}$		
HLWE-Al-23	43.5	$Na_{6.3}(Al_{6.3}Si_{9.7}O_{32})$	9.2	Fe_3O_4						
HLWE-Al-24			0.6	Fe_3O_4						
HLWE-Al-25			6.3	Fe_3O_4						
HLWE-Al-26			6.6	Fe_3O_4						
HLWE-Al-27			6.1	Fe_3O_4						
HLWE-Al-29			0.6	Fe_3O_4						

Table 3.3. X-Ray Diffraction Data for CCC Heat-Treated Glasses Made at PNNL (various) and at VSL (HWI-Al-#)

GLASS ID	Nepheline		Spinel		Fluorapatite		Silicate		Other	
	Vol%	Structure	Vol%	Structure	Vol%	Structure	Vol%	Structure	Vol%	Structure
HWI-Al-2			6.2	Fe_3O_4	1.1	$Ca_5(PO_4)_3F$				
HWI-Al-3			4.1	Fe_3O_4	2.9	$Ca_5(PO_4)_3F$				
HWI-Al-4			6.1	Fe_3O_4+ Chromite						
HWI-Al-6			5.2	Fe_3O_4						
HWI-Al-10			4.2	Fe_3O_4						
HWI-Al-11			7.0	Fe_3O_4						
HWI-Al-12			7.4	Fe_3O_4						
HWI-Al-14			8.4	Fe_3O_4	2.8	$Ca_5(PO_4)_3F$				
HWI-Al-20			4.6	Fe_3O_4						
A0			7.3	Fe_3O_4						
A1			4.6	Fe_3O_4						
A2			4.5	Fe_3O_4						
A3	26.5	$NaAlSiO_4$	3.4	$MgAl_{.8}Fe_{1.2}O_4$			0.9	$Na_8(AlSiO_4)_6(MnO_4)_2$		
A4	20.8	$NaAlSiO_4$	5.4	$MgAl_{.8}Fe_{1.2}O_4$			1.4	$Na_8(AlSiO_4)_6(MnO_4)_2$		
A5			4.8	Fe_3O_4						
EM09-Li20m-B-04									100	Amorphous
EM09-Li20m-B-09			7.0	Fe_3O_4						
EM09-Li20m-B-10			3.7	Fe_3O_4						
EM09-Li20m-B-16			8.9	Fe_3O_4			32.2	$(Li_2Al_2Si_3O_{10})_{.6}$		
EM09-Li20m-B-26			8.3	Fe_3O_4			44.5	$Li_{0.9}AlSiO_4$		
EM09-Li20m-B-29			6.1	Fe_3O_4			28.9	$Li_{0.9}AlSiO_4$		
EM09-Li20m-B-34			3.6	Fe_3O_4			5.6	$(Li_2Al_2Si_3O_{10})_{.6}$		
EM09-Li20m-B-38			11.2	Fe_3O_4			4.6	$(Li_2Al_2Si_3O_{10})_{.6}$		
EM09-Ca20m-B			4.7	$NiFe_2O_4$			46.0	$CaAl_2Si_2O_8$		
EM09-Mg20m-B			22.3	$MgAl_2O_4$						
HLW-ALG-27	33.8	$Na_{6.65}Al_{6.24}Si_{9.76}O_{32}$							3.0	Fe_2O_3
DZr-CV-2									100	Amorphous
DZr-CV-4									100	Amorphous
DZr-CV-20									100	Amorphous
DZr-CV-21							9.9	$Na_8Al_6Si_6O_{24}SO_4$		

Table 3.4. X-Ray Diffraction Data for CCC Heat-Treated Glasses Made and Heat-Treated at SRNL (NE3)

GLASS ID	Nepheline		Spinel		Silicate		Other	
	Vol%	Structure	Vol%	Structure	Vol%	Structure	Vol%	Structure
NE3_01			13.3	$NiFe_2O_4$				
NE3_03							100	Amorphous
NE3_04	5.6	$Na_{2.8}K_{.6}Ca_{.2}Al_{3.8}Si_{4.2}O_{16}$						
NE3_06			10.6	Fe_3O_4				
NE3_07			13.6	Fe_3O_4				
NE3_08			0.8	$NiFe_2O_4$				
NE3_09							100	Amorphous
NE3_10	21.7	$Na_{6.8}(Al_{6.3}Si_{9.7}O_{32})$			1.9	Li_2SiO_3	5.2	Fe_2O_3
NE3_11	9.2	$K_{0.24}Na_{6.00}Al_{6.24}Si_{9.76}O_{32}$	11.1	$Fe_{.99}Fe_{1.97}Cr_{.03}N_{i.01}O_4$	2.1	Li_2SiO_3		
NE3_12							100	Amorphous
NE3_13	43.6	$Na_{6.8}(Al_{6.3}Si_{9.7}O_{32})$	10.4	$NiFe_2O_4$	14.6	Li_2SiO_3		
NE3_14	37.1	$Na_{6.8}(Al_{6.3}Si_{9.7}O_{32})$	10.6	$NiFe_2O_4$	14.0	Li_2SiO_3		
NE3_21	32.1	$Na_6K_{1.2}Al_{7.1}Si_{.9}O_{32}$	8.9	Fe_3O_4	14.5	Li_2SiO_3		
NE3_24	19.0	$Na_{7.11}(Al_{7.2}Si_{8.8}O_{32})$						
NE3_25	30.6	$Na_{6.8}(Al_{6.3}Si_{9.7}O_{32})$	5.8	Fe_3O_4	12.6	Li_2SiO_3		
NE3_26	30.2	$Na_6K_{1.2}Al_{7.1}Si_{8.9}O_{32}$	5.7	Fe_3O_4	12.4	Li_2SiO_3		
NE3_27	40.9	$Na_{6.8}(Al_{6.3}Si_{9.7}O_{32})$	16.5	$MgFe_2O_4$	17.8	Li_2SiO_3		
NE3_28			0.4	$NiFe_2O_4$				
NE3_29	45.1	$Na_{7.11}(Al_{7.2}Si_{8.8}O_{32})$	6.2	Fe_3O_4				

Table 3.5. X-Ray Diffraction Data for CCC Heat-Treated Glasses Made and Heat-Treated at SRNL (NP2)

GLASS ID	Nepheline		Spinel		Silicate		Other	
	Vol%	Structure	Vol%	Structure	Vol%	Structure	Vol%	Structure
NP2_03							100	Amorphous
NP2_06	7.2	$Na(AlSiO_4)$	2.1	$Ni(Fe_2O_4)$				
NP2_11	27.2	$Na_{6.8}(Al_{6.3}Si_{9.7}O_{32})$						
NP2_14	18.6	$Na(AlSiO_4)$	7.9	$Ni(Fe_2O_4)$				
NP2_16	39.0	$K_{0.24}Na_{6.00}Al_{6.24}Si_{9.76}O_{32}$			8.3	Li_2SiO_3	11.5	Fe_2O_3
NP2_18	15.8	$K_{0.24}Na_{6.00}Al_{6.24}Si_{9.76}O_{32}$			11.9	Li_2SiO_3		
NP2_20	26.3	$Na_{6.65}Al_{6.24}Si9.76O32$			10.5	Li_2SiO_3		
NP2_21	39.4	$Na_6K_{1.2}Al_{7.1}Si_{8.9}O_{32}$	4.8	$Li_{.35}\ Zn_{.3}\ Fe_{2.35}\ O_4$	0.7	SiO_2	13.1 8.1	$Ca_2\ Fe_{1.28}\ Al_{0.72}\ O_5$ $Li_{.25}\ Ni_{1.75}\ O_2$
NP2_22							100	Amorphous
NP2_23	4.0	$K_{0.24}Na_{6.00}Al_{6.24}Si_{9.76}O_{32}$						
NP2_24	7.1	$K_{0.24}Na_{6.00}Al_{6.24}Si_{9.76}O_{32}$	10.8	$Ni_{1.43}Fe_{1.7}O_4$				

Table 3.6. PDF Database Identification Numbers used for XRD Phase Identification (JADE 6)

Structure	PDF- #	Structure	PDF- #
$Na_{7.11}(Al_{7.2}Si_{8.8}O_{32})$	63-2072	Fe_2O_3	33-0664
$K_{0.25}Na_6A_{l6.24}Si_{9.76}O_{32}$	70-1260	$(Fe_{0.793}Al_{0.207})(Al_{1.793}Fe_{0.207})O_4$	65-0508
$Na_{6.65}(A_{l6.24}Si_{9.76}O_{32})$	65-4626	$CaAl_2Si_2O_8$	70-0287
$Na_6K_{1.2}A_{l7.2}Si_{8.8}O_{32}$	71-0594	$Na_8(AlSiO_4)_6(MnO_4)_2$	82-1813
$NaAlSiO_4$	76-1558	$MgAl_{.8}Fe_{1.2}O_4$	73-2159
$K_{0.24}Na_{6.00}Al_{6.24}Si_{9.76}O_{32}$	83-2279	$Ca_{5.06}1(P_{2.87}O_{11.46})F_{0.89}$	83-0556
$Na_{6.8}(Al_{6.3}Si_{9.7}O_{32})$	79-0994	$Ca_5\ (P\ O_4)_3\ F$	71-0881
$Na_{2.8}K_{.6}Ca_{.2}Al_{3.8}S_{i4.2}O_{16}$	60-9771	$(Li_2Al_2Si_3O_{10})_{.6}$	73-2335
Fe_3O_4	61-3889	$Li_{0.9}\ Al\ Si\ O_4$	61-5972
$NiFe_2O_4$	61-2928	$Li_{0.9}\ Al\ Si\ O_4$	61-5972
$(Zn_{0.3}\ Al_{0.7})\ Al_{1.7}\ O_4$	61-9741	Li_2SiO_3	83-1517
$MgAl_2O_4$	75-1799	$Na_{8.56}(Al_6Si_6O_{24})(SO_4)_{1.56}$	62-5676
$LiFe_3Cr_2O_8$	60-8143	$Li_2Fe_5Cr_5O_{16}$	73-0213

Data from the XRD analysis were plotted in the ND versus OB quadrant system. All of the datasets described in Appendix A were included in Figure 3.1. All the data appear in the quadrant projection, including those with zero nepheline, so other plots were created filtering the data for all points >1 vol% nepheline. It is apparent from the two-dimensional (2-D) and three-dimensional (3-D) figures that most of the nepheline crystallization occurs for compositions in Quadrant I (Fail ND, Fail OB), while some crystallization does take place in Quadrant IV (Fail ND, Pass OB). Those that crystallize nepheline in Quadrant IV (and nearby in Quadrant I) are all of the HLW-E-ANa or HLW-E-ANa(X) glass series (green diamonds). These have very high Al_2O_3 (>21.3 mass%) and Na_2O (>12.7 mass%) concentrations and typically produce at least 25 vol% nepheline (not another NLAS) with a CCC heat-treatment. For 37 glasses studied in these two series, the average nepheline crystallization was 32.5 vol% with five of these glasses producing no nepheline and two producing <15 vol% nepheline. If it were desired to have a maximum threshold OB value that would not permit any nepheline formation, including all the new data discussed herein, the value would have to be OB=0.555 to account for the behavior in the HLW-E-ANa and HLW-E-ANa(X) series glasses.

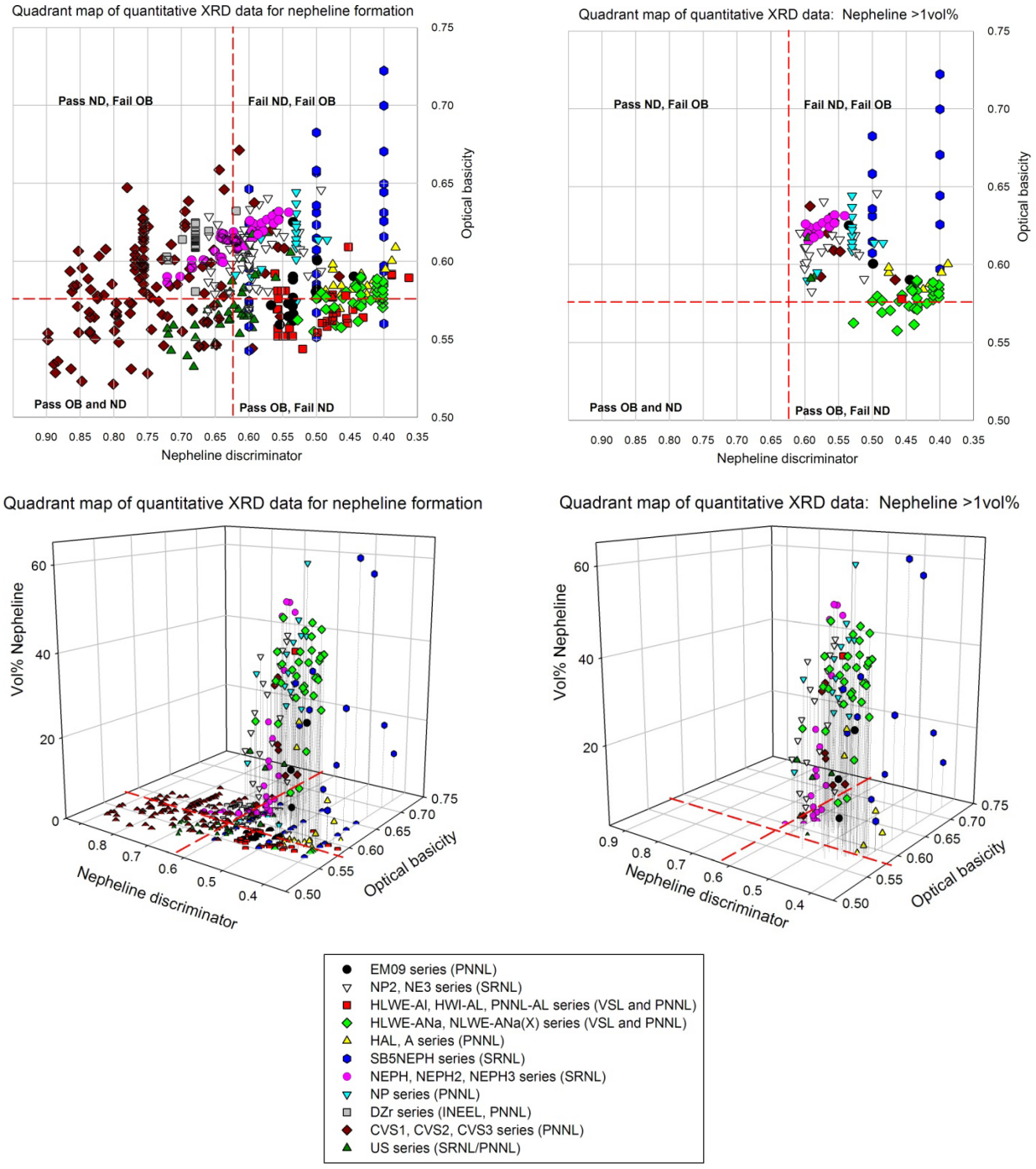

Figure 3.1. ND Versus OB Plot Showing the Composition Locations of Data Sets Studied in this Report and Described in Appendix A. Lines are drawn at the OB = 0.575 and ND = 0.62 threshold values. The figure to the left shows all data, while the figure to the right shows data with nepheline >1 vol%. Figures on the top row are projections, while figures on the bottom row are 3-D depictions of the volume of nepheline precipitation.

3.2 Product Consistency Test (PCT) Analysis

Glasses for PCT were prepared as described previously. Results shown in Table 3.7 are normalized values derived with Equation 3.1 (Hrma et al. 1994):

$$r_i = \frac{c_i}{f_i\left(\frac{A}{V}\right)} \tag{3.1}$$

where r_i = normalized mass release of element i (in g/m^2)
c_i = concentration of element i in solution (in g/m^3)
f_i = mass fraction of element i in the glass
A/V = the glass surface area to solution volume ratio (m^{-1}). An A/V value of 2000 m^{-1} was assumed based on glass mass, solution mass, and particle size range.

Collected data are shown in Table 3.7. Not all glasses were measured in both quenched and CCC configurations. Some glasses were measured only in one or the other condition. This is reflected by blank cells in the table. Additionally, the PCT analysis sets performed at SRNL (applicable to some of the quenched data) did not measure Al release.

Data are also plotted in Figure 3.2 (normalized boron release) and Figure 3.3 (normalized sodium release). From these plots, all quenched glasses tested and all PNNL-AL-# new glasses are under the standard glass (EA) release limits. On the other hand, most of the HLWE-ANa-# and HLWE-ANa-#(X) glasses are above the standard glass release limits for both boron and sodium. These glasses as a group tended to precipitate large amounts of nepheline.

Figure 3.4 shows the natural logarithm of PCT-B (horizontal-axis) versus PCT-Na (vertical-axis) for the quenched and CCC measurements. For the most part, the dissolution of B and Na from the glasses is similar and shows little systematic difference between quenched and CCC series.

Figure 3.5 shows the natural logarithm of quenched PCT-B (horizontal-axis) versus CCC PCT-B (vertical-axis) for those glasses in this study where both quenched and CCC data are available. Different symbols are used for samples crystallizing nepheline (red circles), eucryptite/spodumene/lithium aluminosilicate (orange diamonds), and no NLAS (green triangles). Similar to the conclusions from Kim et al (1995) and McCloy and Vienna (2010), samples with large amounts of crystallization lie on the upper side of the 1:1 control limit line. This plot emphasizes, then, that other NLAS phases, such as lithium aluminosilicate phases (eucryptite or spodumene) or calcium aluminosilicate phases (anorthite) can also have an adverse effect on CCC PCT. Note that all the nepheline and NLAS points on the graph showed at least 13 vol% NLAS in the XRD data.

Further quantitative correlation is warranted to understand the quantitative relationship between nepheline precipitation and PCT response.

Table 3.7. PCT Normalized Released Data for CCC and Quenched Glasses. (-) Denotes Data Not Measured

	PCT_{CCC} (g/m^2)					PCT_Q (g/m^2)				
Glass ID	**Al**	**B**	**Li**	**Si**	**Na**	**Al**	**B**	**Li**	**Si**	**Na**
ARM	-	-		-	-	-	0.833	0.262	0.060	0.240
EA	0.042	8.508	4.561	2.253	6.574	-	-	-	-	-
EM09-Ca20m-B	0.093	1.862	1.758	0.006	0.937	-	0.081	0.453	0.010	0.131
EM09-Li20m-B-4	0.472	2.439	2.049	0.426	1.412		2.714	2.351	0.230	1.646
EM09-Li20m-B-16	-	-	-	-	-	0.137	0.205	0.288	0.305	0.018
EM09-Li20m-B-26	0.223	16.846	3.148	0.063	9.315		0.318	0.324	0.094	0.093
EM09-Li20m-B-29	0.117	12.529	2.985	0.066	7.688	0.223	0.259	0.342	0.220	0.091
EM09-Li20m-B-38	0.225	4.853	1.396	0.085	1.073	-	-	-	-	-
HLWE-AL-3	0.117	2.137	29.399	0.149	1.456	-	-	-	-	-
HLWE-AL-17	0.252	1.819	1.745	0.109	1.693	-	-	-	-	-
ALWE-AL-23	0.290	31.200	19.867	0.070	6.510	-		-	-	-
HLWE-AL-24	0.169	0.472	0.482	0.161	0.352	0.126	0.714	0.558	0.134	0.252
HLWE-AL-26	0.180	0.737	0.666	0.192	0.468	0.188	0.638	0.597	0.183	0.410
HLWE-AL-27	0.068	0.097	0.156	0.066	0.100	-				
PNNL-AL-24-1	0.137	0.707	0.647	0.141	0.372	-	0.592	0.549	0.061	0.319
PNNL-AL-24-4	-	-	-	-	-	-	3.948	2.992	0.039	1.665
PNNL-AL-24-12	0.128	0.668	0.596	0.134	0.316	-	0.724	0.623	0.062	0.333
PNNL-AL-24-13	-	-	-	-	-	-	1.642	1.234	0.047	0.682
PNNL-AL-24-18	0.100	2.272	1.722	0.100	1.000	-	-	-	-	-
PNNL_AL-24-22	0.097	5.194	3.888	0.093	2.145	-	-	-	-	-
PNNL_AL-24-28	-	-	-	-	-	-	0.520	0.506	0.071	0.292
PNNL-AL-24-33	0.137	0.201	0.304	0.141	0.146	-	-	-	-	-
PNNL-AL-24-41	0.092	3.000	2.219	0.093	1.161	0.089	2.963	2.296	0.091	1.192
PNNL-AL-24-53	0.140	0.179	0.287	0.148	0.127	0.147	0.206	0.338	0.150	0.133
PNNL-AL-24-65	0.121	0.478	0.407	0.142	0.321	-	0.291	0.207	0.062	0.238
HLWE-ANa-4	0.215	14.004	7.782	0.066	3.330	-	0.246	0.296	0.250	0.064
HLWE-ANa-9(0.5B-.5Li)	-	-	-	-	-	0.372	1.110	0.868	0.183	0.761
HLWE-ANa-10	0.107	38.683	16.219	0.038	11.896	0.283	1.050	0.836	0.177	0.709
HLWE-ANa-11	0.029	32.462	23.048	0.015	7.042		0.926	0.713	0.098	0.730
HLWE-ANa-13	0.151	19.046	18.660	0.059	4.391	0.086	0.140	0.198	0.081	0.167
HLWE-ANa-13(3Al+2B-5Si)	0.103	34.618	32.323	0.018	9.704	-	-	-	-	-
HLWE-ANa-15	0.480	13.477	10.763	0.025	4.420	-	0.207	0.216	0.040	0.210
HLWE-ANA-16	-	-	-	-	-	-	0.302	0.285	0.124	0.159
HLWE-ANa-16(2Mg-2Ca)	0.068	43.461	43.291	0.025	8.389	-	-	-	-	-
HLWE-ANA-25	0.288	26.985	13.174	0.075	8.674	-	1.406	1.113	0.068	0.799
HLWE-ANa-26	0.278	16.921	8.421	0.070	6.471	0.156	1.468	1.171	0.147	0.844

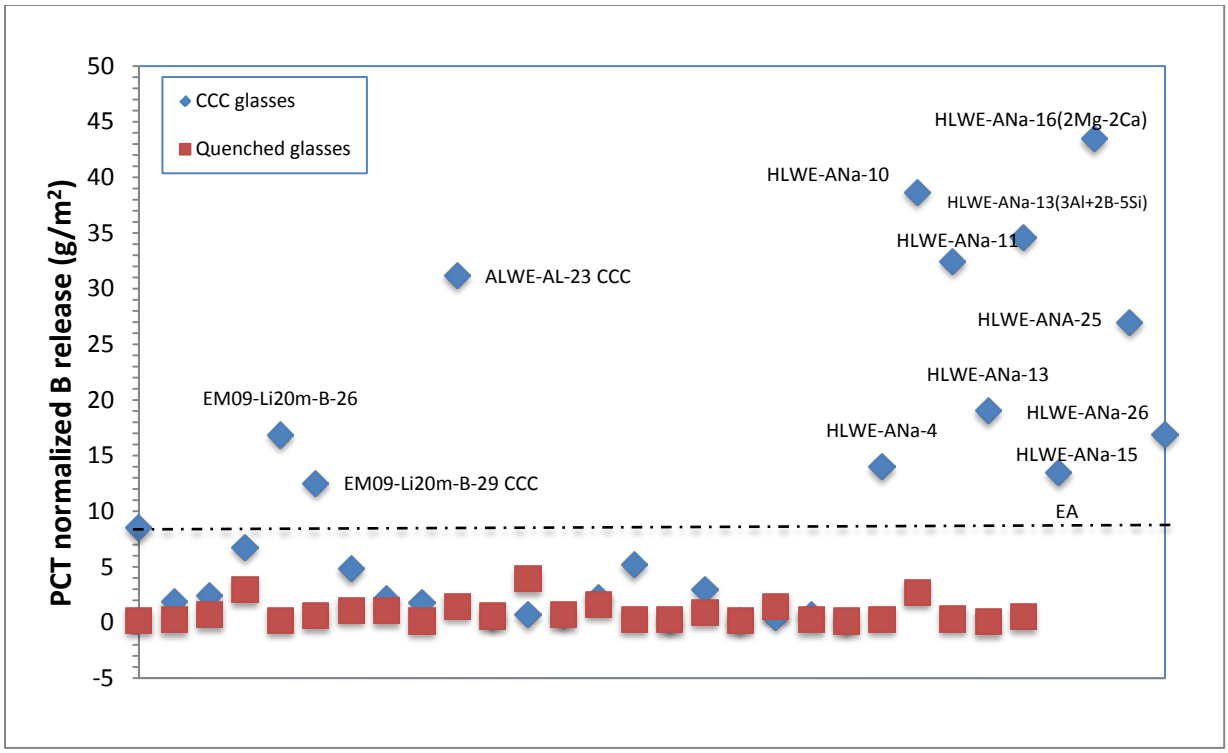

Figure 3.2. Plot of Normalized Boron Release Data for Quench and CCC Heat-Treated Glasses

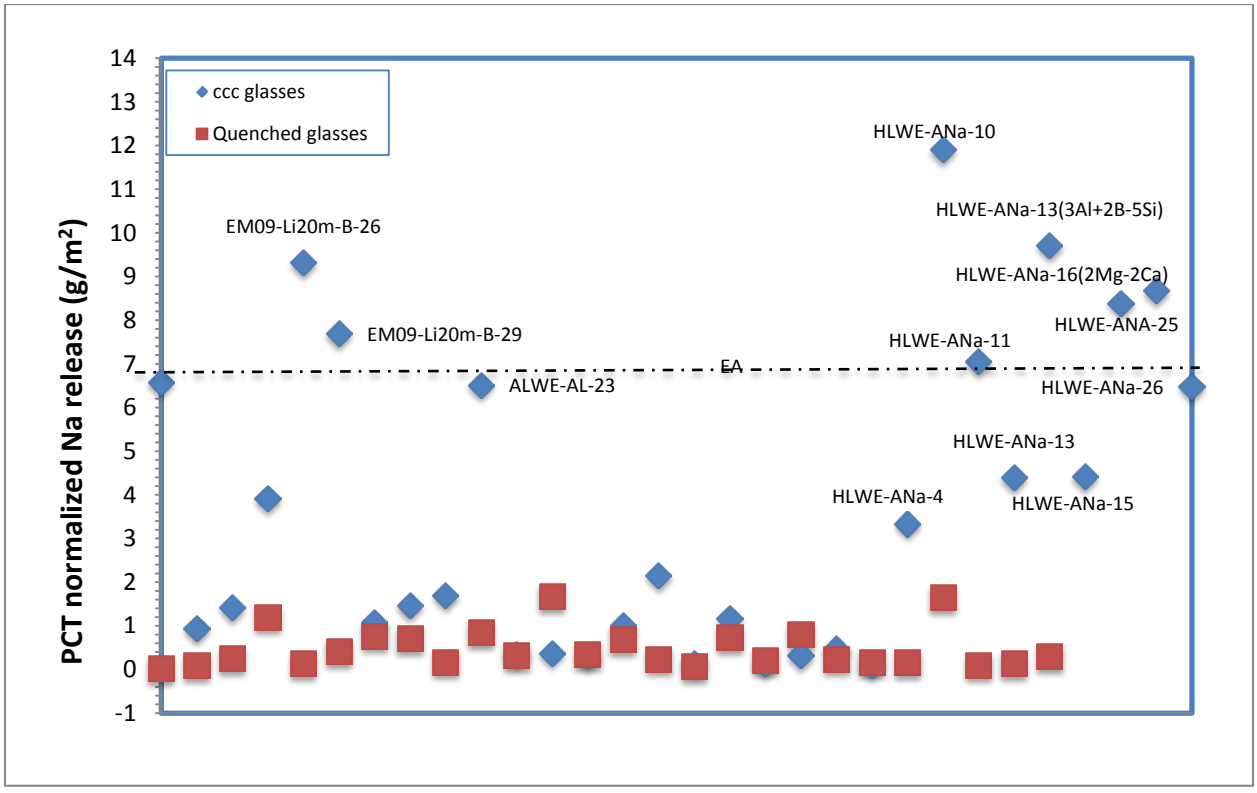

Figure 3.3. Plot of Normalized Sodium Release Data for Quench and CCC Heat-Treated Glasses

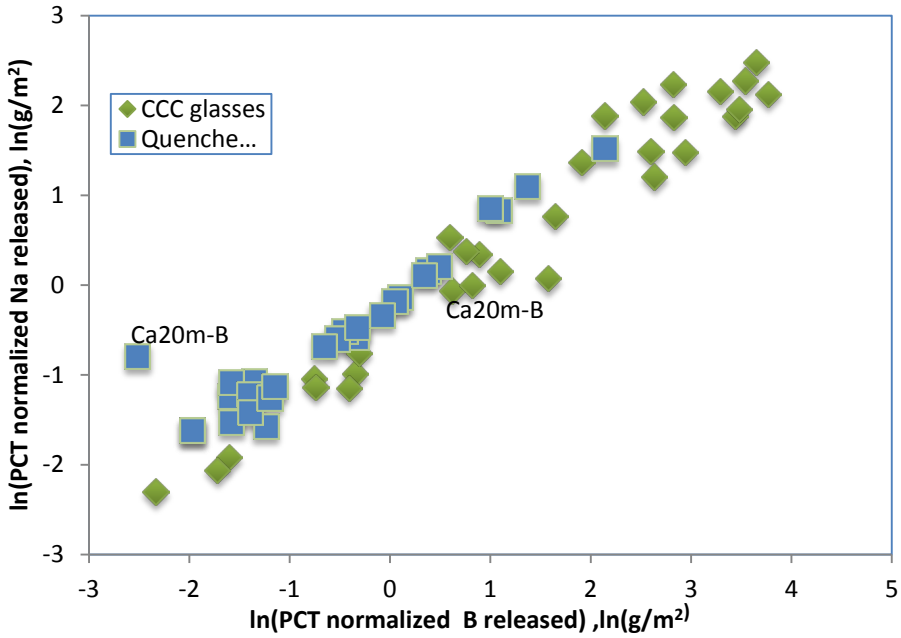

Figure 3.4. Ln-Ln Plot for Na and B Normalized Release for Quenched and CCC Glasses

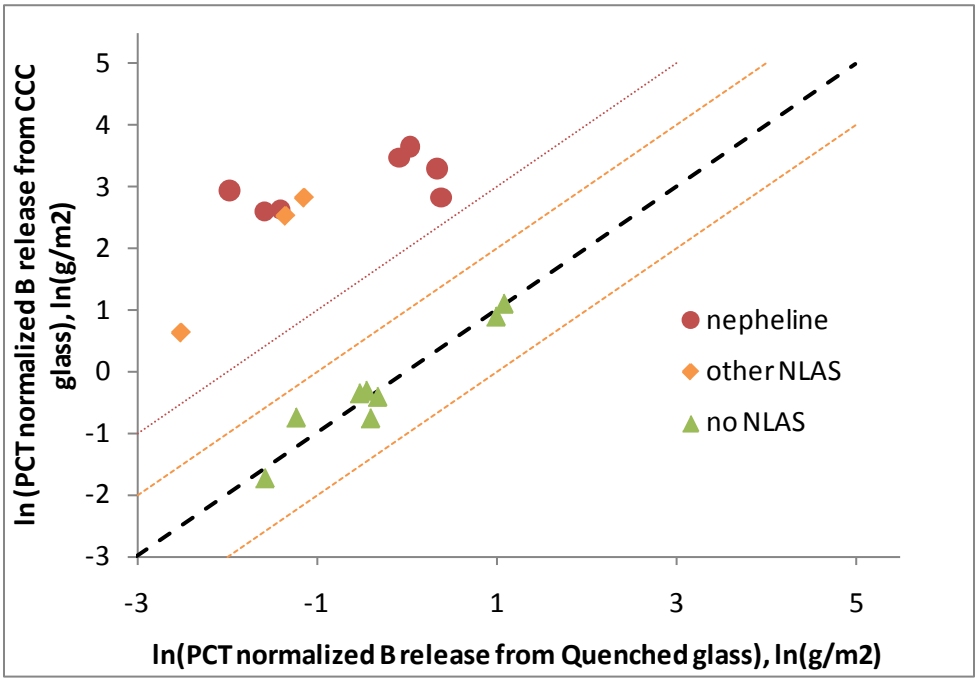

Figure 3.5. Ln-Ln Plot for Quenched Versus CCC Normalized B Release Emphasizing Crystallization Effects on CCC PCT

4.0 Conclusions

The purpose of this study was to find compositions that increase waste loading of high-alumina wastes beyond what is currently acceptable while avoiding crystallization of nepheline ($NaAlSiO_4$) on slow cooling. It was hypothesized that there would be some composition regions where high-alumina would not result in nepheline crystal production.

Sixty-eight glasses were made. About half of the glasses were used to fill the data gaps, and the remaining glasses were used to determine nepheline inhibition. Figure 3.1 shows as red squares the PNNL-AL-24 series that filled in a composition region previously that had little data. The PNNL-Al-24 glass series showed no nepheline formation. Note that adding EM09-Li20m-B glasses shown in Figure 3.2 as dark circles also helped fill in this region. Additional study of this region would also help better understand the growth of nepheline and its limits.

HLWE-ANa and HLWE-ANa(X) glasses shown in Figure 3.1 as green circles were an attempt to diminish nepheline formation by adjusting Na, Li, B, Al, and Si. Adjustments in composition were minor and showed minor changes in nepheline formation. It was anticipated that a greater impact on nepheline formation would be observed.

The introduction of the OB concept as a means of describing a glass composition has continued to proved useful. We have generated a large amount of quantitative XRD data to test the previously suggested OB = 0.575 constraint. There continues to be a small subset of compositions that does indeed crystallize nepheline at OB values below the constraint (i.e., in Quadrant IV), but these seem to be limited to one family of glasses, those based on HLW-E-ANa and its derivatives HLW-E-ANa(X). Changing the OB constraint to 0.555 would shift these glasses to Quadrant I where the other nepheline-prone glasses predominate. There were a few glasses in this family that did not have a problem with nepheline formation, and we will continue to attempt to understand what sets these apart. With this exception, all other nepheline precipitation seems to occur in Quadrant I.

This study differed somewhat from the previous one (McCloy and Vienna 2010) in that we considered only those crystalline phases that could be strictly assigned to nepheline. It was found, however, that PCT was compromised when other NLAS phases (eucryptite, spodumene, anorthite) precipitated. It is therefore important to continue to understand not only nepheline precipitation, but also all alkali and possibly alkaline earth aluminosilicate precipitation in HLW glasses. While the glass precipitating calcium NLAS had a composition lying in Quadrant I, the glasses precipitating lithium NLAS had compositions lying in Quadrant IV.

5.0 References

ASTM. 2008. *Standard Test Methods for Determining Chemical Durability of Nuclear, Hazardous, and Mixed Waste Glasses and Multiphase Glass Ceramics: The Product Consistency Test (PCT)*. ASTM Committee C26 on Nuclear Fuel Cycle.

Edwards TB. 2006. *SME Acceptability Determination for DWPF Process Control (U).* WSRC TR-95-00364 Revision 5, Savannah River National Laboratory, Aiken, South Carolina.

Fox KM, JD Newell, TB Edwards, DR Best, IA Reamer, and RJ Workman. 2007. *Refinement of the Nepheline Discriminator: Results of a Phase I Study*, WSRC-STI-2007-00659 Revision 0, Savannah River National Laboratory, Aiken, South Carolina.

Fox KM and TB Edwards. 2008. *Refinement of the Nepheline Discriminator: Results of a Phase II Study*, SRNS-STI-2008-00099 Revision 0, Savannah River National Laboratory, Aiken, South Carolina.

Fox KM, TB Edwards, and DK Peeler. 2008 "Control of Nepheline Crystallization in Nuclear Waste Glass." *Int. J. Appl. Ceram. Technol*. 5(6):666-673.

Fox KM and TB Edwards. 2009. *Experimental Results of the Nepheline Phase III Study.* SRNL STI-2009-00608, Savannah River National Laboratory, Aiken, South Carolina.

Hrma P, GF Piepel, MJ Schweiger, DE Smith, DS Kim, PE Redgate, JD Vienna, CA LoPresti, DB Simpson, DK Peeler, and MH Langowski. 1994. *Property/Composition Relationships for Hanford High-Level Waste Glasses Melting at 1150ºC.* PNL-10359, Pacific Northwest Laboratory, Richland, Washington.

Hrma P, MJ Schweiger, CJ Humrickhouse, JA Moody, RM Tate, TT Rainsdon, NE TeGrotenhuis, BM Arrigoni, J Marcial, CP Rodriguez, and BH Tincher. 2010. "Effect of glass batch makeup on the melting process." *Ceramics-Silikaty* 54:193-211.

Jantzen CM, NE Bibler, DC Beam, CL Crawford, and MA Pickett. 1993. *Characterization of the Defense Waste Processing Facility (DWPF) Environmental Assessment (EA) Glass Standard Reference Materials (U)*. WSRC-TR-92-346, Rev. 1, Westinghouse Savannah River Company, Savannah River Site, Aiken, South Carolina.

Kim DS, DK Peeler, and P Hrma. 1995. "Effect of Crystallization on the Chemical Durability of Simulated Nuclear Waste Glasses," In *Ceramic Transactions* 61*, Environmental Issues and Waste Management Technologies*, American Ceramic Society, Westerville, Ohio, 177-185.

Li H, JD Vienna, P Hrma, DE Smith, and MJ Schweiger. 1997. "Nepheline Precipitation in High-level waste glasses: compositional effects and impact on the waste form acceptability." In *Materials Research Society Vol. 465 Scientific Basis for Nuclear Waste management XX*, Materials Research Society. Pittsburgh, Pennsylvania,:261-268. Materials Research Society.

Li H, P Hrma, JD Vienna, M Qian, Y Su, and DE Smith. 2003. "Effects of Al_2O_3, B_2O_3, Na_2O, and SiO_2 on nepheline formation in borosilicate glasses: chemical and physical correlations." *Journal of Non-Crystalline Solids* 331(1-3):202-216.

Marra JC and CM Jantzen. 1993. *Characterization of projected DWPF glasses heat treated to simulate canister centerline cooling*. WSRC-TR-92-142, rev 1, Westinghouse Savannah River Company, Aiken, South Carolina.

Matlack KS, H Gan, M Chaudhuri, W Kot, W Gong, T Bardakci, IL Pegg, and I Joseph. 2008. *Melt Rate Enhancement for High Aluminum HLW Glass Formulations.* VSL-089R1360-1, Vitreous State Laboratory, the Catholic University of America, Washington, D.C.

Matlack KS, H Gan, W Gong, IL Pegg, CC Chapman, and I Joseph. 2007. *High Level Waste Vitrification System Improvements*. VSL-07R1010-1, Vitreous State Laboratory, the Catholic University of America, Washington, D.C.

McCloy J and JD Vienna. 2010. *Glass Composition Constraint Recommendations for Use in Life-Cycle Mission Modeling*. PNNL-19372, Pacific Northwest National Laboratory, Richland, Washington.

McCloy JS, C Rodriguez, C Windisch, C Leslie, MJ Schweiger, BJ Riley, and JD Vienna. 2010. "Alkali/ Alkaline-Earth Content Effects of Properties of High-Alumina Nuclear Waste Glasses," In *Ceramic Transactions*, 222, *Advances in Materials Science for Environmental and Nuclear Technology*, ed K.M. Fox et al., John Wiley & Sons, Hoboken, New Jersey, pp. 63-76.

Mellinger GB and JL Daniel. 1984. *Approved Reference and Testing Materials for Use in Nuclear Waste Management Research and Development.* PNL-4955-2, Pacific Northwest Laboratory, Richland, Washington.

National Research Council, Committee on Long-Term Research Needs for Radioactive High Level Waste at Department of Energy Sites. 2001. *Research Needs for High-Level Waste Stored in Tanks and Bins at U.S. Department of Energy Sites*. National Academy Press, Washington, D.C.

Riley BJ, JA Rosaria, and P Hrma. 2001. *Impact of HLW Glass Crystallinity on PCT Response.* PNNL-13491, Pacific Northwest National Laboratory, Richland, Washington.

Vienna JD and DS Kim. 2008. *Preliminary IHLW Formulation Algorithm Description*. 24590- HLW-RPT-RT-05-001, Rev 0, River Projection Project, Waste Treatment Plant, Richland, Washington.

Vienna JD, A Fluegel, DS Kim, and P Hrma. 2009. *Glass Property Data and Models for Estimating High-Level Waste Glass Volume.* PNNL-18501, Pacific Northwest National Laboratory, Richland, Washington.

Appendix A

Critical Assessment of Existing Database

Appendix A: Critical Assessment of Existing Database

Table A.1 summarizes the critically assessed data sets, including the new data described in this report. This data was used in a companion recent publication for assessment of the quantitative formation of nepheline as a function of position optical basicity and position in the Na_2O-SiO_2-Al_2O_3 ternary (McCloy et al. 2011). The table describes the laboratory that made the glasses, the laboratory that performed the heat treatment (and the details of the heat treatment schedule), and the references for the glass compositions and semi-quantitative x-ray crystallization data. Data sets chosen were primarily limited to those whose heat treatments simulated a CCC treatment (Marra and Jantzen 1993), which is a stepped slow cool from high temperature representative of the glass in the interior of a poured canister. There were two exceptions to this requirement. The EM09 data set (McCloy et al. 2010) and the SB5-NEPH data set (Fox et al. 2007) were included because of their extreme compositions, despite having 24-hour isothermal heat treatments at 950°C. These glasses tended to crystallize large amounts of nepheline or other alkali aluminosilicates, so prove to further limit rather than extend the region of acceptable glass compositions. In the following section, the individual data sets used are briefly discussed.

Some datasets had semi-quantitative XRD analysis performed by fitting spectra that did not have internal CaF_2 standards in them. These data were previously unpublished and were separate from the main study of this report. However, it was felt that it would be useful to include the data here for future studies since it is not publically available anywhere else. This semi-quantitative data for SRNL glasses is listed in Table A.2 (NEPH), Table A.3 (NEPH2), and Table A.4 (NEPH3). Table A.5 (SB5-NEPH) is XRD data performed with CaF_2 internal standards, but after a 950°C-24 hour heat treatment. Additionally, some of the glasses from this series were remade at PNNL, and the composition was modified slightly to remove minor components that were not thought to have any influence on nepheline formation. The details of this process are described below under SB5-NEPH, and the glass identification in Table A.5 is modified with a –PNL suffix.

- **NE3 glasses**: All glasses reported by SRNL to contain nepheline (Fox and Edwards 2009) (19 of 29) were obtained from them as CCC samples and XRD'd with CaF_2. Primary crystal phases include nepheline, lithium silicate (Li_2SiO_3), hematite (Fe_2O_3,), and spinels (usually assigned to trevorite ($NiFe_2O_4$), magnetite (Fe_3O_4), and magnesioferrite ($MgFe_2O_4$), but probably more accurately represented as a solid solution $[Mg,Ni,Fe][Fe,Cr]_2O_4$). In a number of cases, qualitative XRD phase identification in previous SRNL work on these glasses did not agree with PNNL's assessment of nepheline for 7 of the 19 samples tested (-03, -06, -07, -08, -09, -12, -28) where SRNL indicated nepheline and PNNL saw none.
- **NP2 glasses**: All glasses reported by SRNL to contain nepheline (Fox and Edwards 2008) (12 of 25) were obtained as CCC samples from them and XRD'd with CaF_2. Primary crystal phases include nepheline, lithium silicate, hematite, cristobalite (SiO_2), and spinels. XRD phase identification in previous SRNL work on these glasses did not agree with PNNL's assessment of nepheline for 3 of the 12 samples tested (-03, -15, -22) where SRNL indicated nepheline and PNNL saw none.
- **HWI-Al glasses**: A subset of VSL glasses in this series (Matlack et al. 2008) (9 of 20) were obtained as quenched glass, heat treated using the WTP-CCC profile at PNNL, and XRD'd with CaF_2. Samples tested were -02, -03, -04, -06, -10, -11, -12, -14, -20. No nepheline was found in any glasses. Previously VSL had reported no nepheline in -07, -09, -13, -16, -18, and -19, so these data

were included as well, bringing the total number of glasses used in this study to 15 out of 20 from this dataset. Primary crystal phases were spinels (chromite ($FeCr_2O_4$) and magnetite).

- **HLW-E-Al glasses**: A subset of VSL glasses in this series (Matlack et al. 2007) (14 of 27) were obtained as quenched glass, heat treated using the WTP-CCC profile at PNNL, and XRD'd with CaF_2. Samples tested were -03, -08, -09, -10, -14, -15, -16, -17, -23, -24, -25, -26, -27, -29. Primary crystal phases included nepheline (-23), lithium aluminum silicate (-15, -17) hematite, and spinels (magnetite, chromite, hercynite ($FeAl_2O_4$), and $Zn(AlFe)O_4$). Only -23 was considered to have nepheline for the purposes of this study, even though -15 and -17 showed substantial crystallization of the lithium aluminosilicate (probably eucryptite).

- **PNNL-24-# glasses**: Thirteen new glasses based on HLW-E-Al-24 (Matlack et al. 2007) were formulated, melted, heat treated, and examined with XRD by PNNL. These glasses are described in this report. These had suffixes of -01, -04, -06, -11, -12, -13, -16, -18, -19, -22, -28, -53, -63. All compositions showed only magnetite. These particular compositions were selected to attempt to fill in gaps in the OB-versus-ND quadrant plot, particularly in Quadrant IV. These glasses are described in detail in the main body of this report.

- **HLW-E-ANa glasses**: These glasses were VSL compositions (Matlack et al. 2007) but were made, heat treated, and XRD'd at PNNL. Glasses investigated were 12 of the 26 compositions, with a 13th (-22) being included as a zero nepheline per VSL data. Glasses made were -04, -05, -09, -10, -11, -13, -14, -15, -16, -24, -25, -26. All except -24 contained substantial amounts of nepheline, 14-51 vol%. Primary crystal phases included nepheline, fluorapatite ($Ca_5(PO_4)_3F$), hematite, and spinels (magnetite, trevorite, Mg Al iron oxide).

- **HLW-E-ANa-#(X) glasses**: Twenty-four new compositions were formulated, fabricated, heat treated, and XRD'd. Samples were based on HLW-E-ANa-05, -09, -10, -11, -13, -15, -16 from VSL (Matlack et al. 2007). These glasses are described in this report. Primary crystalline phases include nepheline, fluorapatite, and spinels (trevorite, magnetite, Zn-Al oxide). All but 2 of the compositions contained at least 13 vol% nepheline, and all but 3 contained over 30 vol% nepheline. These glasses are described in detail in the main body of this report.

- **EM09-Li20m-B-# glasses**: Eight new high Li_2O compositions based on EM09-Li20m-B (McCloy et al. 2010) were formulated, fabricated, heat treated, and XRD'd. These glasses are described in this report. Five of the 8 glasses formed lithium aluminum silicates in amounts from 4 to 45 vol%. The 3 other glasses did not form aluminosilicates. Other phases formed in this series were hematite and magnetite. Only the 3 glasses not forming lithium aluminosilicate were included in this study, in order to maintain integrity of the Na_2O-Al_2O_3-SiO_2 phase diagram and not confound it with the Li_2O phases. These glasses are described in detail in the main body of this report.

- **A glasses**: Five high-Al_2O_3 compositions (Hrma et al. 2010) were fabricated, heat-treated, and XRD'd. Two of these (-03 and -04) formed nepheline (20-26 vol%) and sodalite ($Na_8(AlSiO_4)_6(MnO_4)_2$, 0.5-1.5 vol%) while the rest formed only spinels (magnetite or Mg-Al-Fe oxide). Only the nepheline content was considered here. These glasses are described in detail in the main body of this report.

- **HAL glasses**: Compositions for this high-Al_2O_3 series are published separately for -01 to -18 (Kim et al. 2008) (note: compositions only listed for -01, -03, -04, -09, -11, -12, -17, and -18) and -19 to -25 (note -19 is the same as -17R in this reference) (Marra et al. 2009). Recently the full dataset of these glasses was published (Schweiger et al. 2011). Nepheline fractions for 12 of the 18 in the first series

were previously estimated (Schweiger et al. 2011) based on the diffraction patterns without a CaF_2 internal standard. Only 2 of these (-15 and -16) showed any nepheline, at levels <5 vol%. Nepheline fractions for the second series are published (Marra et al. 2009) and only two of these (-22, -25) formed any nepheline. Most formed spinel.

- **NP glasses**: 20 glasses from a previous study (Li et al. 1997) were included. Quantitative nepheline fractions were already published in the original study, and were converted to vol% for the current study. Three glasses listed (-BL, -Al-3, -Al-4) had large nepheline fractions (>29 wt% of the crystallized glass) and an additional phase identified as $Na(Si_3Al)O_8$ (5-10 wt% of the crystalline phase). Given its similarity to nepheline, we include this phase also in the total for nepheline formation. Various other phases were produced in this series, including lithium silicate, spinels, and other, rarer borate and phosphate phases.
- **NEPH glasses**: Twelve glasses in the SB4-NEPH series (Peeler et al. 2005) from SRNL were previously estimated based on the diffraction patterns without a CaF_2 internal standard. Only 2 formed nepheline-like phases (-01 nepheline and -04 carnegieite, the high temperature form) and were estimated at 1 vol%. These were noted as surface crystals in the original report. Trevorite was noted in one sample.
- **NEPH2 glasses**: Twenty-eight glasses in the NEPH2 series (Peeler et al. 2006) from SRNL were previously estimated based on the diffraction patterns without a CaF_2 internal standard. Of these 28, one (-25) was noted as nepheline "present" but no quantitative estimate was given so this datapoint was not used. The others varied widely from 0-57 vol% nepheline. Other phases noted include lithium silicate and trevorite spinel. Notes from the original study indicate crystallinity is primarily on the surface, with the bulk being either homogeneous or completely devitrified.
- **NEPH3 glasses**: Sixteen glasses in the NEPH3 series (Fox et al. 2006) from SRNL were previously estimated based on the diffraction patterns without a CaF_2 internal standard. Only two compositions were noted to contain nepheline, -44 (3.3 vol%) and -56 (12.7 vol%). The other primary crystalline phase noted was trevorite spinel.
- **DZr-CV glasses**: Twenty-four glasses of compositions previously described (Riley et al. 2001) were considered. Of these, the ones indicated in the previous report to form nepheline (-2), nosean ($Na_8Al_6Si_6O_{24}SO_4$, -2, -4), sodalite (-20), and sodium aluminum silicate sulfide (-21) were remade, heat-treated, and XRD'd. DZr-CV-2 was found to be amorphous, and was replicated twice to be certain, with the same results. Glasses -4 and -20 were also amorphous, but -21 formed 9.87 vol% nosean. Therefore all the glasses in this series were considered as zero nepheline for the purposes of this study. Various other rare phases were reportedly formed in this series including cuspidine [$Ca_4Si_2O_7(F,OH)_2$], fluorapatite, fluorite (CaF_2), and hiordahlite [$(Ca,Na)_3(Zr,Ti)Si_2O_7(O,F)_2$]. This unique mineral assemblage is likely due to the high fluorine content (4-5 wt%) and high CaO content (9-13 wt%) in this series. Similar glasses were produced in another study (Musick et al. 2000) for DZr-S glasses, but no quantitative crystal fraction data was available for that dataset.
- **US glasses**: Forty-five high Al_2O_3 glasses previously described (Fox et al. 2008) were considered. Nepheline fractions for 44 of the 45 were analyzed based on samples from the liquidus measurements with a CaF_2 internal standard. The original report describes nepheline in CCC samples of -18, -25, -27, -37, -42, and -43 made at SRNL. Other phases observed include SiO_2, hematite, spinels (trevorite, magnetite, jacobsite ($MnFe_2O_4$), and mixed spinels with Fe, Mn, Zn). PNNL also made these glasses for liquidus temperature measurements, and noted nepheline in -28 and -42 and nosean

in -28 and -33. Quantitative measurements indicated the following vol% nepehline after CCC treatment: -03 (4.7%), -11 (0.9%), -12 (11.8%+1.05% nosean), -37 (12.5%), -42 (two chemistries of nepheline, one with iron and one with potassium, identified but not quantified), -43 (17.8%). These quantitative numbers were used in this work, while -42 was eliminated due to lack of quantitative data. It is recognized that there are some discrepancies (-25, -26) between what was seen qualitatively on XRD at SRNL and quantitatively at PNNL on the CCC liquidus samples. These probably involved very small amounts of nepheline. However, -42 should be remade at some point and quantified.

- **CVS1 and CVS2 glasses**: There are 23 glasses in CVS1 and 100 in CVS2, nearly all of which have quantitative crystal fractions previously published (Hrma et al. 1994). All glasses except CVS2-53 and -54 (glasses with depleted uranium that never had crystallization identified) were included for this study. Note that glasses CVS2-101 though -123 were also produced, but no crystallization data were collected or published. In the CVS1 series, only -16 formed nepheline (18 vol%). In the CVS2 series, several glasses formed nepheline: -33 (15 vol%), -35 (10 vol% + 7 vol% gehlenite ($Ca_2Al_2SiO_7$)), -63 (15 vol%), -85 (33 vol%), and -96 (5 vol%). Three glasses formed a Li-Al silicate, probably spodumene ($LiAlSi_2O_6$): -68 (8 vol%), -70 (10 vol%), -90 (1 vol%). Many glasses formed pyroxenes (olivine, clinopyroxene, orthopyroxene), some of which remove alkali or alkaline earth, aluminum, and silicon from the network but are not thought to be as detrimental to chemical durability as nepheline (Kim et al. 1995). Various other crystalline phases were noted and have been discussed (Kim et al. 1993).
- **CVS3 glasses**: These glasses were high-melting-temperature glasses previously reported (Vienna et al. 1996). Quantitative XRD data is included in that report. Crystallinity data is available for all 40 glasses except -26, with many different phases being reported. Only -16 contained nepheline (40 wt%) and also contained Li-Al-silicate (45 wt%, either spodumene or eucryptite). Only the nepheline composition was included in the model for this report, with the other compositions having zero nepheline.
- **EM09 glasses**: These glasses were high-Al_2O_3 glasses, whose compositions and crystal fractions were previously reported (McCloy et al. 2010). Heat treatments were not CCC, but 950°C for 24 hours. This data set is included because of the interesting results in substituting alkali (K or Li) or alkaline earths (Ca or Mg) for sodium, either nearly totally (20 mol% of alkali or alkaline earth) or partially (10 mol% of alkali/ alkaline earth + 10 mol% Na_2O). Two additional glasses in this series were made for this current study (data in this report), substituting 20 mol% CaO or MgO in the same manner described in the previous work, except heat treatment was CCC. Suffix "-B" or "+B" referred to the boron/aluminum ratios. The "-B" ratio was found to precipitate nepheline on heat treatment (EM09-Na20m-B, ~28 vol%). The potassium version (K20m-B) precipitated >50 vol% kalsilite ($KAlSiO_4$) on quenching so was not heat-treated. The lithium version (Li20m-B) precipitated >50 vol% eucryptite ($LiAlSiO_4$) on heat treatment. The calcium version (Ca20m-B) precipitated 46 vol% anorthite with CCC, while the magnesium version (Mg20m-B) did not crystallize with CCC. Glasses substituted at 10 mol% formed nepheline (K10m-B, ~15 vol%), labradorite ($Ca_{0.86}Na_{0.14}Al_{1.86}Si_{0.14}Si_2O_8$, Ca10m-B, ~7 vol%), or nothing (Li10m-B, Mg10m-B). For the purposes of this study, glasses precipitating phases other than nepheline are considered as zero. For future investigation of the importance of crystallization of other alkali and alkaline earth aluminosilicates, however, this data set is particularly important.

- **SB5-NEPH glasses**: This series formulated by SRNL was specifically designed to test the nepheline discriminator by fixing the value at 0.6, 0.5, and 0.4 for a series of glasses and adding or subtracting reasonably high levels of B_2O_3 and CaO (Fox et al. 2007). The result was a wide range of crystallization that had not previously been reported, so it is reviewed in some detail below. Qualitative evaluation of crystals was performed by SRNL on quenched and CCC glasses. Quenched glasses were amorphous or had various crystalline phases including spinels (trevorite, magnetite, jacobsite, mixed Fe,Al oxide), bunsenite (NiO), corundum (Al_2O_3), hematite, gregoryite (Na_2CO_3 and its hydrated form thermonatrite), alkaline earth silicates (Ca_2SiO_4), mullite ($Al_{2.4}Si_{0.6}O_{4.8}$), and nepheline (of various stoichiometries: $(Na_2O)_{0.33}NaAlSiO_4$, $Na_{1.55}Al_{1.55}Si_{0.45}O_4$, $NaAlSiO_4$). Glasses heat treated by CCC were amorphous or showed SiO_2, corundum, spinels ($NiAl_2O_4$, hercynite, jacobsite, magnetite, trevorite, mixed Fe,Mn oxide), pyroxenes (aegirine ($NaFeSi_2O_6$)), $NaFeO_2$, borates (tincalconite ($Na_2B_4O_7{\cdot}5H_2O$), borax ($Na_2B_4O_5(OH)_4(H_2O)_8$), CaB_4O_7, $Ca_2B_2O_5$, $Al_4B_2O_9$, $Na_4B_{10}O_{17}$), alkali or alkaline earth silicates (combeite ($Na_4Ca_4Si_6O_{18}$ or $Na_{4.24}Ca_{3.8}Si_6O_{18}$), rankinite ($Ca_3Si_2O_7$), nekoite [$Ca_3Si_6O_{12}(OH)_6{\cdot}5H_2O$], ($Na_{1.74}Mg_{0.865}Si_{1.135}O_4$), ($Na_2SiO_3$), ($Ca_2SiO_4$), alkaline earth aluminates [$Ca_8Al_2Fe_2O_{12}CO_3(OH)_2{\cdot}22H_2O$, $Ca_2Al_2O_5{\cdot}6H_2O$], alkaline earth aluminosilicates [anorthite ($Ca_{0.66}Na_{0.34}Al_{1.66}Si_{2.34}O_8$, $CaAl_2Si_2O_8$), ($Na_3MgAlSi_2O_8$)], and nepheline ($Na_6K_{1.2}A_{l7.2}Si_{8.8}O_{32}$, $Na_{1.67}AlSiO_{4.33}$, $NaAlSiO_4$, $Na_{1.55}Al_{1.55}Si_{0.45}O_4$, $Na_{1.75}Al_{1.75}Si_{0.25}O_4$). Quantitative XRD was performed at PNNL on a subset of these glasses. Glasses investigated by PNNL included all those reported by SRNL to include nepheline. Quenched glass samples received from SRNL included -02, -03, -10, -11, -12, -25, -27, -30, -34, -36, -37, -39. Glasses made at PNNL that were nearly identical compositions but without a few minor components (BaO, CuO, La_2O_3, PbO, ZnO removed and remaining constituents renormalized), included -17, -19, -31, -33, and -35. All the glasses received or processed at PNNL were heat treated at 950°C for 24 hours rather than subjected to CCC heat treatment.

Table A.1. Summary of 523 Glasses Considered in Recent Nepheline Modeling Efforts

Glass family	Glass #s	Produced by	Heat treat by	Ref for glass comp	Ref for Quant XRD	Notes
NE3	01-29	SRNL	SRNL (CCC-DWPF)	(Fox and Edwards 2009)	This work	CaF_2 spiked; measured 19, rest reported as zero
NP2	01-25	SRNL	SRNL (CCC-DWPF)	(Fox and Edwards 2008)	This work	CaF_2 spiked; measured 12, rest reported as zero
HWI-Al	Subset of 15	VSL	PNNL (CCC-WTP)	(Matlack et al. 2008)	This work	CaF_2 spiked
HLW-E-Al	Subset of 14	VSL	PNNL (CCC-WTP)	(Matlack et al. 2007)	This work	CaF_2 spiked
PNNL-Al-24-#	13 total	PNNL	PNNL (CCC-WTP)	This work	This work	CaF_2 spiked
HLW-E-ANa	Subset of 13	VSL (PNNL)	PNNL (CCC-WTP)	(Matlack et al. 2007)	This work	CaF_2 spiked; PNNL made VSL compositions
HLW-E-ANa-#(X)	24 total	PNNL	PNNL (CCC-WTP)	This work	This work	CaF_2 spiked
EM09Li20m-B-#	8 total	PNNL	PNNL (CCC-WTP)	This work; based on (McCloy et al. 2010)	This work	CaF_2 spiked; only 3 glasses not forming Li-Al silicates included
A	0-5	PNNL	PNNL (CCC-WTP)	(Hrma et al. 2010)	This work	CaF_2 spiked
HAL	Subset of 18	PNNL	PNNL (CCC-WTP)	(Kim et al. 2008)	(Schweiger et al. 2011)	Evaluation of unspiked XRD
HAL	19-25	PNNL	PNNL (CCC-WTP)	(Marra et al. 2009)	(Marra et al. 2009)	
NP	20 total	PNNL	PNNL (CCC-WTP)	(Li et al. 1997)	(Li et al. 1997)	
NEPH	1-12	SRNL	SRNL (CCC-DWPF)	(Peeler et al. 2005)	This work	Evaluation of unspiked XRD
NEPH2	13-40	SRNL	SRNL (CCC-DWPF)	(Peeler et al. 2006)	This work	Evaluation of unspiked XRD
NEPH3	41-56	SRNL	SRNL (CCC-DWPF)	(Fox et al. 2006)	This work	Evaluation of unspiked XRD
DZr	24			(Riley et al. 2001)	This work	Remade and CaF_2 quant on 4 comps; rest were zero
US	01-45 (ex)	SRNL	SRNL (CCC-DWPF)	(Fox et al. 2008)	(Fox et al. 2008)	As published
CVS1, CVS2	23 (CVS1) + 98 (CVS2)	PNNL	PNNL (CCC-WTP)	(Hrma et al. 1994)	(Hrma et al. 1994)	As published
CVS3	40	PNNL	PNNL (CCC-WTP)	(Vienna et al. 1996)	(Vienna et al. 1996)	As published
EM09-	14 total	PNNL	PNNL (950C-24h) except Ca20m-B and Mg20m-B (CCC-WTP)	(McCloy et al. 2010)	(McCloy et al. 2010), this work	As published, except Ca20m-B and Mg20m-B, new here and described in text
SB5NEPH	01-40	SRNL	PNNL (950-24)	(Fox et al. 2007)	This work	

Table A.2. Previously Unpublished Semi-Quantitative XRD Data for CCC Heat Treated Glasses (NEPH)

GLASS ID	Nepheline		Spinel		Fluorapatite		Silicate		Other	
	Vol%	Structure	Vol%	Structure	Vol%	Structure	Vol%	Structure	Vol%	Structure
NEPH-01	0.9	$Na(AlSiO_4)$?								
NEPH-02										Amorphous
NEPH-03			1.9	$NiFe_2O_4$						
NEPH-04	0.9	$Na(AlSiO_4)$ carnegieite								
NEPH-05										Amorphous
NEPH-06										Amorphous
NEPH-07										Amorphous
NEPH-08										Amorphous
NEPH-09										Amorphous
NEPH-10										Amorphous
NEPH-11										Amorphous
NEPH-12										Amorphous

Table A.3. Previously Unpublished Semi-Quantitative XRD Data for CCC Heat Treated Glasses (NEPH2)

GLASS ID	Nepheline		Spinel		Fluorapatite		Silicate		Other	
	Vol%	Structure	Vol%	Structure	Vol%	Structure	Vol%	Structure	Vol%	Structure
NEPH2-13										Amorphous
NEPH2-14	1.7	$Na(AlSiO_4)$?	3.4	$NiFe_2O_4$			2.2	Li_2SiO_3		
NEPH2-15										Amorphous
NEPH2-16	4.5	$Na(AlSiO_4)$?	1.6	$NiFe_2O_4$			1.2	Li_2SiO_3		
NEPH2-17	3.8	$Na(AlSiO_4)$?	5.4	$NiFe_2O_4$			4.5	Li_2SiO_3		
NEPH2-18			2.0	$NiFe_2O_4$						
NEPH2-19	2.4	$Na(AlSiO_4)$?	6.6	$NiFe_2O_4$						
NEPH2-20	9.7	$Na(AlSiO_4)$?	8.4	$NiFe_2O_4$			1.8	Li_2SiO_3		
NEPH2-21										Amorphous
NEPH2-22	1.0	$Na(AlSiO_4)$?	16.6	$NiFe_2O_4$			0.3	Li_2SiO_3		
NEPH2-23	35.4	$Na(AlSiO_4)$?	1.9	$NiFe_2O_4$			4.2	Li_2SiO_3		
NEPH2-24										Amorphous
NEPH2-26	51.2	$Na(AlSiO_4)$?	4.7	$NiFe_2O_4$			3.9	Li_2SiO_3		
NEPH2-27			1.9	$NiFe_2O_4$						
NEPH2-28										Amorphous
NEPH2-29	49.1	$Na(AlSiO_4)$?	6.1	$NiFe_2O_4$			17.3	Li_2SiO_3		
NEPH2-30										Amorphous
NEPH2-31	13.8	$Na(AlSiO_4)$?	5.3	$NiFe_2O_4$			4.8	Li_2SiO_3		
NEPH2-32	51.5	$Na(AlSiO_4)$?	3.8	$NiFe_2O_4$			14.5	Li_2SiO_3		
NEPH2-33			2.0	$NiFe_2O_4$						
NEPH2-34	23.3	$Na(AlSiO_4)$?	2.1	$NiFe_2O_4$			0.4	Li_2SiO_3		
NEPH2-35	48.2	$Na(AlSiO_4)$?	4.8	$NiFe_2O_4$			9.2	Li_2SiO_3		
NEPH2-36			2.0	$NiFe_2O_4$						
NEPH2-37	7.6	$Na(AlSiO_4)$?	7.2	$NiFe_2O_4$						
NEPH2-38	19.3	$Na(AlSiO_4)$?	4.1	$NiFe_2O_4$			1.5	Li_2SiO_3		
NEPH2-39			1.9	$NiFe_2O_4$						
NEPH2-40			1.9	$NiFe_2O_4$						

Table A.4. Previously Unpublished Semi-Quantitative XRD Data for CCC Heat Treated Glasses (NEPH3)

GLASS ID	Nepheline		Spinel		Fluorapatite		Silicate		Other	
	Vol%	Structure	Vol%	Structure	Vol%	Structure	Vol%	Structure	Vol%	Structure
NEPH3-41										Amorphous
NEPH3-42										Amorphous
NEPH3-43										Amorphous
NEPH3-44	2.9	$Na(AlSiO_4)$?	20.2	$NiFe_2O_4$						
NEPH3-45										Amorphous
NEPH3-46										Amorphous
NEPH3-47										Amorphous
NEPH3-48										Amorphous
NEPH3-49										Amorphous
NEPH3-50										Amorphous
NEPH3-51										Amorphous
NEPH3-52										Amorphous
NEPH3-53										Amorphous
NEPH3-54										Amorphous
NEPH3-55										Amorphous
NEPH3-56	11.4	$Na(AlSiO_4)$?	23.1	$NiFe_2O_4$						

Table A.5. Previously Unpublished Quantitative XRD Data for 950°C-24 hr Heat Treated Glasses with CaF_2 Standard (SB5-NEPH)

GLASS ID	Nepheline		Spinel		Fluorapatite		Lithium Aluminum Silicate		Other	
	Vol%	Structure	Vol%	Structure	Vol%	Structure	Vol%	Structure	Vol%	Structure
SB5NEPH-02 (950-24 h)										
SB5NEPH-03 (950-24 h)			2.5	Fe_3O_4			11.6	$Na_{5.27}Ca_3(Si_6O_{18})$ - high combeite		
SB5NEPH-10 (950-24 h)			21.1	Fe_3O_4						
SB5NEPH-11 (950-24 h)			16.8	$ZnFe_2O_4$			6.6	$Na_{0.34}Ca_{0.66}Al_{1.66}Si_{2.34}O_8$ - labradorite		
SB5NEPH-12 (950-24 h)			11.8	Fe_3O_4						
SBNEPH-13 (950-24 h)										
SB5NEPH-15 (950-24 h)	10.0	$NaAlSiO_4$	3.4	Fe_3O_4			14.0	$Na_4Ca_4(Si_6O_{18})$ - combeite		
SB5NEPH-17-PNL (950-24 h)	26.9	$NaAlSiO_4$	4.4	$MgFe_2O_4$			5.1	$Na_{8.56}(Al_6Si_6O_{24})(SO_4)_{1.56}$ - lazurite		
SB5NEPH-19-PNL (950-24 h)	5.6	$NaAlSiO_4$	4.7	Fe_3O_4			4.1	$Na_{8.56}(Al_6Si_6O_{24})(SO_4)_{1.56}$ - lazurite		
SB5NEPH-21 (950-24 h)	34.4	$NaAlSiO_4$	10.8	Fe_3O_4						
SB5NEPH-23 (950-24 h)	35.8	$NaAlSiO_4$	9.9	Fe_3O_4						
SB5NEPH-25 (950-24 h)			22.2 11.6	$Li_2Fe_5Cr_5O_{16}$ - chromite $MgFe_{.2}Al_{1.8}O_4$					3.7	Al_2O_3
SB5NEPH-27 (950-24 h)	24.2	$K_{0.24}Na_{6.00}Al_{6.24}Si_{9.76}O_{32}$	19.5	Fe_3O_4			27.7	$CaAl_2Si_2O_8$ - anorthite		
SB5NEPH-29 (quenched)	20.9	$NaAlSiO_4$ - carnegieite								
SB5NEPH-30 (950-24 h)										
SB5NEPH-31-PNL (950-24 h)	12.3	$NaAlSiO_4$							3.7	$Na_{0.5}FeO_2$
SB5NEPH-32 (950-24 h)										
SB5NEPH-33-PNL (950-24 h)	62.0	$Na_{7.11}(Al_{7.2}Si_{8.8}O_{32})$	17.9	Fe_3O_4			2.9	$Na_6Ca_2Al_6SiO_{24}(SO_4)_2$ - hauyne		
SB5NEPH-34 (950-24 h)			8.8	Fe_3O_4						
SB5NEPH-35-PNL (950-24 h)	32.0 10.1 15.8	$Na_6Al_4Si_4O_{17}$ $Na_{7.11}(Al_{7.2}Si_{8.8}O_{32})$ $NaAlSi_2O_6$ - jadeite	6.8	Fe_3O_4			1.4	$Na_8(AlSi_6O_{24})(MnO_4)_{1.46}(OH)_{0.54}$ - sodalite		
SB5NEPH-36 (950-24 h)			7.7	Fe_3O_4						
SB5NEPH-37 (950-24 h)	7.7	$NaAlSiO_4$	57.2	$MgFeAlO_4$					30.6	Al_2O_3
SB5NEPH-39 (950-24 h)	29.3	$K_{0.24}Na_{6.00}Al_{6.24}Si_{9.76}O_{32}$	8.8	Fe_3O_4						

References

Fox KM and TB Edwards. 2008. *Refinement of the Nepheline Discriminator: Results of a Phase II Study.* SRNS-STI-2008-00099, Savannah River National Laboratory, Aiken, South Carolina.

Fox KM and TB Edwards. 2009. *Experimental Results of the Nepheline Phase III Study.* SRNL- STI-2009-00608, Savannah River National Laboratory, Aiken, South Carolina.

Fox KM, DK Peeler, TB Edwards, DR Best, IA Reamer, RJ Workman, JC Marra, BJ Riley, JD Vienna, JV Crum, J Matyas, AB Edmondson, JB Lang, NM Ibarra, A Fluegel, A Aloy, AV Trofimenko, and R Soshnikov. 2008. *International Study of Aluminum Impacts on Crystallization in U.S. High Level Waste Glass.* SRNS-STI-2008-00057, Savannah River National Laboratory, Aiken, South Carolina.

Fox KM, JD Newell, TB Edwards, DR Best, IA Reamer, and RJ Workman. 2007. *Refinement of the Nepheline Discriminator: Results of a Phase I Study.* WSRC-STI-2007-00659, Savannah River National Laboratory, Aiken, South Carolina.

Fox KM, TB Edwards, DK Peeler, DR Best, IA Reamer, and RJ Workman. 2006. *Nepheline Formation Study For Sludge Batch 4 (SB4): Phase 3 Experimental Results.* WSRC-TR-2006 00093, Savannah River National Laboratory, Aiken, South Carolina.

Hrma P, GF Piepel, MJ Schweiger, DE Smith, DS Kim, PE Redgate, JD Vienna, CA LoPresti, DB Simpson, DK Peeler, and MH Langowski. 1994. *Property/Composition Relationships for Hanford High-Level Waste Glasses Melting at 1150ºC.* PNL-10359, Pacific Northwest Laboratory, Richland, Washington.

Hrma P, MJ Schweiger, CJ Humrickhouse, JA Moody, RM Tate, TT Rainsdon, NE TeGrotenhuis, BM Arrigoni, J Marcial, CP Rodriguez, and BH Tincher. 2010. "Effect of Glass Batch Makeup on the Melting Process." *Ceramics-Silikaty* 54:193-211.

Kim DS, DK Peeler, and P Hrma. 1995. "Effect of Crystallization on the Chemical Durability of Simulated Nuclear Waste Glasses," In *Ceramic Transactions* 61, *Environmental Issues and Waste Management Technologies,* American Ceramic Society, Westerville, Ohio, pp 177-185.

Kim DS, P Hrma, DE Smith, and MJ Schweiger. 1993. "Crystallization in Simulated Glasses from Hanford High-Level Nuclear Waste Composition Range," In *Ceramic Transactions*, 39*, Environmental and Waste Management Issues in the Ceramic Industry*, ed GB Mellinger, American Ceramic Society, Westerville, Ohio, pp 179-189.

Kim, DS, JD Vienna, DK Peeler, KM Fox, A Aloy, AV Trofimenko, and KD Gerdes. 2008. *Improved Alumina Loading in High-Level Waste Glasses – 8460.* Proc. WM2008 Waste Management Conference, WM2008 Waste Management Conference.

Li H, JD Vienna, P Hrma, DE Smith, and MJ Schweiger. 1997. "Nepheline Precipitation in High Level Waste Glasses: Compositional Effects and Impact on the Waste Form Acceptability," *Proc. Materials*

Research Society Vol. 465 Scientific Basis for Nuclear Waste management XX, Materials Research Society. Pittsburgh, Pennsylvania, pp 261-268.

Marra JC and CM Jantzen. 1993. *Characterization of projected DWPF glasses heat treated to simulate canister centerline cooling*. WSRC-TR-92-142, rev 1, Westinghouse Savannah River Company, Aiken, South Carolina.

Marra, JC, KM Fox, GT Jannik, EB Farfan, DS Kim, JD Vienna, JA Roach, A Aloy, SV Stefanovsky, DP Lopukh, MD Bondarkov, KD Gerdes, and AM Han. 2009. "The DOE Office of Environmental Management International Cooperative Program: Overview of Technical Tasks and Results," Proc., WM2010 Waste Management Conference.

Matlack KS, H Gan, M Chaudhuri, W Kot, W Gong, T Bardakci, IL Pegg, and I Joseph. 2008. *Melt Rate Enhancement for High Aluminum HLW Glass Formulations.* VSL-089R1360-1, Vitreous State Laboratory, the Catholic University of America, Washington, D.C.

Matlack KS, H Gan, W Gong, IL Pegg, CC Chapman, and I Joseph. 2007. *High Level Waste Vitrification System Improvements.* VSL-07R1010-1, Vitreous State Laboratory, the Catholic University of America, Washington, D.C.

McCloy JS, C Rodriguez, C Windisch, C Leslie, MJ Schweiger, BJ Riley, and JD Vienna. 2010. "Alkali/ Alkaline-Earth Content Effects of Properties of High-Alumina Nuclear Waste Glasses," In *Ceramic Transactions 222, Advances in Materials Science for Environmental and Nuclear Technology*, ed KM Fox, et al. John Wiley & Sons, Hoboken, New Jersey, pp 63-76.

McCloy JS, MJ Schweiger, CP Rodriguez, and JD Vienna. 2011. "Nepheline Crystallization in Nuclear Waste Glasses: Progress toward acceptance of high-alumina formulations," *International Journal of Applied Glass Science*, submitted.

Musick CA, BA Scholes, RD Tillotson, DM Bennert, JD Vienna, JV Crum, DK Peeler, IA Reamer, DF Bickford, JC Marra, and NL Waldo. 2000. *Technical Status Report: Vitrification Technology Development Using INEEL Run 78 Pilot Plant Calcine*. INEEL/EXT-2000-00110.

Peeler DK, TB Edwards, DR Best, IA Reamer, and RJ Workman. 2006. *Nepheline Formation Study for Sludge Batch 4 (SB4): Phase 2 Experimental Results.*WSRC-TR-2006 00006, Savannah River National Laboratory, Aiken, South Carolina.

Peeler DK, TB Edwards, IA Reamer, and RJ Workman. 2005. *Nepheline Formation Study for Sludge Batch 4 (SB4): Phase 1 Experimental Results.* WSRC-TR-2005-00371, Savannah River National Laboratory, Aiken, South Carolina.

Riley BJ, JA Rosaria, and P Hrma. 2001. *Impact of HLW Glass Crystallinity on PCT Response.* PNNL-13491, Pacific Northwest National Laboratory, Richland, Washington.

Schweiger MJ, BJ Riley, JV Crum, PR Hrma, CP Rodriguez, BM Arrigoni, JB Lang, DS Kim, JD Vienna, FC Raszewski, DK Peeler, TB Edwards, DR Best, IA Reamer, WT Riley, PT Simmons, and RJ

Workman. 2011. *Expanded High-Level Waste Glass Property Data Development: Phase I.* PNNL-17950, Rev 0, Pacific Northwest National Laboratory, Richland, Washington.

Vienna JD, P Hrma, MJ Schweiger, MH Langowski, PE Redgate, DS Kim, GF Peipel, DE Smith, CY Chang, DE Rinehart, SE Palmer, and H Li. 1996. *Effect of Composition and Temperature on the Properties of High-Level Waste (HLW) Glass Melting Above 1200°C.* PNNL-10987, Pacific Northwest National Laboratory, Richland, Washington.

Appendix B

Compilation and Critical Comparison of Optical Basicities

Appendix B: Compilation and Critical Comparison of Optical Basicities

Optical basicity values have been compiled and computed for 97 oxides (88 elements) using electronegativity, ionic-covalent parameter, and optical properties methods. The various scales were compared and found to be incompatible when viewed as large datasets, but some subsets of oxides compared well. The merits of the various scales are discussed. A current, self-consistent set of values is recommended for use until systematic measurements on less common components such as actinides can be obtained. These oxide optical basicity values should prove useful for assessing complex compounds and glasses such as encountered in nuclear waste vitrification.

B.1 Introduction

Complex silicate glasses and slags are technologically important for various processes from metallurgical processing to nuclear waste immobilization to extraction geochemistry. In these fields, the idea of "basicity" as it applies to oxides, particularly melts, is an analogy between the dissociation of acids to produce hydrogen ions and the dissociation of network anions such as silicates to produce oxygen ions (Bach et al. 2001). Various conceptions of basicity in oxides have been employed (Mills 1995) as measures of free oxygen ion thermodynamic activity, ranging from simple ones like the ratio of CaO to SiO_2, (Susa et al. 1992) to more physically grounded ones based on the Coulomb force between the cation and oxygen (Moringa et. al 1994).

Perhaps the most useful and longstanding conception of basicity has been that of optical basicity (OB), first introduced in the early 1970's by Duffy and Ingram (1971, 1976). OB was originally conceived as the measurement of the oxygen donation power relative to CaO, based on a systematic red shift of a probe ion absorption band with increasingly basic glasses or complex oxides. Since then, various methods besides ultraviolet (UV) probe ion spectroscopy have been used to obtain OB values for constituent oxides, including such various considerations as electron density (Nakamura et al. 1986), electronegativity (Duffy and Ingram 1973, Duffy 1986a), energy gap (Duffy 1986a), refractive index (Iwamoto et al. 1984, Duffy 1986b), thermochemical properties (Duffy 1993), and extraction capacities of sulfur, vanadium, or phosphorus (Bergman 1988, Yang and Somerville 2001). OB has since been shown to have great predictive power for correlating trends in transport properties, including viscosity, electrical and thermal conductivity, and diffusion (Mills 1993, Mitchell et al. 1997) thermochemical properties such as heats of formation and thermodynamic activity coefficients, (Duffy 2004b, Beckett 2002) and even magnetic (Lenglet 2000), catalytic (Bordes 2000, Moriceau et al. 2000), and lubrication (Prakash and Celis 2007) properties. OB has been shown to be closely related to other structural descriptors of glasses such as non-bridging oxygen per tetrahedron (NBO/T), and thus represents an overall average state of oxygen in the system, though in certain cases individual oxygen local states can be distinguished (Iwamoto and Makino 1979, Duffy and Ingram 1976).

B.1.1 Optical Basicity Scales

Several different scales of optical basicities have been proposed which are mutually exclusive (McCloy et al. 2010). In general, the OB can be computed for any given glass from the OB of constituents as:

$$\Lambda_{glass} = \sum_i x_i q_i \Lambda_i \Big/ \sum_i x_i q_i \tag{B.1}$$

where q_i is the number of oxygen atoms in the *i*-th component oxide, x_i is the *i*-th component oxide mole fraction, and Λ_i is the *i*-th oxide OB (Mills 1995, Verein-Deutscher-Eisenhuttenleute 1995). Note that it is also straightforward to apply Equation B.1 to computing OB for a complex oxide with more than one cation, provided that it can be converted stoichiometrically into a sum of simple oxides (e.g. $MgAl_2O_4$ = $MgO + Al_2O_3$, with each of the components contributing 0.5 moles to the compound), and that the molecular weight and corresponding number of ions is carefully considered. Note that where the term "glass" is used below, the procedure is equally valid for a compound oxide or mixture of oxide phases. OB of the simple oxides, compound oxides, or glasses can be computed in various ways as follows. The theoretical derivation of these various scales is discussed in greater depth in a recent paper (McCloy et al. 2010).

B.1.2 1a) OB from UV probe spectroscopy (Λ_{exp})

This method uses the spectral absorption shift of the $^1S_0 \rightarrow {}^3P_1$ electronic excitation of a $6s^2$ electronic configuration probe ion (Tl^+, Pb^{2+}, or Bi^{3+}), placed in the medium for optical measurement, in order to determine the OB. Probe ion spectroscopy works very well for oxides of alkali, alkaline earth, and first and second row cations (i.e. B, C, N, Al, Si, P, S), but fails when working with transition metals due to the large absorption of these ions in the ultraviolet and visible (Duffy 1989d). For this reason, the other methods below have been developed. It has been shown that there are subtle but telling differences in choice of probe ion in determining local environments of oxygen (Duffy et al. 1993), but for the present purposes it will be assumed that the OB determined is representative of the average oxygen environment.

B.1.3 1b) OB from the refractive index (Λ_n)

This method uses computation of the molar polarizability from the Lorentz-Lorenz equation and the composition to get the average oxygen polarizability and thus the OB (Duffy 1989b). The refractivity method requires knowledge of the oxide molar composition, the density, the molecular weight (normalized to 1 mole of glass), the number of cations and oxygens in oxides, the cation polarizabilities, and the refractive index (preferably in the visible region). Procedurally, first the Lorentz-Lorenz equation is solved for the molar polarizability (α_m) using Equation B.2a:

$$\alpha_m(\mathring{A}^3) = \frac{3}{4\pi}\frac{M}{\rho N_{Av}}\left(\frac{n^2-1}{n^2+2}\right) \tag{B.2a}$$

$$\alpha_m(\mathring{A}^3) = \sum_i \left(x_i q_{ox,i}\alpha_{ox,i} + x_i p_{cat,i}\alpha_{cat,i}\right) = F_{ox}\alpha_{ox} + \alpha_{m,cat} = \alpha_{m,ox} + \alpha_{m,cat} \tag{B.2b}$$

with input data of the refractive index (n), the density (ρ), the molecular weight (M), and Avogadro's number (N_{Av}). The total molar polarizability (α_m) is then decomposed via Equation B.2b into its

contributions from the cations ($\alpha_{m,cat}$) and the oxygens ($\alpha_{m,ox}$), according to the mole fractions of the oxides (x_i), and numbers of cations ($p_{cat,i}$) and oxygens ($q_{ox,i}$) per A_pO_q oxide. The values for the individual cation polarizabilities are found in the literature (see Table B.1 for compilation). Finally, the polarizability per oxygen (or average oxygen polarizability) (α_{ox}) is determined from the total oxygen polarizability ($\alpha_{m,ox}$) dividing by the fractional oxygens (F_{ox}, i.e., mole fraction oxide $x_i q_{ox,i}$, oxygens per oxide). Having obtained the average oxygen polarizability (α_{ox}), the OB of the glass or oxide is obtained from Equation B.3:

$$\Lambda = 1.67\left(1-\frac{1}{\alpha_{ox}}\right) \tag{B.3}$$

Note that this equation does not show a subscript since it can, in principle, be used to obtain the OB from oxygen polarizability obtained using any method, including correlations with energy gap (see below). This relation was obtained by Duffy (1989b) by a very good linear fit between OB (as determined by measured probe ion spectroscopy or Pauling electronegativity, see Equation B.13 and Discussion) and oxygen polarizability (as determined by Equation B.2 and measured refractivity data) of a number of simple and multicomponent oxide compounds. Note that the OB from refractive index can be determined from multicomponent glass data ($\Lambda_{n,glass}$) or from refractivity of simple oxides ($\Lambda_{n,oxide}$), and both have been presented in the literature and generally produce OB values in good agreement, with the possible exception of the lanthanides as discussed below.

B.1.4 1c) OB from the energy gap (Λ_{Eg})

Basicity can also be computed from the energy gap via an empirical correlation (Banu et al. 2003, Vithal et al. 1997, Duffy 1986a) between energy gap and refractivity (e.g. Equation B.4). This method of obtaining OB requires all the same inputs as above except the energy gap rather than the refractive index is required. Several different energy gap/ refractivity correlations have appeared in the literature, but the one shown below is the most used, obtained by Duffy (1986a) from the correlation of measured energy gap and the refractivity of many simple oxides.

$$E_g = 20(1-R_m/V_m)^2 \tag{B.4}$$

$$V_m\left(\frac{cm^3}{mol}\right) = \sum x_i M_i \big/ \rho_{glass} \tag{B.5}$$

$$R_m\left(\frac{cm^3}{mol}\right) = \frac{4\pi}{3} N_{Av}\alpha_m\left(cm^3\right) = 2.52\left(\frac{cm^3}{\mathring{A}^3 mol}\right)\alpha_m(\mathring{A}^3) \tag{B.6}$$

To obtain the OB (Λ_{Eg}), Equation B.4 is used with the energy gap (E_g) and the molar volume (V_m) to obtain the molar refractivity (R_m). The molar volume is computed from Equation B.5 using the molecular weight of each oxide (M_i), the mole fraction of each oxide (x_i), and the density of the glass (ρ_{glass}) (measured or computed; see Appendix). In computing the molar volume, it is convenient to normalize to one mole of glass. From the molar refractivity (R_m), the molar polarizability (α_m) can be directly obtained through Equation B6. From the molar polarizability, the average oxygen polarizability (α_{ox}) (via Equation B.2b) and then the OB (in this case Λ_{Eg} via Equation B.3) are obtained. For the purposes of subsequent discussion, the OB as determined from UV probe ion spectroscopy (Λ_{exp}), glass refractivity ($\Lambda_{n,glass}$), oxide refractivity ($\Lambda_{n,oxide}$), and energy gap ($\Lambda_{n,Eg}$) are considered to be roughly interchangeable and self-

consistent. In this paper, they are collectively referred to as "OB based on optical properties" (Λ_{opt}) to distinguish them from those determined from electronegativity or ionic-covalent character as described below.

B.1.5 2) OB from the average electronegativity (EN) ($\Lambda_{\chi av}$)

For this formulation of OB, only the EN of the elements and number of atoms of each element are required (Reddy et al. 2001). The concept of "average EN" was originally introduced to help understand the behavior of oxide superconductors (Asokamani and Manjula 1989).

$$\chi_{av} = \sum_{i=1}^{n} \chi_i N_i \Big/ \sum_{i=1}^{n} N_i \tag{B.7}$$

Here, the average EN (χ_{av}) depends on the number of atoms of a particular element (N_i) and the EN of the element (χ_i). Originally, Pauling EN values were used in calculating average EN, but more recently a different tabulated EN scale has been used in the context of OB. (Zhao et al. 2008b). Li and Xue's EN (χ_{LX}) (Li and Xue 2006) is tabulated up through actinium (atomic number = 89), but values for the other actinides would have to be derived as follows.

$$\chi_{LX} = 0.105\frac{Z^*}{r_{cryst}} + 0.863 = 0.105\frac{n^*\left(I_z / R_\infty\right)^{1/2}}{r_{cryst}} + 0.863 \tag{B.8}$$

Li and Xue's EN (χ_{LX}) is derived from a consideration of quantum mechanics, specifically the effective nuclear charge on the valence electrons (Z^*), along with Shannon's (1976) "crystal radii" for six coordinated ions (r_{cryst}). The numerical coefficients were originally obtained by plotting the effective ion potential (Z^*/ r_{cryst}) versus the Pauling EN. Z^* is itself a function of the effective principle quantum number (n^*) (Li and Xue 2006), the ultimate ionization potential (electron affinity) (I_z), and the Rydberg constant (R_∞ = 13.6 eV). Procedurally, the electronegativity values, in this case those from Li and Xue (χ_{LX}), are taken from the literature or computed via Equation B.8. Next, the average EN (χ_{av}) is computed using Equation B.7 from the number of atoms of a particular element (N_i) and the EN of the element (χ_i), where the scale of EN used (e.g. Pauling (Pauling 1932) or Li and Xue (2006)) partially determines the coefficients B and C in Equation B.9 used to compute OB ($\Lambda_{\chi av}$). The significance of coefficients B and C is discussed later in this paper.

$$\Lambda_{\chi av} = B - C\chi_{ave} \tag{B.9}$$

B.1.6 3) OB from the ionic-covalent parameter (ICP) (Λ_{ICP})

The ICP contains contributions from both the iconicity and covalency of the chemical bonding, and contains terms containing the polarizing power of the cation (P) and its electronegativity (EN, in this case χ_{Port}) (Portier et al. 1994b)

$$ICP_{(Port)} = \log P - 1.38\chi_{Port} + 2.07 = \log\left(z / r_{ion}^2\right) - 1.38\chi_{Port} + 2.07 \tag{B.10}$$

The polarizing power (P) is defined as the cation charge (z) divided by the radius (r_i) squared. Two numerical fit coefficients in the ICP depend on the choice of EN and radius scales (e.g., Shannon's

[1976]) "ionic" radii [r_{ion}] as used in this case or "crystal" radii). The ICP of Au^{+} is always set equal to zero. EN as defined by Portier et al. (1994a) (χ_{Port}) depends only on z, r_{ion} ("ionic" radius), and a small tabulated elemental specific correction term β (the authors use α but to avoid confusion here with polarizability, the correction term is β) (see Equation B.11).

$$\chi_{Port} = 0.274z - 0.15zr_{ion} - 0.01r_{ion} + 1 + \beta \tag{B.11}$$

Subsequently, Lebouteiller and Courtine (1998) computed $ICP_{(Port)}$ for various ions in specific coordinations (e.g. tetrahedral, octahedral) and correlated it to OB (determined by refractivity or UV probe spectroscopy). They then separated out the ions (i.e. B^{3+} for B_2O_3) into groups of the same valence electronic configuration (i.e. sp, $d^{10}s^2$, d^0, d^{10}, and d^1-d^9), drew linear fits in each electronic configuration group between the ICP and the known OB, and postulated that these relations could be extrapolated to ions in coordinations, spin states, and valence states where OB was not known experimentally. Hence, all that is needed to calculate OB (Λ_{ICP}) is the cation charge (z), ionic radius (r_{ion}) (which depends on coordination number), an elemental correction term (available through atomic number = 102) (Portier et al. 1994a), and the empirical formulas below (Equation B.12a through Equation B.12e).

sp: $$ICP = -0.676\Lambda + 1.452 \tag{B.12a}$$

$d^{10}s^2$: $$ICP = -13.844\Lambda + 17.134 \tag{B.12b}$$

d^0: $$ICP = 3.007\Lambda + 1.336 \tag{B.12c}$$

d^{10}: $$ICP = -0.729\Lambda + 1.390 \tag{B.12d}$$

d^1-d^9: $$ICP = -0.643\Lambda + 1.143 \tag{B.12e}$$

Procedurally, the OB of a simple oxide is thus obtained by first computing the Portier EN (χ_{Port}) via Equation B.11, then the ICP via Equation B.10. From this ICP, the OB (Λ_{ICP}) is determined from a different empirical equation (Equation B.12a through Equation B-12e), depending on the valence state of the ion. Thus, for example, the compounds studied by Duffy by UV spectroscopy are the sp ions (Pb^{5+}, Si^{4+}, B^{3+}, Al^{3+}, Mg^{2+}, Na^{+}, etc.). One clear disadvantage of this method is that no relationships yet exist for *f* electrons, for which a relationship has not been found in this study either (see Discussion).

B.1.7 4) OB from some other methods

Early on it was pointed out that there existed some empirical correlations between the OB of oxides and Pauling electronegativity (EN). Pauling (1932) thought of EN as the power of the atom in a molecule to attract electrons to itself, and derived his scale from thermochemical heats of formation on an arbitrary scale from 4 (fluorine) to 0.7 (cesium). He did not account for valence state or ionic radius but had a single value for each element, as it was conceived of as an assessment of the ionic contribution to essentially covalent bonding. The Pauling EN for the cation ($\chi_{M,Paul}$) can be correlated to optical basicity, but only for cations whose oxidation state corresponds to a noble gas electron configuration (Duffy and Ingram 1992, Duffy and Ingram 1991, Binks and Duffy 1985).

$$\Lambda = \frac{0.75}{\chi_{M,Paul} - 0.25} \tag{B.13}$$

For these same binary oxides (e.g. alkali oxides, alkaline-earth oxides, Al_2O_3, B_2O_3, TiO_2, SiO_2, H_2O, P_2O_5, and SO_3), the corresponding Pauling EN of the oxygen is (Binks and Duffy 1985).

$$\chi_{O,Paul} = 4.1 - \frac{0.86}{\chi_{M,Paul} - 0.25} \tag{B.14}$$

Despite these limitations, these relations have been used to predict optical basicities for fluorides (Duffy 1989a) and sulfides (Duffy 1992) (but not successfully for chlorides and bromides), with the increasing basicity going as $F^- < O^{2-} < S^{2-}$. Detailed consideration of basicity for non-oxides is beyond the scope of this paper. Later, Nakamura et al. (1986) proposed that the OB was related to the electron density (D) as defined by

$$D = a\frac{z}{\left(r_{cat} + r_{an}\right)^3} \tag{B.15}$$

Where z is the cation valence, r_{cat} and r_{an} are the radii of the cation and anion, respectively, and a is a parameter defined as unity for oxides but takes on other values for fluorides and chlorides. From this value of electron density D, the optical basicity is calculated as

$$\frac{1}{\Lambda} = 1.34(D + 0.6) \tag{B.16}$$

These authors found this relation to hold for CaO, Al_2O_3, SiO_2, B_2O_3, and P_2O_5, and so extended it to other oxides, most notably transition metals. In theory this expression is quite useful as it only requires knowing the ionic radii and the a factor for oxides (1), fluorides (3.7), or chlorides (4.9). These a factors were derived for the non-oxide systems using photoacoustic spectroscopy.

A comparison of optical basicities of some oxides as determined by UV probe spectroscopy (Λ_{exp}), glass refractivity ($\Lambda_{n,glass}$), oxide refractivity ($\Lambda_{n,oxide}$), oxide energy gap (Λ_{Eg}), and Pauling electronegativity ($\Lambda_{\chi P}$), is shown in Table B.2. Additionally, basicities calculated from electron density (Λ_D) (assuming the radius of oxygen is 1.40 Å), average electronegativity ($\Lambda_{\chi av}$) (assuming the EN of oxygen is $\chi_{LX} = 3.758$) (Zhao et al. 2008a) and ionic-covalent parameter (Λ_{ICP}) (Lebouteiller and Courtine 1998) for a given coordination number (CN) are also shown. Yang and Somerville (Yang and Somerville 2001) previously recommended a set of values for these oxides, so the current recommended values (Λ_{rec}) (see below) are shown for comparison with the previous ones.

B.2 Methods

Literature sources were assessed and compiled to ascertain the largest dataset possible of OB values in the three primary scales described above. Where possible, new OB values were derived using the methods described above. Representative subsets of oxides were tested to see if a systematic linear relationship was apparent between the scales that would allow conversion among all three scales if necessary.

B.3 Results

OB of some oxides was determined from refractive index data (sodium D-line at 589 nm) or energy gap using the equations discussed previously (see Table B.3). In some cases, the cation polarizability had to be estimated based on the cube of the ionic radius (Prakash and Celis 2007). Refractive index of the oxide was used to determine the OB of As_2O_3, Au_2O_3, PtO_2, SeO_2, ThO_2, UO_2, and UO_3. Note that now the OB of U_3O_8 can be calculated as $\frac{1}{3}\Lambda_{UO3}+\frac{2}{3}\Lambda_{UO2}=\frac{1}{3}(1.03)+\frac{2}{3}(0.97) = 0.99$. Band gap was used to determine the OB of As_2O_3, Co_2O_3, Cu_2O, HfO_2, HgO, IrO_2, OsO_2, PbO_2, PdO, PtO_2, Re_2O_7, Rh_2O_3, RuO_2, ThO_2, TiO, Tl_2O_3, and UO_3.

No index or energy gap data could be located for the oxides As_2O_5 and Tl_2O, but substantial glass refractivity data exists. Seventeen glass compositions from Vogel (1994) were investigated where As_2O_5 was present in 2 to 9 mol% along with substantial amounts of As_2O_3 (27–51 mol%). Six glass compositions from Fuijino et al. (1995a, 1995b) were investigated which contained 10–40 mol% Tl_2O. Using the published composition, refractive index, and density of the glasses, the molar polarizability and ultimately the per-oxygen polarizabilities were calculated (Equation B.2a, B.2b), and from this the OB of the glasses (Equation B.3).

The optimum value of the OB for As_2O_5 and for Tl_2O for each glass was found by computing the OB using Equation B.1 and equating the glass OB to that calculated from the refractivity (refractive index and density). It was found that the value for polarizability of Tl^+ of 5.2 $Å^3$ (Tessman et al. 1953) was too large and the value 3.81 $Å^3$ (Fajans and Kreidl 1948) was preferred as it is also close to the cube of the ionic radius (3.375 $Å^3$). The basicity of Tl_2O was computed using both polarizabilities, and the average was 0.995 for the larger cation polarizability and 1.487 for the smaller (preferred) cation polarizability. The latter value is deemed appropriate, especially in comparison with K_2O (OB=1.32), Cs_2O (OB = 1.52), and Rb_2O (OB = 1.41). The OB of As_2O_5 was more difficult to establish, since the optimum value in several individual glass cases was negative. This could be due to the low molar content and possible confusion of As_2O_3 and As_2O_5 in the compositional analysis. If the negative values are removed, the average basicity goes from As_2O_5 0.29 to 0.40, but this is still very acidic, on the order of B_2O_3 and P_2O_5. The latter value of 0.40 is chosen for As_2O_5 since it is chemically similar to P_2O_5.

A summary table of optical basicities of all oxides in this study (in alphabetical order) is shown in Table B.1, including much of the same information for the more limited set of Table B.2. Additionally, cation electronic polarizabilities (α_{cation}) as well as coefficients for computing density (Vienna et al. 2009) (see Appendix) are tabulated. A recommended set of OB values for oxides has been provided and is shown in Table B.1 as Λ_{rec}. The justification for these choices is presented in the Discussion below.

Figure B.1 shows the results of plotting the optical basicities of the various scales (of 69 oxides where values were available in all three scales) against one another. No satisfying correlation could be made. This was somewhat unexpected, since previously some 20 component oxide nuclear waste glasses were investigated where the correlations between scales was nominally very good (not shown). It was determined, however, that this was due to the very good linear correlations of the major components of these glasses (>10 mol%), which were Al_2O_3, B_2O_3, CaO, Na_2O, and SiO_2. Figure B.2 shows the 20 oxides in these glasses (those previously listed plus K_2O, MgO, BaO, ZnO, NiO, CuO, MnO, PbO, Fe_2O_3, Cr_2O_3, La_2O_3, Ce_2O_3, TiO_2, ZrO_2, and SO_3) with a linear fit to the major glass components (Al_2O_3, B_2O_3, CaO, Na_2O, and SiO_2) showing good correlation among scales for these.

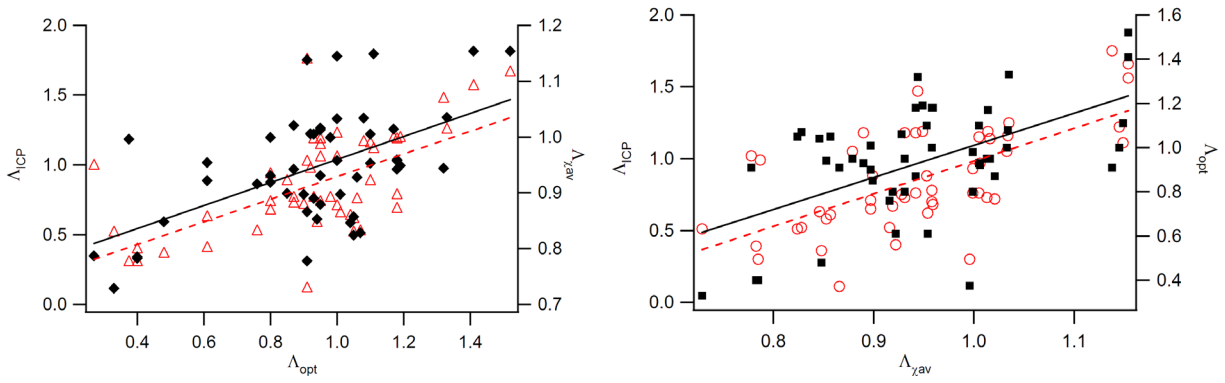

Figure B.1. Comparison of Optical Basicity of 69 Binary Oxides in Three Scales: (a,L): Λ_{ICP} (open triangles) and $\Lambda_{\chi av}$ (solid diamonds) versus Λ_{opt}. Equations for Λ_{ICP} ($y = 0.8118x+0.1034$, $R^2 = 0.3687$, dotted line) and for $\Lambda_{\chi av}$ ($y = 0.206x + 0.7538$, $R^2 = 0.2993$, solid line) indicate no correlations can be made. (b, R): Λ_{ICP} (open circles) and Λ_{opt} (solid squares) versus $\Lambda_{\chi av}$. Equations for Λ_{ICP} ($y = 2.2729x$ - 1.2903, R^2=0.4097, dotted line) and for Λ_{opt} ($y = 1.453x$ - 0.4435, $R^2 = 0.2993$, solid line) indicate no correlations can be made.

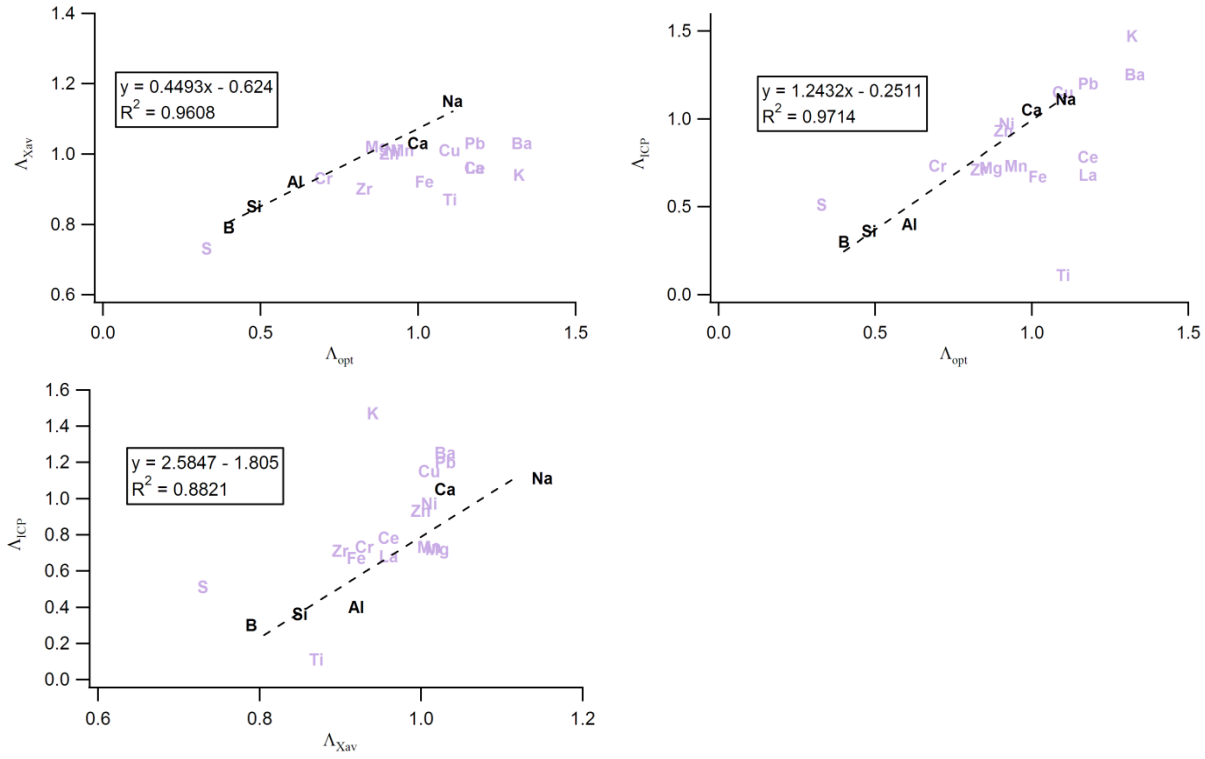

Figure B.2. Comparison of optical basicity values from three scales for 20 binary oxides components common in nuclear waste glasses. Data points are the elemental symbols. Light symbols are the 20 oxides (listed in text) and dark symbols are the major components (Al_2O_3, B_2O_3, CaO, Na_2O, and SiO_2). Linear fit to the major components is shown.

B.4 Discussion

The primary disadvantage of using the optical properties for obtaining OB for a binary oxide is the necessity of not only an optical property (energy gap or refractive index), but also the cation polarizability and the oxide density. For some of the more uncommon oxides this can be difficult.

One potential disadvantage of using the ICP method strictly from the equations (Equations B.10-B.12) is the problem with B_2O_3 and BeO. Both B^{3+} and Be^{2+} are *sp* configuration cations, but using the equation for *sp* (Equation B.12a) gives a negative value for Λ since the ionic radii are so small. One alternative is to use the Λ values from another scale or, perhaps, an estimated value, and that is the work-around adopted here. This is indicated in Table B.1 where this correction is applied for the aforementioned oxides, in addition to Re_2O_7. Another disadvantage of this method is that no empirical relations exist for ions with valence *f* electrons, and these relations would have to be derived. Such an attempt was made by the author, but no satisfying fit could be obtained between known OB data (Duffy 2005b) and ICP for CN = 8.

The basicity based on average EN is attractive due to its dependence only on tabulated EN data, in this case that of Li and Xue (χ_{LX}) (Li and Xue 2006). One disadvantage for this method is that the χ_{LX} values are not tabulated for actinides (atomic number >89) and hence would have to be derived where some of the necessary parameters in Equation B.8, notably the ionization energy, may not be known. It was discovered, however, that there is a close correlation between ionic field strength *F* and $\Lambda_{\chi av}$ (see Figure B.3). Field strength is here defined as $Z_{cat}/(r_{cat}+r_{ox})^2$, where Z_{cat} is the cation valence, r_{cat} is the cation radius, and r_{ox} is the oxygen ionic radius, here taken to be 1.40 Å (Shannon 1976). It is interesting to note that the main deviation from the linear fit is from the oxides of Li, Na, and K, the reason for which is not understood at this time. It is also not immediately obvious why the correlation with field strength should be so strong, since the average EN is computed with a term of $1/r_{cryst}$ (Equation B.8), not $1/ r_{ion}^2$ as is the ICP (Equation B.10) and the field strength.

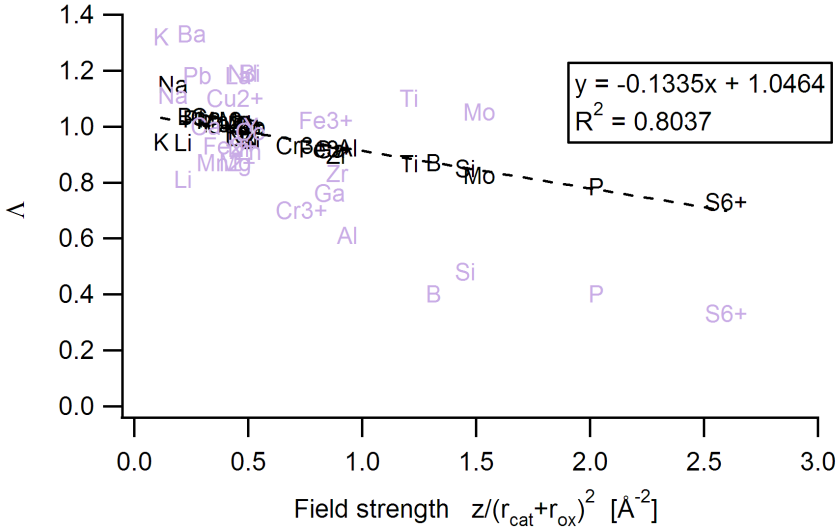

Figure B.3. Optical basicity of 30 oxides versus field strength. Data points are the elemental symbols. Light symbols are OB from optical properties, dark symbols and linear fit are OB from average EN (Li and Xue), which is calculated using the same coordination as that used in the field strength calculation.

Since almost no refractivity or band gap data was available for the actinides and other radioactive elements (except UO_2, UO_3, and ThO_2), other means of estimating the OB was needed. For this purpose, methods based solely on ionic radii and valences were desirable, such as the electron density and field strength correlations with OB. Table B.4 shows the six-fold coordinated atomic radii, calculated field strengths ($Å^{-2}$) and electron densities ($Å^3$). From these values the OB was calculated based on the empirical field strength equation (from Figure B.3) and the empirical electron density equation (Equation B.16). These values all seemed too low when compared to the UO_2, UO_3, and ThO_2 values from refractivity, and so an average scaling factor was derived for each scale depending on the relative value for these three oxides. For the electron density values the scaling factor was 1.35, and for the field strength values the scaling factor was 1.07. Since this was an average and the UO_3 value was much farther off than the others, neither scaled series faithfully reproduces the three oxide OBs used for scaling. However, the scaled values from the electron density seem as a whole too high and the values from the field strength series are more in line with the known values of UO_2, UO_3, and ThO_2. Therefore, as provisional values, these OB values ($\Lambda_{FS,scaled}$) are preferred until more definite oxide band gap or refractive index data is available.

The use of the average EN for determining OB also has its problems. There are a total of four different data fits proposed by Reddy et al. (2001) depending on the composition, and all were based on Pauling EN values. The empirical equation Zhao et al. (2008b) used with average EN (Li and Xue 2006) EN values originally proposed by Reddy et al. (2001) for "binary oxides," was one of several linear fits to OB data, and was based on Pauling EN values.

$$\Lambda_0 = 1.59 - 0.2279\chi_{ave} \text{ for "binary oxides"} \quad \text{(B.17a)}$$

Therefore the application of Equation B.17a by Zhao et al. (2008b) to their lanthanide data is questionable, though they do show some rough correlation with OB determined other ways. For the calculations of optical basicity in Table B.1, Equation B.17a was used.

Reddy et al. (2001) also calculated the average EN (Pauling) for the same binary glass systems whose OB was studied by Dimitrov and Komatsu (1999b) who had previously determined OB for these glasses by two methods: 1) using the measured refractive index of the glass, Lorentz-Lorenz equation, and empirical Equation B.3 above, and 2) calculating from known tabulated OB values of component oxides. Reddy et al. (2001) noted that their results of the OB to average EN (Pauling) fits compared "favorably" with the OB determined by other methods. However, they found several different correlations between OB and average EN of the glasses depending on the composition. The separation of validity ranges for their linear fit equations seems somewhat arbitrary, but to an extent corresponds to the three groupings of oxides (I, II, and III) as described by Dimitrov and Komatsu (2002) which takes into account various factors as summarized in Table B.5. In any case, the three relations give values that bin the OB of the glass into three ranges. First, the relation for binary oxide glasses "except those containing TeO_2, GeO_2, or TiO_2" (originally proposed in Reddy et al. 1999):

$$\Lambda_1 = \frac{0.75}{\chi_{ave,glass} - 1.35}, \; 0.44<\Lambda<0.68 \quad \text{(B.17b)}$$

Second, for those containing TeO_2, GeO_2, or TiO_2:

$$\Lambda_2 = 0.04375 + 0.3097\chi_{ave,glass}\text{ , } 0.88<\Lambda<0.97 \quad \text{(B.17c)}$$

Third, for systems of alkali and alkaline earth binary oxide glasses:

$$\Lambda_3 = 1.152 - 0.2298\chi_{ave,glass}\text{ , } 0.50<\Lambda<0.62 \quad \text{(B.17d)}$$

The first group of binary glasses, which are described by Equation B.17b, all contain at least 14 mol% of a primary acidic glass forming oxide (e.g. SiO_2 and others in Dimitrov and Komatsu's [DK] Group I). The second group of binary glasses, described by Equation B.17c, consists of combinations of oxides in DK Groups II and III, except a couple with GeO_2 (Group I) in combination with Bi_2O_3, Sb_2O_3, or V_2O_5, and MgO (Group I) combined with TeO_2, all of which have high optical basicities. It may be that in this case GeO_2 and MgO are changing their coordination from the normal one due to the other highly polarizing cations (Duffy 2004a). The third group of glasses, described by Equation B17d, consists of all the glasses containing alkali oxides, most of which are considered to be in DK Group III, except Li_2O which is Group II, in combination with SiO_2, B_2O_3, or P_2O_5.

The Yamashita-Kurosawa interaction parameter (Yamashita and Kurosawa 1955) (A) is another way to describe the interaction between cations and anions in terms of the change in polarizability of the free anion due to the cation:

$$A = \frac{\alpha_f - \alpha_{ox}}{2\left(\alpha_f - \alpha_{cat}\right)\left(\alpha_{ox} - \alpha_{cat}\right)} \quad \text{(B.18)}$$

Here, α_f is the electronic polarizability of the free oxide ion, taken to be 3.921 $Å^3$ (Pauling's value), α_{ox} is the per oxygen polarizability in the oxide as determined by the refractive index and the Lorentz-Lorenz equation (Equation B.2a, B.2b), and α_{cat} is the tabulated cation polarizability (assumed to be the same value for the free cation and the cation in the oxide since the electron cloud of the cation is not as deformable as the oxygen ion). This interaction parameter represents the charge overlapping of the anion with its nearest-neighbor cation, and hence is a measure of covalency. Therefore, the interaction parameter is inversely proportional to OB, which is a measure of iconicity (Dimitrov and Komatsu 2000). Dimitrovand Komatsu (1999a) have shown strong correlation between the Yamashita-Kurosawa interaction parameter, OB, and oxygen-binding energy.

Based on these assessments, the following set of recommended values is offered for 88 elements (97 oxides). The rationale behind the choice of recommended data was as follows, and is described in the notes for Table B.1 for each oxide. In general, glass refractivity data is preferred, especially when considering properties of complex oxide glasses such as encountered in nuclear waste vitrification. When both UV probe and glass refractivity data are available, choose the latter, though they are generally very close in value. For this reason it seems acceptable to use UV probe data where no other data is available (e.g. for H_2O and CO_2). Where band gap, refractive index of oxide, and refractive index from glass largely disagree, take the average of the closest two (e.g. Ga_2O_3).

Traditionally, it has been difficult to assign OB values to transition metals because of their natural absorption in the region of the UV probe, so many sets of values have been proposed based on various criteria. In this compilation, for some first row transition metals and a few other oxides, choose the value that fits the trends with several sets of properties investigated (e.g. FeO, MnO, Fe_2O_3, Cr_2O_3, ZnO, Ag_2O,

CdO). Details on these choices are provided in the notes to the table. For lanthanides, choose the glass refractivity rather than the oxide refractivity or band gap data. For the newly acquired OB values from energy gap and refractive index (shown in this paper), use these individually or their average if both are available. For the actinides and Tc, use the values based on the field strength empirical equation, scaled to the UO_2, UO_3, and ThO_2 OB values obtained from refractivity as provisional estimates.

B.6 Estimating Density

In determining refractivity of complex glasses without resorting to measurements, a method can be used whereby the optical basicity and density are computed from composition and the refractive index is calculated by taking Equation B.3 and B.2 in reverse (McCloy et al. 2010). Densities can be obtained by using the semi-empirical approach developed for multi-component alumino-boro-silicate nuclear waste glasses (Vienna et al. 2009). In this approach, a value for the partial-specific volume of each component (v_i) is determined as

$$v_i = a\frac{4}{3}\pi r_{O,cryst}^3 \frac{n_{ox,i}}{M_i} + b\frac{4}{3}\pi r_{cryst}^3 \frac{m_{cat,i}}{M_i} \tag{B.19}$$

from the crystal radii of the cation (r_{cryst}) and oxygen ($r_{O,cryst}$ = 1.28 pm) which corresponds to a coordination of 8) as listed in Shannon (1976) the molecular weight (M in g/mol) of the component, and two fit parameters (a, b) accounting for non-ideality in oxygen volume. Measured density data of 415 glasses was used by the authors to obtain the fit parameters a and b. Densities can then be calculated as

$$\rho_{calc} = \frac{1}{v} = \frac{1}{\sum_{i=1}^{n} y_i v_i} \tag{B.20}$$

where y_i is the i-th oxide component *mass* fraction and v_i is the i-th component partial specific volume and ρ_{calc} is in g/cm^3. Partial specific volume coefficients for component oxides are shown in Table B.1 for many oxides common in nuclear waste glasses.

B.5 Conclusions

The most robust scale of optical basicity (OB) appears to be that based on optical properties, i.e., UV probe ion absorption shift, energy gap, or refractive index (of oxide or from assessment of multicomponent glasses). Correlations between this composite scale (Λ_{opt}) and those based on average electronegativity (EN) ($\Lambda_{\chi av}$) or ionic-covalent parameter (ICP) (Λ_{ICP}) are not systematic; however, some common oxide materials (SiO_2, B_2O_3, Al_2O_3, CaO, Na_2O) do correlate well among the scales. The EN and ICP scales are still useful for comparison among materials as they can be calculated from physical and chemical properties (ionization energy, ionic radii, etc.).

Most of the work in glasses, such as redox couples, has been done with basicity determined from optical properties, so the empirical equations that exist for these must be used with that particular scale. Though it is tempting to use the other scales due to the lesser requirements for data, it seems that other

scales simply beg a proliferation of empirical equations, such as the various ones required for the EN model of basicity or the ICP model.

That being said, the latter models do seem to indicate additional nuances in the physico-chemical behavior of oxides. For instance, the EN models seem to indicate a differentiation of behavior among the various groups of oxides with characteristic polarizability behavior. Also, the ICP models indicate differing basicity behavior depending on the electronic configuration.

Given this, it may prove fruitful to reinvestigate the commonly used empirical equation (Equation B.3) for oxygen polarizability as a function of OB, with special consideration of highly polarizable cations, to see if any additional nuances can be gathered. In the meantime, a self-consistent basicity scale has been compiled including 97 oxides for 88 elements, and is now available for use in calculating optical basicities of very complex oxide glasses such as those encountered in nuclear waste vitrification.

Table B.1. Optical Basicity, Polarizability, and Density Parameters for Oxides

	Λ_{rec}	$\Lambda_{n,glass}$	Λ_{exp}	$\Lambda_{n,\ oxide}$	Λ_{Eg}	CN	$\Lambda_{\chi av}$	Λ_{ICP}	α_{cation}	v_i
Oxides	Recommended values	Glass refractivity data	Probe ion (Duffy and Ingram 1976; Duffy 2002)	Refractive index of oxide (Dimitrov and Sakka 1996)	Band gap of oxide (Dimitrov and Sakka 1996)	Assumed in $\Lambda_{\chi av}$ and Λ_{ICP} calcs.	Tabulated electronegativity (Li and Xue 2006)	Ionic-covalent parameter (Lebouteiller and Courtine 1998)	Cation electronic polarizability (Å^3)	Specific volume coefficient (cm^3/g) (Vienna et al. 2009)
Ac_2O_3	1.06 (h)	-	-	-	-	-	-	-	-	-
Ag_2O	0.91 (Duffy 2006) (d)	-	-	-	-	6	1.138	1.75	1.63 (b) (Kordes 1939)	0.088013
Al_2O_3	0.61 0.40	0.5 –0.61 - 0.40 (Duffy 2003)	0.59 (Duffy and Ingram 1973) - -	- - 0.45	-	4 5 6	0.922 0.933 0.938	0.40 0.58 0.67	0.052	0.356339
Am_2O_3	1.05	-	-	-	-	-	-	-	-	-
As_2O_3	1.01 (e)	-	-	0.95 (a)	1.02 (a)	6	0.931	1.18	0.67 (b) (Fanderlik 1983)	0.259265 (As^{5+})
As_2O_5	0.40 (a)	0.40 (a)	-	-	-	6	0.816	0.82	0.10 (b) (Kordes 1939)	0.259265
At_2O_7	0.88 (h)	-	-	-	-	-	-	-	-	-
Au_2O_3	1.13 (a)	-	-	1.13 (a)	-	4	0.922	1.07	0.31 (a)	-
B_2O_3	0.40	0.40 (Duffy 2004a) (n)	0.43 (Duffy and Ingram 1973)	-	-	3 4	0.785 0.870	0.30 (c) 0.35 (c)	0.003	0.508767
BaO	1.33	1.23–1.43	1.15 (m)	1.21	1.23	8	1.035	1.25	1.55	0.161534
BeO	0.375 (Dimitrov and Komatsu 2002) (e)	-	-	-	-	4	0.996	0.30 (c)	0.007 (Dimitrov and Komatsu 1999a)	-
Bi_2O_3	1.19	-	-	-	1.19	6	0.949	1.19	1.508 (Dimitrov and Sakka 1996)	0.09932
Bk_2O_3	1.05 (h)	-	-	-	-	-	-	-	-	-
CO_2	0.33 (m) (Duffy et al. 1978)	-	-	-	-	-	-	-	0.0013	-
CaO	1.00	1.0	1.0 (Duffy and Ingram 1973)	1.00	0.95	8	1.033	1.05	0.47	0.332023

Table B.1. Optical Basicity, Polarizability, and Density Parameters for Oxides

	Λ_{rec}	$\Lambda_{n,glass}$	Λ_{exp}	$\Lambda_{n,\ oxide}$	Λ_{Eg}	CN	$\Lambda_{\chi av}$	Λ_{ICP}	α_{cation}	v_i
Oxides	Recommended values	Glass refractivity data	Probe ion (Duffy and Ingram 1976; Duffy 2002)	Refractive index of oxide (Dimitrov and Sakka 1996)	Band gap of oxide (Dimitrov and Sakka 1996)	Assumed in $\Lambda_{\chi av}$ and Λ_{ICP} calcs.	Tabu-lated electro-negativity (Li and Xue 2006)	Ionic-covalent parameter (Lebouteiller and Courtine 1998)	Cation electronic polarizability ($Å^3$)	Specific volume coefficient (cm^3/g) (Vienna et al. 2009)
CdO	0.95 (Lenglet 2004) (f)	-	-	1.10	1.13	6	1.016	1.14	1.054 (Dimitrov and Sakka 1996)	0.142497
CeO_2	1.01	-	-	-	1.01	6	0.897	0.65	0.702 (Dimitrov and Sakka 1996), 0.73	0.139312 (Ce^{3+})
Ce_2O_3	1.18	1.18 (Duffy 2005b)	-	1.038 (Zhao et al. 2007)	1.421 (Zhao et al. 2007)	8	0.958	0.78	1.28 (Zhao et al. 2007)	0.139312
Cf_2O_3	1.05 (h)	-	-	-	-	-	-	-	-	-
Cl_2O_7	0.27 (m) (Duffy et al. 1978)	-	-	-	-	-	0.772	1.76	0.01 (b) (Kordes 1939)	0.449721
Cm_2O_3	1.05	-	-	-	-	-	-	-	-	-
CoO	0.98	-	-	-	0.98	4	0.999	0.76	0.508 (Dimitrov and Sakka 1996)	0.188757
Co_2O_3	0.96 (a)					6	0.925	0.85	0.19 (a)	-
Cr_2O_3	0.80 (Mills 1995) (g)	-	-	0.70 (Duffy 1989d)	-	6	0.931	0.73	0.3 (Duffy 1989d)	0.251727
Cs_2O	1.52	1.49–1.54	1.67 (m)	-	-	8	1.154	1.66	2.42	0.203202
Cu_2O	1.36 (a)	-	-	-	1.36 (a)	6	1.005	1.15	0.43 (Fanderlik 1983)	-
CuO	1.10 (e)	-	-	1.08	1.11	6	1.005	1.15	0.437 (Dimitrov and Sakka 1996)	0.176319
Dy_2O_3	1.08	1.08 (Duffy 2005b)	-	0.945 (Zhao et al. 2007)	1.291 (Zhao et al. 2007)	8	0.951	-	1.00 (Zhao et al. 2007)	0.116045
Eu_2O_3	0.95	0.95 (Duffy 2005b)	-	0.976 (Zhao et al. 2007)	1.328 (Zhao et al. 2007)	8	0.950	-	1.12 (Zhao et al. 2007)	0.134467
Fe_2O_3	0.80 (Mills 1995) (g)	0.77 (Duffy 1989d)		1.04	0.99	4 6	0.919 0.930	0.67 0.89	0.3 (Duffy 1989d)	0.231855
FeO	0.93 (Duffy 2006) (d)	-	-	1.0 (Duffy 1989d)	-	4 6	1.005 1.009	0.76 0.94	1.08 (Zhao et al. 2007)	-
Fr_2O	1.11 (h)	-	-	-	-	-	-	-	-	-

Table B.1. Optical Basicity, Polarizability, and Density Parameters for Oxides

	Λ_{rec}	$\Lambda_{n,glass}$	Λ_{exp}	$\Lambda_{n,\ oxide}$	Λ_{Eg}	CN	$\Lambda_{\chi av}$	Λ_{ICP}	α_{cation}	v_i
Oxides	Recommended values	Glass refractivity data	Probe ion (Duffy and Ingram 1976; Duffy 2002)	Refractive index of oxide (Dimitrov and Sakka 1996)	Band gap of oxide (Dimitrov and Sakka 1996)	Assumed in $\Lambda_{\chi av}$ and Λ_{ICP} calcs.	Tabu-lated electro-negativity (Li and Xue 2006)	Ionic-covalent parameter (Lebouteiller and Courtine 1998)	Cation electronic polarizability ($Å^3$)	Specific volume coefficient (cm^3/g) (Vienna et al. 2009)
Ga_2O_3	0.76 (e)	1.4 (Duffy 2005a)	-	0.71 (Dimitrov and Sakka 1996)	0.80 (Dimitrov and Sakka 1996)	4	0.916	0.52	0.195 (Dimitrov and Sakka 1996)	0.196685
Gd_2O_3	1.18	1.18 (Duffy 2005b)	-	0.969 (Zhao et al. 2007)	1.282 (Zhao et al. 2007)	8	0.954	-	1.08 (Zhao et al. 2007)	0.129486
GeO_2	0.61	0.61, 0.4 (Duffy 2004a)	-	0.70	0.94	4 6	0.954 0.878	0.62 0.82	0.137 (Dimitrov and Sakka 1996)	-
H_2O	0.40 (m) (Duffy et al. 1978)	-	0.40 (Duffy and Ingram 1973)	-	-	-	-	-	-	-
HfO_2	0.77 (a)	-	-	-	-	4	0.878	0.71	0.368 (b) (Kordes 1939)	-
HgO	1.25 (a)	-	-	-	1.25 (a)	6	1.011	1.12	1.38 (b) (Kordes 1939)	-
Ho_2O_3	1.04	1.04 (Duffy 2005b)	-	0.945 (Zhao et al. 2007)	1.270 (Zhao et al. 2007)	8	0.951	-	0.91 (Zhao et al. 2007)	-
In_2O_3	1.06	1.05 (Duffy 2005a)	-	-	1.07 (Dimitrov and Sakka 1996)	4 6	0.928 0.941	0.75 0.90	0.662 (Dimitrov and Sakka 1996)	-
IrO_2	0.85 (a)	-	-	-	0.85 (a)	6	0.876	1.16	0.24 (a)	-
K_2O	1.32	1.32	1.37 (m)	-	-	8	0.944	1.47	0.83	0.451472
La_2O_3	1.18	1.18 (Duffy 2005b)	1.07 (Honma et al. 2002)	1.048 (Zhao et al. 2007)	1.315 (Zhao et al. 2007)	8	0.959	0.68	1.32 (Zhao et al. 2007)	0.154555
Li_2O	0.84 (e)	0.81	1.0 (m)	0.87	-	6	0.942	0.76	0.029, 0.024 (Dimitrov and Sakka 1996)	0.483063
Lu_2O_3	0.97	0.97 (Duffy 2005b)	-	0.886 (Zhao et al. 2007)	1.239 (Zhao et al. 2007)	8	0.951	-	0.80 (Zhao et al. 2007)	-

Table B.1. Optical Basicity, Polarizability, and Density Parameters for Oxides

	Λ_{rec}	$\Lambda_{n,glass}$	Λ_{exp}	$\Lambda_{n,\ oxide}$	Λ_{Eg}	CN	$\Lambda_{\chi av}$	Λ_{ICP}	α_{cation}	v_i
Oxides	Recommended values	Glass refractivity data	Probe ion (Duffy and Ingram 1976; Duffy 2002)	Refractive index of oxide (Dimitrov and Sakka 1996)	Band gap of oxide (Dimitrov and Sakka 1996)	Assumed in $\Lambda_{\chi av}$ and Λ_{ICP} calcs.	Tabu-lated electro-negativity (Li and Xue 2006)	Ionic-covalent parameter (Lebouteiller and Courtine 1998)	Cation electronic polarizability (Å^3)	Specific volume coefficient (cm^3/g) (Vienna et al. 2009)
MgO	0.95 (Lenglet 2004) (f)	0.83–0.91	0.78 (m)	0.69	0.67	4 6	1.012 1.021	0.51 0.72	0.094	0.34608
MnO	0.95 (Duffy 2006) (d)	-	-	0.94 (Dimitrov and Sakka 1996), 1.0 (Duffy 1989d)	0.96	6	1.013	0.73	0.544 (Dimitrov and Sakka 1996)	0.209981
MoO_3	1.07	-	-	1.07	1.07	6	0.828	0.52	0.169 (Dimitrov and Sakka 1996)	0.25459
N_2O_5	0.27 (m) (Duffy et al. 1978)	-	-	-	-	6	0.787	0.99	-	-
Na_2O	1.11	1.11	1.0 –1.15 (Duffy and Ingram 1973)	-	-	6	1.149	1.11	0.179	0.362348
Nb_2O_5	1.05	-	-	-	1.05	6	0.857	0.61	0.242 (Dimitrov and Sakka 1996)	0.233644
Nd_2O_3	1.19	1.19 (Duffy 2005b)	-	1.014 (Zhao et al. 2007)	1.333 (Zhao et al. 2007)	8	0.955	-	1.25 (Zhao et al. 2007)	0.144597
NiO	0.92 (e)	-	-	0.91	0.92	6	1.006	0.97	0.266 (Dimitrov and Sakka 1996)	0.1838
NpO_2	1.01 (h)	-	-	-	-	-	-	-	-	0.100612
OsO_2	1.22 (a)	-	-	-	1.22 (a)	6	0.876	1.17	0.25 (a)	-
PaO_2	1.02 (h)	-	-	-	-	-	-	-	-	-
P_2O_5	0.40 (m) (Duffy et al. 1978)	0.36–0.48 (Duffy 2004c)	0.38 (Duffy and Ingram 1973)	-	-	4	0.783	0.39	0.04 (b) (Fajans and Kreidl 1948)	0.416076
PbO	1.18 (e)	-	-	1.19	1.17	4 8	1.014 1.025	1.19 1.20	3.623 (Dimitrov and Sakka 1996)	0.097588
PbO_2	1.22 (a)	-	-	-	1.22 (a)	6	0.921	1.00	1.78 (Fanderlik 1983)	-
PdO	1.19 (a)	-	-	-	1.19 (a)	6	1.008	1.11	0.64 (a)	0.124118
Pm_2O_3	1.19 (k)	-	-	1.010 (Zhao et al.	-	8	1.009	-	1.11 (Zhao et al.	-

Table B.1. Optical Basicity, Polarizability, and Density Parameters for Oxides

	Λ_{rec}	$\Lambda_{n,glass}$	Λ_{exp}	$\Lambda_{n,\ oxide}$	Λ_{Eg}	CN	$\Lambda_{\chi av}$	Λ_{ICP}	α_{cation}	v_i
Oxides	Recommended values	Glass refractivity data	Probe ion (Duffy and Ingram 1976; Duffy 2002)	Refractive index of oxide (Dimitrov and Sakka 1996)	Band gap of oxide (Dimitrov and Sakka 1996)	Assumed in $\Lambda_{\chi av}$ and Λ_{ICP} calcs.	Tabu-lated electro-negativity (Li and Xue 2006)	Ionic-covalent parameter (Lebouteiller and Courtine 1998)	Cation electronic polarizability (Å^3)	Specific volume coefficient (cm^3/g) (Vienna et al. 2009)
				2007)					2007)	
PoO_2	1.02 (a)	-	-	-	-	-	-	-	-	-
Pr_2O_3	1.22	1.22 (Duffy 2005b)	-	1.039 (Zhao et al. 2007)	1.372 (Zhao et al. 2007)	8	0.956	-	1.23 (Zhao et al. 2007)	0.149193
PtO_2	1.06 (e)	-	-	1.05 (a)	1.07 (a)	6	0.875	1.18	0.24 (a)	-
PuO_2	1.01 (h)	-	-	-	-	-	-	-	-	0.099468
RaO	1.09 (h)	-	-	-	-	-	-	-	-	-
Rb_2O	1.41	1.35–1.47	1.49 (m)	-	-	8	1.154	1.56	1.4	0.259259
Re_2O_7	1.30 (a)	-	-	-	1.30 (a)	6	0.797	0.20 (c)	0.11 (b) (Kordes 1939)	0.174351
Rh_2O_3	1.08 (a)	-	-	-	1.08 (a)	6	0.928	0.93	0.29 (a)	0.153206
RuO_2	0.92 (a)	-	-	-	0.92 (a)	6	0.879	1.05	0.24 (a)	0.188211
SO_3	0.33 (m) (Duffy et al. 1978)	-	0.32 (Duffy and Ingram 1973)	-	-	4	0.729	0.51	0.014 (b) (Kordes 1939)	0.441816
Sb_2O_3	1.18 (e)	-	-	1.14	1.22	6	0.942	1.18	1.111 (Dimitrov and Sakka 1996)	0.130656
Sc_2O_3	1.10	1.1 (Duffy 2005a)	-	-	0.87 (Dimitrov and Sakka 1996)	8	0.953	0.88	2.87 (Dimitrov and Sakka 1996)	-
SeO_2	0.95 (a)	-	-	0.95 (a)	-	6	0.833	0.82	0.13 (a)	0.214457
SiO_2	0.48	0.48	0.50 (Duffy and Ingram 1973)	0.48	0.52	4	0.848	0.36	0.0165 0.033 (b) (Kordes 1939)	0.395468
Sm_2O_3	1.14	1.14 (Duffy 2005b)	-	0.984 (Zhao et al. 2007)	1.308 (Zhao et al. 2007)	8	0.953	-	1.16 (Zhao et al. 2007)	0.13683
SnO_2	0.85 (e)	-	-	0.79	0.91	6	0.899	0.88	0.479 (Dimitrov and Sakka 1996)	0.169198

Table B.1. Optical Basicity, Polarizability, and Density Parameters for Oxides

	Λ_{rec}	$\Lambda_{n,glass}$	Λ_{exp}	$\Lambda_{n,\ oxide}$	Λ_{Eg}	CN	$\Lambda_{\chi av}$	Λ_{ICP}	α_{cation}	v_i
Oxides	Recommended values	Glass refractivity data	Probe ion (Duffy and Ingram 1976; Duffy 2002)	Refractive index of oxide (Dimitrov and Sakka 1996)	Band gap of oxide (Dimitrov and Sakka 1996)	Assumed in $\Lambda_{\chi av}$ and Λ_{ICP} calcs.	Tabu-lated electro-negativity (Li and Xue 2006)	Ionic-covalent parameter (Lebouteiller and Courtine 1998)	Cation electronic polarizability ($Å^3$)	Specific volume coefficient (cm^3/g) (Vienna et al. 2009)
SrO	1.08	1.04–1.11	1.11 (m)	1.10	1.18	8	1.034	1.16	0.86	0.204254
Ta_2O_5	0.94	-	-	-	0.94	6	0.853	0.58	0.185 (Dimitrov and Sakka 1996)	-
Tb_2O_3	0.99	0.99 (Duffy 2005b)	-	0.954 (Zhao et al. 2007)	1.340 (Zhao et al. 2007)	8	0.953	-	1.04 (Zhao et al. 2007)	
Tc_2O_7	0.86 (h)	-	-	-	-	6	0.803	-	-	0.276953
TeO_2	0.93 (Aida et al. 2001) (j)	0.87 (Aida et al. 2001) 0.99 (Aida et al. 2001)	-	- 0.99	- 0.96	3 4	- 0.890	1.17 1.18	1.595 (Dimitrov and Sakka 1996)	0.158491
ThO_2	0.97 (e)	-	-	0.95 (a)	0.99 (a)	6	1.019	-	0.97 (b) (Kordes 1939), 1.55 (b) (Fanderlik 1983)	0.105495
TiO	1.30 (a)	-	-	-	1.30 (a)	6	0.932	0.62	0.64 (a)	-
TiO_2	0.91 (e)	1.0–1.1 (Duffy 1989c); 0.75 (Duffy 1989d)	-	0.86-0.96	0.79-0.91	4	0.866	0.11	0.185	0.302252
Tl_2O	1.49 (a)	1.49 (a)	-	-	-	6	1.145	1.22	5.2 (Tessman et al. 1953) 3.81 (preferred) (Fajans 1948)	0.111169
Tl_2O_3	1.21 (a)	-	-	-	1.21 (a)	4	0.928	0.96	0.97 (b) (Kordes 1939)	-
Tm_2O_3	1.0	1.00 (Duffy 2005b)	-	0.913 (Zhao et al. 2007)	1.252 (Zhao et al. 2007)	8	0.949	-	0.87 (Zhao et al. 2007)	-
UO_3	1.04 (a)	-	-	1.03 (a)	1.06 (a)	-	-	-	0.56 (b) (Kordes 1939)	0.131343
UO_2	0.97 (a)	-	-	0.97 (a)	-	-	-	-	0.70 (a)	-
U_3O_8	0.99 (see text)	-	-	0.99 (see text)	-	-	-	-	-	-
V_2O_5	1.04	-	-	-	1.04	6	0.846	0.63	0.122 (Dimitrov	0.335433

Table B.1. Optical Basicity, Polarizability, and Density Parameters for Oxides

	Λ_{rec}	$\Lambda_{n,glass}$	Λ_{exp}	$\Lambda_{n,\ oxide}$	Λ_{Eg}	CN	$\Lambda_{\chi av}$	Λ_{ICP}	α_{cation}	v_i
Oxides	Recommended values	Glass refractivity data	Probe ion (Duffy and Ingram 1976; Duffy 2002)	Refractive index of oxide (Dimitrov and Sakka 1996)	Band gap of oxide (Dimitrov and Sakka 1996)	Assumed in $\Lambda_{\chi av}$ and Λ_{ICP} calcs.	Tabu-lated electro-negativity (Li and Xue 2006)	Ionic-covalent parameter (Lebouteiller and Courtine 1998)	Cation electronic polarizability (Å^3)	Specific volume coefficient (cm^3/g) (Vienna et al. 2009)
									and Sakka 1996)	
WO_3	1.05 (e)	-	-	1.05	1.04	6	0.824	0.51	0.147 (Dimitrov and Sakka 1996)	0.158296
Y_2O_3	1.0	1.0 (Duffy 2005a)	-	0.99 (Dimitrov and Sakka 1996)	-	8	0.958	0.70	0.544 (Dimitrov and Sakka 1996)	0.20359
Yb_2O_3	0.95	0.95 (Duffy 2005b)	-	0.893 (Zhao et al. 2007)	1.269 (Zhao et al. 2007)		0.947	-	0.86 (Zhao et al. 2007)	-
ZnO	0.80 (Lenglet 2004) (f)	-	0.55–0.9 (Duffy and Ingram 1991)	1.03	1.13	4	0.999	0.93	0.283 (Dimitrov and Sakka 1996)	0.173291
ZrO_2	0.85 (e)	-	-	0.87 – 0.9 (Duffy 1989c); 0.86 (Dimitrov and Sakka 1996)	0.79	6	0.897	0.71	0.37 0.357 (Dimitrov and Sakka 1996) 0.434 (b) (Kordes 1939)	0.208725

NOTES: Cation polarizability, unless otherwise noted from Pauling in Kittel (2005); glass refractivity from Duffy (2002) unless otherwise noted

(a) new values as shown in Table 3 and/or described in text

(b) cation polarizability back-calculated from ionic refractivity from reference listed using equation B.5

(c) estimated values for ICP OB since calculations from ionic radii produce negative numbers (see text)

(d) Duffy's (2006) most recent values for first row transition metals obtained by "pragmatic means"

(e) average value from refractive index and energy gap or glass refractivity and oxide refractive index

(f) Lenglet's (2004) values based on consideration of acidity, fractional iconicity, and periodic trends in metal oxides

(g) Mills' (1995) values based on consideration of molar refractivity, electron densities, and heat of formation

(h) provisional values (see text)

(j) value due to combination of trigonal bipryamidal (TeO_4) and trigonal pyramidal (TeO_3) units. Most glasses will have a mix. See (Aida et al. 2001) for details.

(k) assigned same value as Nd_2O_3 due to similarity in OB of oxides

(m) values based on Pauling electronegativity (Duffy et al. 1978)

(n) B^{4+} basicity is lower, about 0.2 on average (Duffy 2004a)

Table B.2. Optical Basicity Comparison for a Few Main Group and Transition Metal Oxides. All calculated values use the Shannon (Shannon 1976) radii.

	Λ_{rec}		$\Lambda_{n,glass}$	Λ_{exp}	$\Lambda_{n,\ oxide}$	Λ_{Eg}	$\Lambda_{\chi P}$	CN	Λ_D	$\Lambda_{\chi av}$	Λ_{ICP}
Oxides	Recommended values (this work)	Recommended by Yang & Somerville (Yang and Somerville 2001)	Glass refractivity data	Probeion (Duffy and Ingram 1976) or (Duffy 2002)	Refractive index of oxide (Dimitrov and Sakka 1996)	Band gap of oxide (Dimitrov and Sakka 1996)	From Pauling EN (Duffy et al. 1978); Yang & Somerville 2001)	Assumed in $\Lambda_{\chi av}$ and Λ_{ICP} calcs.	From average electron density (Nakamura et al. 1986)	Tabulated electronegativity (Li and Xue 2006)	Ionic-covalent parameter (Lebouteiller and Courtine 1998)
Al_2O_3	0.61	0.65	0.5 –0.61	0.60	-	-	0.61	4	0.66	0.922	0.40
B_2O_3	0.40	0.42	0.40 (Duffy, 2004a)	0.43	-	-	0.42	3	0.51	0.785	0.30
BaO	1.33	1.10	1.23–1.43	1.15	1.21	1.23	1.15	8	1.08	1.035	1.25
CaO	1.00	1.00	1.0	1.0	1.00	0.95	1.00	8	1.03	1.033	1.05
Cr_2O_3	0.80 (Mills 1995)	0.69	-	-	0.70 (Duffy 1989d)	-	0.55	6	0.77	0.931	0.73
Fe_2O_3	0.80 (Mills 1995)	0.69	0.77 (Duffy 1989d)		1.04	0.99	0.48	4	0.71	0.919	0.67
FeO	0.93 (Duffy, 2006)	0.93	-	-	1.0 (Duffy 1989d)	-	0.51	6	0.94	1.009	0.94
K_2O	1.32	1.40	1.32	1.37	-	-	1.40	8	1.16	0.944	1.47
Li_2O	0.84	1.05	0.81	1.0	0.87	-	1.07	6	1.07	0.942	0.76
MgO	0.95 (Lenglet 2004)	0.85	0.83–0.91	0.78	0.69	0.67	0.78	6	0.92	1.021	0.72
MnO	0.95 (Duffy, 2006)	0.95	-	-	0.94 (Dimitrov and Sakka 1996)	0.96	0.59	6	0.96	1.013	0.73
Na_2O	1.11	1.20	1.11	1.15	-	-	1.15	6	1.11	1.149	1.11
P_2O_5	0.40	0.40	0.36–0.48 (Duffy 2004c)	-	-	-	0.40	4	0.39	0.783	0.39
SiO_2	0.48	0.48	0.48	0.48	0.48	0.52	0.48	4	0.51	0.848	0.36
SrO	1.08	1.05	1.04–1.11	1.11	1.10	1.18	1.07	8	1.06	1.034	1.16
TiO_2	0.91	0.65	1.0–1.1 (Duffy 1989c); 0.75 (Duffy 1989d)	-	0.86-0.96	0.79-0.91	0.61	4	0.59	0.866	0.11

Table B.3. Determination of New Optical Basicities from Refractive Index and Bad Gap of Oxides

Oxide	$\Lambda_{n,oxide}$	Λ_{Eg}	n	E_G (eV)	ρ (g/cm^3) Ref (Lide 2006)	α_{cat} (Å^3)	α_{ox} (Å^3)	Notes
As_2O_3	0.95	1.02	1.755	6.05	3.86	0.67 (Fanderlik 1983)	2.30	(a), (e)
Au_2O_3	1.13		3.3 (Xia and Birss 2001)		13.68 (Ono and Cuenya 2008)	0.31	3.07	(b)
Co_2O_3		0.96		3.4101 (Prakash and Celis 2007)	5.18	0.19	2.36	(b)
Cu_2O		1.36		2.2 (Duffy 1986)	6.0	0.43 (Fanderlik 1983)	5.47	(a)
HfO_2		0.77		5.54 (Martinez et al. 2007)	9.68	0.368 (Kordes 1939)	1.86	(a)
HgO		1.25		1.9 (Glans et al. 2005)	11.14	1.38 (Kordes 1939)	3.96	(a)
IrO_2		0.85		3.7 (Goel et al. 1981)	11.7	0.24	2.04	(b)
OsO_2		1.22		~0 (Yen et al. 2004)	11.4	0.25	3.74	(b)
PbO_2		1.22		0.61 (Payne et al. 2009)	9.64	1.78 (Fanderlik 1983)	3.71	(a)
PdO		1.19		1.7113 (Prakash and Celis 2007)	8.3	0.64	3.50	(b)
PtO_2	1.05	1.07	3.1 (Naegele and Plieth 1975)	1.2 (Neff and Henkel 1996)	11.8	0.24	2.76	(b)
Re_2O_7		1.30		~0 (Prakash and Celis 2007)	6.1	0.11 (Kordes 1939)	4.50	(a), (d)
Rh_2O_3		1.08		1.41 (Koffyberg 1992)	8.2	0.29	2.81	(b)
RuO_2		0.92		2.8 (Goel et al. 1981)	7.05	0.24	2.23	(b)
SeO_2	0.95		1.8 (Finkelman and Mrose 1977)		3.95	0.28	2.32	(b)
ThO_2	0.95	0.99	2.1113 (Lide 2006)	3.87	10.0	0.97 (Kordes 1939)	2.32	(a), (e)
TiO		1.30		~0 (Duffy 1986)	4.95	0.64	4.48	(b)
Tl_2O_3		1.21		1.6 (Glans et al. 2005)	10.2	0.97 (Kordes 1939)	3.60	(a)
UO_2	0.97		2.2 (International-Nuclear-Safety-Center 1997; Ritchie 1984)		10.97	0.70	2.39	(b)
UO_3	1.03	1.06	2.126	3.07	7.3	0.56 (Kordes 1939)	2.61	(a), (c), (e)

(a) Cation polarizability converted from refractivity.
(b) Estimated cation polarizability from the cube of the ionic radius (CN=6) for all except Au_2O_3 (CN=4), radii from R. D. Shannon (Shannon 1976).
(c) Index estimated by extrapolating hydrated UO_3 compound indices to zero water (Startisky and Walker 1952).
(d) Band gap assumed equal to zero for calculation of basicity.
(e) E_G from $(1-R_m/V_m)$ (Equation B.4), data from J. A. Duffy (Duffy 1986a).

Table B.4. Determination of new optical basicities from field strength of oxides. Note that r_{ox}=1.40 Å; all oxide cations assumed six-fold coordinated; asterisked oxides are those used to derive the scaled values.

Z	Oxide	Ionic radius (Å) (Shannon 1976)	Electron density ($Å^3$)	Field strength ($Å^{-2}$)	Λ_D	Λ_{FS}	$\Lambda_{D,scaled}$	$\Lambda_{FS,scaled}$
43	Tc_2O_7	0.56	0.930	1.82	0.49	0.80	0.66	0.86
84	PoO_2	0.94	0.312	0.73	0.82	0.95	1.11	1.02
85	At_2O_7	0.62	0.849	1.72	0.51	0.82	0.70	0.88
87	Fr_2O	1.8	0.031	0.10	1.18	1.03	1.61	1.11
88	RaO	1.48	0.084	0.24	1.09	1.01	1.48	1.09
89	Ac_2O_3	1.12	0.187	0.47	0.95	0.98	1.29	1.06
90	*ThO_2	0.94	0.312	0.73	0.82	0.95	1.11	1.02
91	PaO_2	0.90	0.329	0.76	0.80	0.95	1.09	1.02
92	*UO_2	0.89	0.333	0.76	0.80	0.94	1.09	1.02
92	*UO_3	0.73	0.621	1.32	0.61	0.87	0.83	0.93
93	NpO_2	0.87	0.342	0.78	0.79	0.94	1.08	1.01
94	PuO_2	0.86	0.347	0.78	0.79	0.94	1.07	1.01
95	Am_2O_3	0.975	0.224	0.53	0.91	0.98	1.23	1.05
96	Cm_2O_3	0.97	0.225	0.53	0.90	0.98	1.22	1.05
97	Bk_2O_3	0.96	0.228	0.54	0.90	0.97	1.22	1.05
98	Cf_2O_3	0.95	0.231	0.54	0.90	0.97	1.22	1.05

Table B.5. Classification of the Oxides, According to Dimitrov and Komatsu (Dimitrov and Komatsu 2002)

	Group I	**Group II**	**Group III**
	Semicovalent, predominantly acidic	Ionic, basic	Very ionic, very basic
Oxides	BeO, MgO, B_2O_3, Al_2O_3, Ga_2O_3, SiO_2, GeO_2, P_2O_5	Li_2O, CaO, In_2O_3, SnO_2, TeO_2; transition metals, lanthanides (per Zhao et al. 2007)	Na_2O, Cs_2O, SrO, BaO, CdO, PbO, Sb_2O_3,Bi_2O_3, (presumably K_2O, Rb_2O also)
Oxide ion polarizability	Low (<1.83 Å^3)	High (1.83 <α_{O2-}< 3.0 Å^3)	Very High (> 3.0 Å^3)
O 1s binding energy	High	Narrow medium range	Low
Cation polarizability	Low	High	Very high
(Non)metal outermost binding energy	High	Low	Very low
Optical basicity	Low (Λ<1)	Narrow range near CaO ($\Lambda \approx 1$)	High (Λ>1)
Interionic interaction (Y-K interaction parameter (Yamashita and Kurosawa 1955))	Strong (large value)	Moderate	Very weak

References

Aida K, T Komatsu, and V Dimitrov. 2001. "Thermal Stability, Electronic Polarisability and Optical Basicity of Ternary Tellurite Glasses." *Physics and Chemistry of Glasses* 42(2):103-111.

Asokamani R and R Manjula. 1989. "Correlation Between Electronegativity and Superconductivity." *Physical Review B* 39(7):4217-4221.

Bach H, FGK Baucke, and D Krause, eds. 2001. *Electrochemistry of Glasses and Glass Melts, Including Glass Electrodes, Schott Series on Glass and Glass Ceramics Science, Technology, and Applications*. Springer, Berlin.

Banu T, KK Rao, and M Vithal. 2003. "Optical, Thermal and Electrical Studies of Nasicon Type $Na_2PbZnMP_3O_{12}$ (M=Al, Fe and Ga) Glasses." *Physics and Chemistry of Glasses* 44(1):30-35.

Beckett JR. 2002. "Role of Basicity and Tetrahedral Speciation in Controlling the Thermodynamic Properties of Silicate Liquids, Part 1: The System CaO-MgO-Al_2O_3-SiO_2." *Geochimica et Cosmochimica Acta* 66(1):93-107.

Bergman A. 1988. "Representation of Phosphorus and Vanadium Equilibria Between Liquid Iron and Complex Steelmaking Slags." *Transactions ISIJ* 28:945-951.

Binks JH and JA Duffy. 1985. "Ionicity of Simple Binary Oxides." *J Chem Soc, Faraday Trans 2*81:473-478.

Bordes E. 2000. "The Role of Structural Chemistry of Selective Catalysts in Heterogeneous Mild Oxidation of Hydrocarbons." *C R Acad Sci Paris, Serie IIc, Chimie* 3:725-733.

Dimitrov V and S Sakka. 1996. "Electronic Polarizability and Optical Basicity of Simple Oxides I." *Journal of Applied Physics* 79(3):1736-1740.

Dimitrov V and T Komatsu. 1999a. "Effect of Interionic Interaction on the Electronic Polarizability, Optical Basicity and Binding Energy of Simple Oxides." *Journal of the Ceramic Society of Japan* 107(11):1012-1018.

Dimitrov V and T Komatsu. 1999b. "Electronic Polarizability, Optical Basicity and Non-Linear Optical Properties of Oxide Glasses." *Journal of Non-Crystalline Solids* 249(2-3):160-179.

Dimitrov V and T Komatsu. 2000. "Interionic Interactions, Electronic Polarizability and Optical Basicity of Oxide Glasses." *Journal of the Ceramic Society of Japan* 108(4):330-338.

Dimitrov V and T Komatsu. 2002. "Classification of Simple Oxides: A Polarizability Approach." *Journal of Solid State Chemistry* 163(1):100-112.

Duffy JA and MD Ingram. 1971. "Establishment of an Optical Scale for Lewis Basicity in Inorganic Oxyacids, Molten Salts, and Glasses." *Journal of the American Chemical Society*, 93(24):6448-6454.

Duffy JA and MD Ingram. 1973. "Nephelauxetic effect and Pauling electronegativity." *J Chem Soc, Chem Commun* 17:635-636.

Duffy JA and MD Ingram. 1976. "An Interpretation of Glass Chemistry in Terms of the Optical Basicity Concept." *Journal of Non-Crystalline Solids* 21(3):373-410.

Duffy JA and MD Ingram. 1991. "Optical Basicity." In *Optical Properties of Glass*, eds. DR Uhlmann and NJ Kreidl. American Ceramic Society, Westerville, Ohio.

Duffy JA and MD Ingram. 1992. "Comments on the Application of Optical Basicity to Glass." *Journal of Non-Crystalline Solids* 144:76-80.

Duffy JA, MD Ingram, and ID Somerville. 1978. "Acid-Base Properties of Molten Oxides and Metallurgical Slags." *J Chem Soc Farad Trans* 74:1410-1419.

Duffy JA, EI Kamitsos, GD Chryssikos, and AP Patsis. 1993. "Trends in Local Optical Basicity I Sodium Borate Glasses and Relation to Ionic Mobility." *Physics and Chemistry of Glasses* 34(4):153-157.

Duffy JA. 1986a. "Chemical Bonding in the Oxides of the Elements: A New Appraisal." *Journal Of Solid State Chemistry* 62(2):145-157.

Duffy JA. 1986b. "The Refractivity and Optical Basicity of Glass." *Journal of Non-Crystalline Solids* 86:149-160.

Duffy JA. 1989a. "A Common Optical Basicity Scale for Oxide and Fluoride Glasses." *Journal of Non-Crystalline Solids* 109(1):35-39.

Duffy JA. 1989b. "Electronic Polarisability and Related Properties of the Oxide Ion." *Physics and Chemistry of Glasses* 30(1):1-4.

Duffy JA. 1989c. "Optical Basicity of Titanium(IV) Oxide and Zirconium(IV) Oxide." *Journal of the American Ceramic Society* 72(10):2012-2013.

Duffy JA. 1989d. "Use of Refractivity Data for Obtaining Optical Basicities of Transition Metal Oxides." *Ironmaking and Steelmaking* 16(6):426-428.

Duffy JA. 1992. "Optical Basicity of Sulfide Systems." *J Chem Soc Faraday Trans* 88(16):2397 2400.

Duffy JA. 2002. "The Electronic Polarisability of Oxygen in Glass and the Effect of Composition." *Journal of Non-Crystalline Solids* 297(2-3):275-284.

Duffy JA. 2003. "Optical Basicity of Aluminosilicate Glasses." *Physics and Chemistry of Glasses* 44(6):388-392.

Duffy JA. 2004a. "Relationship between Cationic Charge, Coordination Number, and Polarizability in Oxidic Materials." *The Journal of Physical Chemistry B* 108(37):14137-14141.

Duffy JA. 2004b. "Relationship between Optical Basicity and Thermochemistry of Silicates." *The Journal of Physical Chemistry B* 108(23):7641-7645.

Duffy JA. 2004c. "Abnormal refractivity trends in phosphate glass systems." *Physics and Chemistry of Glasses* 45(6):322-327.

Duffy JA. 2005a "Optical basicity analysis of glasses containing trivalent scandium, yttrium, gallium and indium." *Physics and Chemistry of Glasses* 46(5):500-504.

Duffy JA. 2005b. "Polarisability and Polarising Power of Rare Earth Ions in Glass: An Optical Basicity Assessment." *Physics and Chemistry of Glasses* 46(1):1-6.

Duffy JA. 2006. "Ionic & Covalent Character of Metal and Nonmetal Oxides." *The Journal of Physical Chemistry A* 110(49):13245-13248.

Fajans K and NJ Kreidl. 1948. "Stability of Lead glasses and Polarization of Ions." *Journal of The American Ceramic Society* 31(4):105-114.

Fanderlik I. 1983. *Optical Properties of Glass, Glass Science and Technology* Vol 5 Elsevier, Amsterdam.

Finkelman RB and ME Mrose. 1977. "Downeyite, the First Verified Natural Occurrence of SeO_2." *American Mineralogist* 62:316-320.

Fujino S, H Takebe, and K Morinaga. 1995a. "Measurements of Refractive Indexes and Factors Affecting Dispersion in Oxide Glasses." *Journal of the American Ceramic Society* 78(5):1179 1184.

Fujino S, H Takebe, and K Morinaga. 1995b. "Effect of PbO, Bi_2O_3 and Tl_2O on Optical Properties of Heavy-Metal Gallate Glasses." *Journal of the Ceramic Society of Japan* 103(4):340 345.

Glans P-A, T Learmonth, KE Smith, J Guo, A Walsh, GW Watson, F Terzi, and RG Egdell. 2005. "Experimental and Theoretical Study of the Electronic Structure of HgO and Tl_2O_3." *Physical Review B* 71(23):235109.

Goel AK, G Skorinko, and FH Pollak. 1981. "Optical Properties of Single-Crystal Rutile RuO_2 and IrO_2 in the Range 05 to 95 eV." *Physical Review B* 24(12):7342-7350.

Honma T, Y Benino, T Fujiwara, T Komatsu, R Sato, and V Dimitrov. 2002. "Electronic Polarizability, Optical Basicity, and Interaction Parameter of La_2O_3 and Related Glasses." *Journal of Applied Physics* 91(5):2942-2950.

International-Nuclear-Safety-Center. 1977. "Emissivity and Optical Constants of Uranium Dioxide."

Iwamoto N and Y Makino. 1979. "Determination of Ionic Distributions of Three Sorts of Oxygens in a Few Binary Silicate Glasses From Molar Refractivity." *Journal of Non-Crystalline Solids* 34(3):381-391.

Iwamoto N, Y Makino, and S Kasahara. 1984. "Correlation Between Refraction Basicity and Theoretical Optical Basicity Part I Alkaline and Alkaline-Earth Silicate Glasses." *Journal of Non Crystalline Solids*, 68(2-3):379-388.

Kittel C. 2005. *Introduction to Solid State Physics.* 8th ed. John Wiley & Sons.

Koffyberg FP. 1992. "Optical Bandgaps and Electron Affinities of Semiconducting Rh_2O_3(I) and Rh_2O_3(III)." *Journal of Physics and Chemistry of Solids* 53(10):1285-1288.

Kordes E. 1939. "Die Ermittlung von Atomabstanden aus der Lichtbrechung." *Zeitschrift fur Physikalische Chemie (B)* 44:249-260.

Lebouteiller A and P Courtine. 1998. "Improvement of a Bulk Optical Basicity Table for Oxidic Systems." *Journal of Solid State Chemistry* 137(1):94-103.

Lenglet M. 2000. "Ligand Field Spectroscopy And Chemical Bonding In Cr^{3+}-, Fe^{3+}-, Co^{2+}- and Ni^{2+}-Containing Oxidic Solids: Influence of The Inductive Effect of the Competing Bonds and Magnetic Interactions on the Degree of Covalency of the 3d M-O Bonds." *Materials Research Bulletin* 35(4):531-543.

Lenglet M. 2004. "Iono-Covalent Character of the Metal-Oxygen Bonds in Oxides: A Comparison of Experimental and Theroretical Data," *Active and Passive Elec Comp* 27:1-60.

Li K and D Xue. 2006. "Estimation of Electronegativity Values of Elements in Different Valence States." *Journal of Physical Chemistry A* 110(39):11332-11337.

Lide DR, ed. 2006. *CRC Handbook of Chemistry and Physics.* 87th ed. Taylor and Francis, Boca Raton.

Martinez FL, M Toledano-Luque, JJ Gandia, J Carabe, W Bohne, J Rohrich, E Strub, and I Martil. 2007. "Optical Properties and Structure Of Hfo2 Thin Films Grown by High Pressure Reactive Sputtering." *Journal of Physics D: Applied Physics* 40(17):5256-5265.

McCloy JS, BR Riley, B Johnson, M Schweiger, H Qiao, and N Carlie. 2010. "The Predictive Power of Electronic Polarizability for Tailoring the Refractivity of High-Index Glasses: Optical Basicity Versus the Single Oscillator Model." *Journal of the American Ceramic Society*, in press.

Mills KC. 1993. "The Influence of Structure on the Physico-Chemical Properties of Slags." *ISIJ International* 33(1):148-155.

Mills KC. 1995. "Basicity and Optical Basicity of Slags," In *Slag Atlas*, Verein-Deutscher Eisenhuttenleute, Verlag Stahleisen GmbH, pp 9-19.

Mitchell F, D Sleeman, JA Duffy, MD Ingram, and RW Young. 1997. "Optical Basicity of Metallurgical Slags: New Computer Based System for Data Visualization and Analysis." *Ironmaking and Steelmaking* 24(4):306-320.

Moriceau P, B Taouk, E Bordes, and P Courtine. 2000. "Correlations Between the Optical Basicity of Catalysts and Their Selectivity in Oxidation of Alcohols, Ammoxidation and Combustion of Hydrocarbons." *Catalysis Today* 61(1-4):197-201.

Moringa K, H Yoshida, and H Takebe. 1994. "Compositional Dependence of Absorption Spectra Of Ti^{3+} In Silicate, Borate, and Phosphate Glasses." *Journal of the American Ceramic Society*, 77(12):3113-3118.

Naegele K and WJ Plieth. 1975. "Kramers-Kronig Analysis for the Determination of the Optical Constants of Thin Surface Films: II Application to Platinum Oxide Films." *Surface Science* 50(1):64-76.

Nakamura T, Y Ueda, and JM Toguri. 1986. "A New Development of the Optical Basicity." *J Japan Inst Metals* 50(5):456-461.

Neff H, S Henkel, E Hartmannsgruber, E Steinbeiss, W Michalke, K Steenbeck, and HG Schmidt. 1996. "Structural, Optical, and Electronic Properties of Magnetron-Sputtered Platinum Oxide Films." *Journal of Applied Physics* 79(10):7672-7675.

Ono LK and B Roldan Cuenya. 2008. "Formation and Thermal Stability of Au_2O_3 on Gold Nanoparticles: Size and Support Effects." *The Journal of Physical Chemistry C* 112(12):4676 4686.

Pauling, L. 1932. "The Nature of the Chemical Bond IV The Energy of Single Bonds and the Relative Electronegativity of Atoms." *Journal of the American Chemical Society* 54:3570-3582.

Payne DJ, G Paolicelli, F Offi, G Panaccione, P Lacovig, G Beamson, A Fondacaro, G Monaco, G Vanko, and RG Egdell. 2009. "A Study of Core and Valence Levels in β-PbO_2 By Hard X Ray Photoemission." *Journal of Electron Spectroscopy and Related Phenomena* 169(1):26-34.

Portier J, G Campet, J Etourneau, and B Tanguy. 1994a. "A Simple Model for the Estimation of Electronegativities of Cations in Different Electronic States and Coordinations." *Journal of Alloys and Compounds* 209(1-2):285-289.

Portier J, G Campet, J Etourneau, MCR Shastry, and B Tanguy. 1994b. "A Simple Approach to Materials Design: Role Played by an Ionic-Covalent Parameter Based on Polarizing Power and Electronegativity." *Journal of Alloys and Compounds* 209(1-2):59-64.

Prakash B and J Celis. 2007. "The Lubricity of Oxides Revised Based on a Polarisability Approach." *Tribology Letters* 27(1):105-112.

Reddy RR, YN Ahammed, KR Gopal, PA Azeem, and TVR Rao. 1999. "Correlation Between Optical Basicity, Electronegativity and Electronic Polarizability for Some Oxides and Oxysalts." *Optical Materials* 12(4):425-428.

Reddy RR, YN Ahammed, PA Azeem, KR Gopal, and TVR Rao. 2001. "Electronic Polarizability and Optical Basicity Properties of Oxide Glasses Through Average Electronegativity." *Journal of Non-Crystalline Solids* 286(3):169-180.

Ritchie AG. 1984. "The Kinetics and Mechanism of The Uranium-Water Vapour Reaction—An Evaluation of Some Published Work." *Journal of Nuclear Materials* 120(2-3):143-153.

Shannon RD. 1976. "Revised Effective Ionic Radii And Systematic Studies Of Interatomic Distances in Halides and Chalcogenides." *Acta Crystallographica Section A* 32:751-767.

Startisky E and DI Walker. 1952. *Optical properties of some compounds of uranium, plutonium, and related elements,* LA-1439, Series A, Los Alamos Scientific Laboratory of the University of California, Los Alamos, New Mexico.

Susa M, F Li, and K Nagata. 1992. "Determination of Refractive Index and Absorption Coefficient of Iron- Oxide-Bearing Slags." *Metallurgical and Materials Transactions B*, 23(3):331-337.

Tessman JR, AH Kahn, and W Shockley. 1953. "Electronic Polarizabilities of Ions in Crystals." *Physical Review* 92(4):890-895.

Verein-Deutscher-Eisenhuttenleute, ed. 1995. *Slag Atlas.* 2nd ed. Verlag Stahleisen GmbH.

Vienna, JD, A Fluegel, DS Kim, and P Hrma. 2009. *Glass Property Data and Models for Estimating High-Level Waste Glass Volume.* PNNL-18501, Pacific Northwest National Laboratory, Richland, Washington.

Vithal M, P Nachimuthu, T Banu, and R Jagannathan. 1997. "Optical and Electrical Properties of PbO-TiO_2, PbO-TeO_2, and PbO-CdO Glass Systems." *Journal of Applied Physics* 81(12):7922 7926.

Vogel W. 1994. *Glass Chemistry.* 2nd ed. Springer-Verlag, Berlin.

Xia SJ and VI Birss. 2001. "A Multi-Technique Study of Compact and Hydrous Au Oxide Growth in 0.1 M Sulfuric Acid Solutions." *Journal of Electroanalytical Chemistry* 500(1-2):562 573.

Yamashita J and T Kurosawa. 1955. "The Theory of the Dielectric Constant of Ionic Crystals III." *Journal of the Physical Society of Japan* 10(8):610-633.

Yang YD and ID Somerville. 2001. "Relationship Between Optical Basicity and Various Capacities in Metallurgical Slags." *Phys Chem Glasses: Eur J Glass Sci Technol B* 43C:362 371.

Yen PC, RS Chen, CC Chen, YS Huang, and KK Tiong. 2004. "Growth and Characterization of OsO_2 Single Crystals." *Journal of Crystal Growth* 262(1-4):271-276.

Zhao X, X Wang, H Lin, and Z Wang. 2007. "Electronic Polarizability and Optical Basicity of Lanthanide Oxides." *Physica B* 392:132-136

Zhao X, X Wang, H Lin, and Z Wang. 2008a. "A New Approach to Estimate Refractive Index, Electronic Polarizability, and Optical Basicity of Binary Oxide Glasses." *Physica B: Condensed Matter* 403(13-16):2450-2460.

Zhao X, X Wang, H Lin, and Z Wang. 2008b. "Average Electronegativity, Electronic Polarizability and Optical Basicity of Lanthanide Oxides for Different Coordination Numbers." *Physica B: Condensed Matter* 403(10-11):1787-1792.

Distribution

No. of Pages

OFFSITE

1 Tommy Edwards
Savannah River National Laboratory
999-W
Aiken, South Carolina 29808

1 Kurt Gerdes
U.S. Department of Energy, EM-32
19901 Germantown Road
Germantown, Maryland 20874

1 Carol Jantzen
Savannah River National Laboratory
773-A
Aiken, South Carolina 29808

1 Wing Kot
Vitreous State Laboratory
620 Michigan Ave., N.E.
Washington, D.C. 20064

3 Ernie Lee
Waste Treatment and Immobilization Plant
2435 Stevens Center Place
Richland, Washington 99354

1 David Peeler
Savannah River National Laboratory
999-W
Aiken, South Carolina 29808

1 Ian Pegg
Vitreous State Laboratory
Hannan Hall
620 Michigan Avenuse, NE
Washington, DC 20064

No. of Pages

ONSITE

31 Hanford Site & Pacific Northwest National Laboratory

PR Bredt (PNNL)	K6-24
PJ Certa (WRPS)	B1-55
TW Crawford (WRPS)	B1-55
JV Crum (PNNL)	K6-24
PA Empey (WRPS)	B1-55
RA Gilbert (ORP)	H6-60
PR Hrma (PNNL)	K6-24
RT Jasper (WRPS)	B1-55
BR Johnson (PNNL)	K6-24
GB Josephson (PNNL)	K9-69
D-S Kim (PNNL)	K6-24
AA Kruger (ORP)	H6-60
BM Mauss (ORP)	H6-60
2 JS McCloy (PNNL)	K6-24
3 FL Meinert (WRPS)	B1-55
LM Peurrung (PNNL)	K9-09
TL Sams (WRPS)	B1-55
JG Reynolds (WRPS)	B1-55
BJ Riley (PNNL)	K6-24
2 C Rodriguez (PNNL)	K6-24
PL Rutland (WRPS)	B1-55
JV Ryan (PNNL)	K6-24
MJ Schweiger (PNNL)	K6-24
GL Smith (EM-31)	H6-60
3 JD Vienna (PNNL)	K6-24

Pacific Northwest
NATIONAL LABORATORY

U.S. DEPARTMENT OF
ENERGY

902 Battelle Boulevard
P.O. Box 999
Richland, WA 99352
1-888-375-PNNL (7665)
www.pnl.gov